2024

Development and characterization of glial cell models of Autosomal Recessive Spastic Ataxia of Charlevoix-Saguenay

Fernanda Ivanira Henriques Murtinheira Ferreira

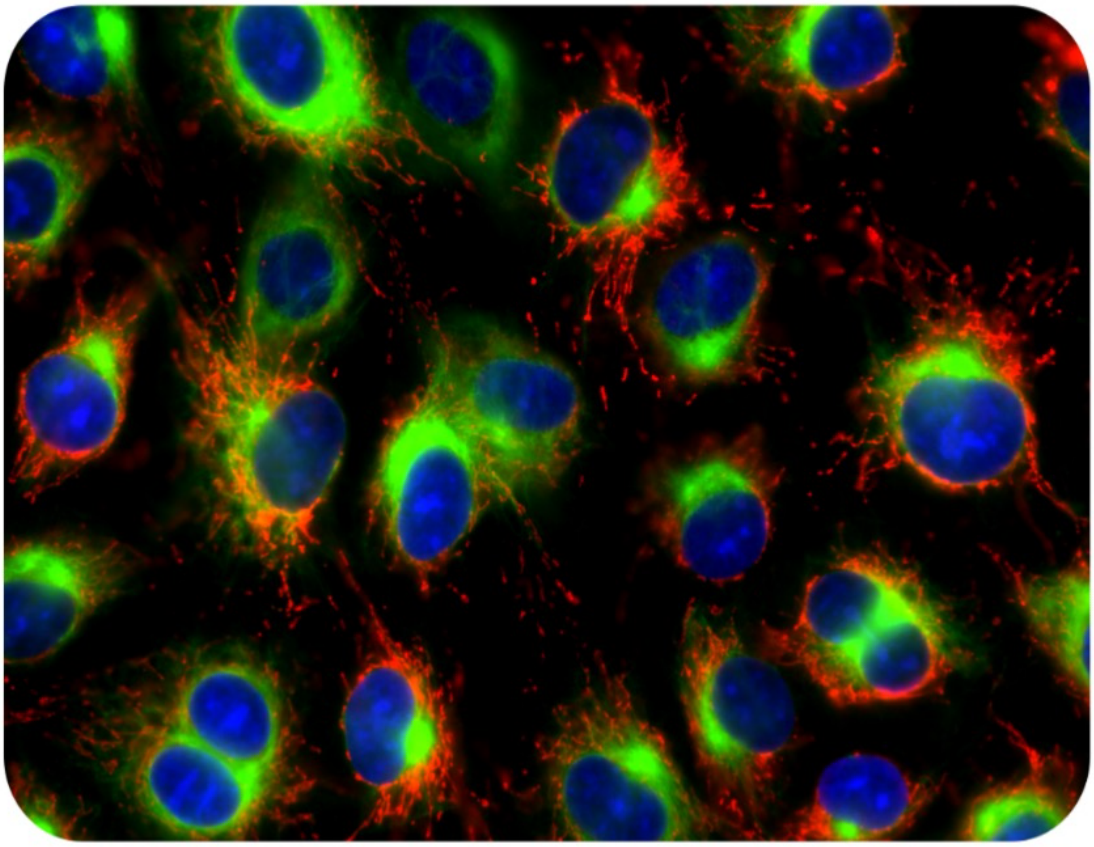

Dissertation presented to obtain the

Ph.D degree in Molecular Biosciences

Speciality Biochemistry

Oeiras, December, 2024

INSTITUTO DE TECNOLOGIA QUÍMICA E BIOLÓGICA ANTÓNIO XAVIER | UNIVERSIDADE NOVA DE LISBOA

Development and characterization of glial cell models of Autosomal Recessive Spastic Ataxia of Charlevoix-Saguenay

Fernanda Ivanira Henriques Murtinheira Ferreira

Dissertation presented to obtain the Ph.D degree in Molecular Biosciences

Instituto de Tecnologia Química e Biológica António Xavier | Universidade Nova de Lisboa

Oeiras, December, 2024

I declare that this dissertation is based on work developed during my PhD research project, except where otherwise stated. I have clearly stated the contribution by others to jointly authored works that I have included in my thesis. Experimental work was performed at Instituto de Tecnologia Química e Biológica António Xavier, Universidade Nova de Lisboa, in Oeiras, Portugal and Faculdade de Ciências, Universidade de Lisboa, in Lisbon, Portugal. Doctor Federico Herrera supervised all work.

Fernanda Murtinheira was supported by a PhD fellowship from Fundação para a Ciência e Tecnologia (Ref. SFRH/BD/133220/2017). We acknowledge the Bioimaging facilities at BioISI/FCUL, Gulbenkian Institute of Science and Instituto de Medicina Molecular João Lobo Antunes, all of them part of the Portuguese Platform of BioImaging supported by FEDER funds (Ref. PPBI-POCI-01-0145-FEDER-022122). Mass spectrometry-based proteomics was performed at the ITQB NOVA and FCUL Proteomics Scientific Platforms with the assistance of Dr. Vukosava Torres (BioISI/FCUL), and had support from the Portuguese Mass Spectrometry Network, integrated in the National Roadmap of Research Infrastructures of Strategic Relevance (ROTEIRO/0028/2013; LISBOA-01-0145-FEDER-022125). This work was also supported by: center grants LISBOA-01-0145-FEDER-007660 (Cellular Structural and Molecular Microbiology) and https://doi.org/10.54499/UIDP/04046/2020 and https://doi.org/10.54499/UIDB/04046/2020 (BioISI Research Unit); individual grants from FCT (Refs. PTDC/MED-NEU/31417/2017 and https://doi.org/10.54499/PTDC/FIS-MAC/2741/2021) and the ARSACS Foundation (Canada); and a European Union Twinning consortium (TWIN2PIPSA, GA 101079147). Views and opinions expressed are those of the author(s) only and do not necessarily reflect those of the European Union or European Research Executive Agency (REA). Neither the European Union nor the granting authority can be held responsible for them.

Oeiras, December 2024

Ao meu filho.

Ao meu marido.

Aos meus pais.

Aos meus irmãos.

“Everyone you meet is fighting a battle you know nothing about.
Be kind. Always.”

Robin Williams

TABLE OF CONTENTS

ACKNOWLEDGEMENTS

I want to thank those who have supported me throughout my PhD journey. First, I want to express my sincere thanks and appreciation to Professor Federico Herrera, my supervisor, for having accepted me to work in his laboratory. His passion for science, attention to detail, guidance, and support have been essential.

I also thank the current and former Cell Structure and Dynamics Lab members. To the former member of the laboratory, Ricardo Vilela, for introducing me to the laboratory and helping me take my first steps. To all the colleagues I have had the pleasure of having during all these years: Beatriz Cardoso, Ricardo Quiteres, Beatriz Teixeira, Mafalda, Daniela, Patricia, Mickael, Andrea, Fabiana, Cristina, Pedro, André and Catarina. All of you make me feel at home in the lab. The PhD journey is a whirlwind of emotions, and the opportunity to work in a safe and familiar environment like the laboratory allowed me to carry out better research. I thank Ana Sofia, Carina and Constança for providing pleasant conversations and relaxing experiences on this journey, having coffee and eating lots of sweets.

My sincere gratitude goes to my son Guilherme for having to share his mother with science and for supporting and facilitating my commitment to my work. Thank you to my parents, Agostinho and Conceição, who allowed me to achieve all my goals from the beginning and to whom I owe what I am. Thank you also to my brothers for all their support and encouragement.

I thank Nuno for being my rock from the beginning. Thank you for listening to me, for supporting me and for having the ability to bring calm on stormy days.

SUMMARY

Autosomal recessive spastic ataxia of Charlevoix-Saguenay (ARSACS) is the third most prevalent recessive ataxia, characterized by childhood onset of progressive cerebellar ataxia, spasticity, motor sensory neuropathy, axonal demyelination, and Purkinje cell loss. ARSACS is caused by loss-of-function mutations in the *SACS* gene, which encodes sacsin, a 520 kDa multimodular protein with a partially understood function. Several lines of evidence suggest that sacsin is involved in chaperone activities, promotes the proper polymerization of the neuronal intermediate filaments (i.e., neurofilaments and vimentin), is linked to mitochondrial dynamics, and bioenergetics and regulates organelle positioning by regulating cytoskeletal dynamics. Although Purkinje cell dysfunction in ARSACS is well-established, the role of glial cells in the pathology remains unexplored. This study aims to uncover the cellular and molecular consequences of sacsin loss in new glial cell models of ARSACS. We demonstrated that primary astrocytes, C6 rat glioma cells, N9 mouse microglia, and HMC3 human microglial cells, among other non-neuronal cell lines, express sacsin protein. This suggests a broader role for sacsin beyond neuronal cells. We generated two new glial cell models of ARSACS by knocking out sacsin in C6 (rat glioblastoma, astroglial-like) and HMC3 (human microglia) cell lines by means of a CRISPR/Cas9 approach. In both cases, knocking out sacsin disrupted the subcellular distribution of glial intermediate filaments, as well as organelles like mitochondria and the Golgi apparatus. It also impaired autophagic and stress pathways in the endoplasmic reticulum. $C6^{Sacs-/-}$ cells displayed defective STAT3 signalling in response to inflammatory cytokines and increased susceptibility to several forms of stress, such as inhibition of mitochondrial respiration, serum deprivation and irradiation. The proteomic profile of $C6^{Sacs-/-}$ cells showed 196 differentially expressed proteins (DEPs)

(36 upregulated and 104 downregulated) related to some of these alterations. The proteomic analysis also revealed changes in pathways that affect cellular mechanical and viscoelastic properties, for which intermediate filaments are the main responsible structure. Atomic Force Microscopy corroborated these findings, indicating lower elasticity and increased stiffness of the cytoplasmic regions of $C6^{Sacs-/-}$ cells. The elasticity of the nuclear region appears to be unaffected by the loss of sacsin.

In summary, our findings revealed that glial cells also express sacsin and that its deletion in glial-like and microglial cells mimics the pathological features of ARSACS observed in neuronal cells. These results shed light on a pivotal role for sacsin in glial cells and highlight astroglia and microglia as crucial players in ARSACS. Future research should validate our findings in *post-mortem* brain tissues from ARSACS patients and existing mouse models of the disease and analyse how sacsin loss disrupts astroglia and microglia functions. Given the developmental nature of ARSACS, these studies should focus on embryonic or perinatal stages. Our findings strongly indicate that the $C6^{Sacs-/-}$ and $HMC3^{Sacs-/-}$ models of ARSACS serve as valuable tools to study sacsin functions beyond neurons, as well as in other human pathologies caused by disruption of intermediate filament networks, such as Alexander disease and Giant Axonal Neuropathy.

RESUMO

A ataxia espástica autossómica recessiva de Charlevoix-Saguenay (ARSACS) é uma doença neurodegenerativa rara, inicialmente descrita na região de Charlevoix-Saguenay, no Québec, Canadá. Atualmente, ARSACS é uma das ataxias recessivas mais prevalentes a nível mundial. As características histopatológicas de ARSACS incluem atrofia da verme anterior, associada à perda seletiva de células de Purkinje e depósitos de lipofuscina nos neurónios cerebelares e na pele. As primeiras manifestações da doença ocorrem frequentemente na primeira infância, e o diagnóstico é feito através de teste genético, uma vez que ARSACS se deve a mutações no gene *SACS*, que codifica a proteína sacsina (520 kDa). Ratos e peixe-zebra knockout para sacsina apresentam características histopatológicas e neurológicas consistentes com ARSACS, indicando que a doença é provocada pela perda de função da sacsina. A função da sacsina ainda não é totalmente compreendida, mas as evidências sugerem que está envolvida no controlo de qualidade de proteínas, na organização dos filamentos intermédios neuronais (ou seja, neurofilamentos e vimentina), e na dinâmica e atividade mitocondrial. Adicionalmente, os modelos celulares de ARSACS apresentam fluxo autofágico desregulado e localização aberrante de proteínas e organelos, nomeadamente, lisossomas, complexo de Golgi e retículo endoplasmático.

O estudo da ARSACS e da função da sacsina tem sido focado sobretudo em células neuronais. Contudo, tem vindo a ser cada vez mais reconhecida a importância das células gliais no neurodesenvolvimento, neuroinflamação e neurodegeneração. Este trabalho tem como objetivo investigar as consequências celulares e moleculares da perda de sacsina em células gliais e a sua contribuição para a patologia ARSACS. Demonstrámos que a

proteína sacsina é expressa em astrócitos primários, células de glioma de rato C6, microglia de rato N9 e células microgliais humanas HMC3, entre outras linhas e tipos celulares não neuronais. Desenvolvemos dois novos modelos celulares de ARSACS, eliminando a sacsina nas células C6 (astrogliais) e nas células HMC3 (microgliais) com recurso à técnica de CRISPR/Cas9.

A deleção da sacsina nas células C6 (semelhantes a astroglia de rato) e nas HMC3 (microglia humana) provocou um aumento da expressão dos principais filamentos intermédios gliais (por exemplo, *glial fibrillary acidic protein* (GFAP), nestina e vimentina) e à sua agregação na zona justanuclear. Foram também observadas alterações na morfologia e distribuição da rede mitocondrial e um aumento dos níveis basais de espécies reativas de oxigénio (ROS). Nas células sacsina knockout observámos mudanças na distribuição do complexo de Golgi e da proteína de ligação ao citoesqueleto, plectina. A ausência de sacsina comprometeu ainda vias específicas de autofagia e de stress no retículo endoplasmático. As células $C6^{Sacs-/-}$ exibiram anomalias na sinalização STAT3 em resposta a citocinas inflamatórias e maior suscetibilidade a várias formas de stress, como a inibição da respiração mitocondrial, privação de soro e irradiação. A análise proteómica também revelou mudanças em vias que afetam as propriedades mecânicas e viscoelásticas celulares, para as quais os filamentos intermédios são a principal estrutura responsável. Através da Microscopia de Força Atómica, verificámos a redução da elasticidade e o aumento da rigidez das regiões citoplasmáticas das células $C6^{Sacs-/-}$, corroborando os resultados de proteómica obtidos. A elasticidade da região nuclear parece não ser afetada pela perda de sacsina.

Em suma, demonstrámos que as células gliais também expressam sacsina e que a sua deleção em células semelhantes a astroglia e

microgliais mimetiza as características patológicas de ARSACS observadas nas células neuronais. Estes resultados sugerem que a sacsina desempenha uma função essencial nas células gliais e apontam para os astrócitos e a microglia como intervenientes cruciais na patologia de ARSACS. Estudos futuros devem testar as nossas descobertas em tecidos cerebrais pós-morte de pacientes com ARSACS e em modelos de ratinho existentes da doença, além de analisar como a perda de sacsina perturba as funções dos astrócitos e da microglia. Considerando que ARSACS apresenta características de uma doença de neurodesenvolvimento, estes estudos devem focar-se em estágios embrionários ou perinatais. As nossas descobertas sugerem que os modelos $C6^{Sacs-/-}$ e $HMC3^{Sacs-/-}$ de ARSACS são ferramentas valiosas para estudar as funções da sacsina em células não neuronais, bem como outras patologias humanas causadas pela perturbação das redes de filamentos intermédios, como a doença de Alexander e a Neuropatia Axonal Gigante.

LIST OF THESIS PUBLICATIONS

JOURNAL ARTICLES

Three scientific papers are the result of the current dissertation, two of which have already been published, and another one is currently under revision. A large part of the results was deposited as an article in the BioRxiv public repository, and the results related to stress sensitivity upon sacsin deletion will be part of a fourth article submission during 2025:

1. **Fernanda Murtinheira**, Mafalda Migueis, Ricardo Letra-Vilela, Mickael Diallo, Andrea Quezada, Cláudia A. Valente, Abel Oliva, Carmen Rodriguez, Vanesa Martin, and Federico Herrera (2022). Sacsin Deletion Induces Aggregation of Glial Intermediate Filaments. Cells 11, nº. 2: 299. https://doi.org/10.3390/cells11020299

2. **Fernanda Murtinheira**, Elisa Farsetti, Luana Macedo, Ana Sofia Boasinha, Mário S. Rodrigues, Adelaide Fernandes and Federico Herrera (2024). A human microglial cell model of autosomal recessive spastic ataxia of Charlevoix-Saguenay. Biochimica et Biophysica Acta (BBA) - Molecular Basis of Disease, 1870, 8. https://doi.org/10.1016/j.bbadis.2024.167452

3. **Fernanda Murtinheira**, Ana Sofia Boasinha, João Belo, Luana Macedo, Elisa Farsetti, Tiago T. Robalo, Vukosava M. Torres, Francisco R. Pinto, Adelaide Fernandes, Patricia Nascimento, Mario S. Rodrigues, Federico Herrera (2024). Subcellular, biochemical and biophysical alterations in two glial cell models of ARSACS. bioRxiv 2024.04.15.589510; doi: https://doi.org/10.1101/2024.04.15.589510.

4. **Fernanda Murtinheira**, João Belo, Ana Sofia Boasinha, Tiago T. Robalo, Vukosava M. Torres, Francisco R. Pinto, Patricia Nascimento, Mario S. Rodrigues, and Federico Herrera. Mechanical alterations in a glial model of autosomal recessive spastic ataxia of Charlevoix-Saguenay. *Under revision in Movement Disorders*.

Additionally, six other scientific articles were published during the thesis period due to the author's participation in other projects carried out by other members of the same research group. However, the content of these papers has not been included in the core thesis as they go beyond its scope, and the author contributed as a collaborator rather than leading the research.

1. Susana G Martins, Vanessa Ribeiro, Catarina Melo, Cláudia Paulino-Cavaco, Dario Antonini, Sharadha Dayalan Naidu, **Fernanda Murtinheira**, Inês Fonseca, Bérénice Saget, Mafalda Pita, Diogo R Fernandes,Pedro Gameiro dos Santos, Gabriela Rodrigues, Rita Zilhão, Federico Herrera, Albena T Dinkova-Kostova, Ana Rita Carlos, Sólveig Thorsteinsdóttir (2024). Laminin-α2 chain regulates muscle cell homeostasis. Life Science Alliance, 7 (12) e202402829. https://doi.org/10.26508/lsa.202402829

2. Mickael Diallo, Constança Pimenta, **Fernanda Murtinheira**, Daniela Martins-Alves, Francisco R. Pinto, André Abrantes da Costa, Ricardo Letra-Vilela, Vanesa Martin, Carmen Rodriguez, Mário S. Rodrigues, Federico Herrera (2023). Asymmetric post-translational modifications regulate the nuclear translocation of STAT3 homodimers in response to leukemia inhibitory factor. Cell Oncol. https://doi.org/10.1007/s13402-023-00911-9

3. Maria Inês Leitão, Giulia Orsini, **Fernanda Murtinheira**, Clara Gomes, Federico Herrera, Ana Petronilho (2023). Synthesis, Base Pairing Properties, and Biological Activity Studies of Platinum(II) Complexes Based on Uracil Nucleosides. Inorg. Chem. 2023, 62, 40, 16412–16425. https://doi.org/10.1021/acs.inorgchem.3c02071

4. Pedro Ferreira-Peralta, Brenda França, **Fernanda Murtinheira**, Mário S. Rodrigues, Federico Herrera, (2023). Is spastic ataxia 8 a protein misfolding disorder?. Biochim Biophys Acta Mol Basis Dis.,1870(1):166882. 10.1016/j.bbadis.2023.166882

5. Ricardo Letra-Vilela, Beatriz Cardoso, Catarina Silva-Almeida, Ana Maia Rocha, **Fernanda Murtinheira**, Joana Branco-Santos, Carmen Rodriguez, Vanesa Martin, Mariana Santa-Marta, Federico Herrera, (2020). Can asymmetric post- translational modifications regulate the

behavior of STAT3 homodimers?. FASEB BioAdvances, 2, 116-125. http://dx.doi.org/10.1096/fba.2019-00049

6. Ricardo Letra-Vilela, Ricardo Quiteres, **Fernanda Murtinheira**, Alvaro Crevenna, Zach Hensel, Federico Herrera, (2020). New tools for the visualization of glial fibrillary acidic protein in living cells. Experimental Results, 1, E4. http://dx.doi.org/10.1017/exp.2020.1

COMMUNICATIONS IN SCIENTIFIC MEETINGS

The scientific outputs of the thesis and the extra contributions were shared with the scientific community in different national and international congresses as poster presentations, as well as oral presentations in research meetings.

Oral communications (Only as 1st author, 9 as a co-author)

1. **Fernanda Murtinheira**, Ana Sofia Boasinha, Luana Macedo, Patrícia Nascimento, Francisco Pinto, Vukosava Torres, Mário S. Rodrigues, Federico Herrera (2023). Proteomic profiling of astroglial and microglial cell models of the Autosomal Recessive Ataxia of Charlevoix-Saguenay (ARSACS). 3rd Chem&Biochem Students Meeting, Faculdade de Ciências da Universidade de Lisboa, Lisboa, Portugal.

2. **Fernanda Murtinheira**, Cristina Duarte Olivenza, Ricardo Letra-Vilela, Beatriz Cardoso, Vanesa Martin, Carmen Rodriguez, Federico Herrera (2022). Sacsin deletion promotes intermediate filament aggregation in glial cells: potential implications for ARSACS. 12th ITQB NOVA PhDStudents' Meeting, Instituto de Tecnologia Química e Biológica, Universidade Nova de Lisboa, Oeiras, Portugal.

3. **Fernanda Murtinheira**, Mafalda Miguéis, Ricardo Letra-Vilela R., Vanesa Martin, Carmen Rodriguez, Claúdia Valente, Cristina Duarte-Olivenza, Federico Herrera (2021). Sacsin deletion promotes intermediate filaments aggregation in glial cells: potential implications for ARSACS. V Symposium of the Portuguese Glial Network. Coimbra, Portugal.

Poster communications (Only as 1st author, 35 as a co-author)

1. **Fernanda Murtinheira**, Ana Sofia Boasinha, João Belo, Luana Macedo, Elisa Farsetti, Tiago T. Robalo, Vukosava Torres, Francisco Pinto, Patrícia Nascimento, Adelaide Fernandes, Mário S. Rodrigues, Federico Herrera (2024). Glial cell models of Autosomal Recessive Spastic Ataxia of Charlevoix-Saguenay. International Congress of Ataxia Research 2024. London, England.

2. **Fernanda Murtinheira**, Ana Sofia Boasinha, Luana Macedo, Patrícia Nascimento, Francisco Pinto, Vukosava Torres, Mário S. Rodrigues, Federico Herrera (2023). Biochemical and biophysical alterations in glial cell models of the Autosomal Recessive Ataxia of Charlevoix-Saguenay (ARSACS). Ciências Research and Innovation Week. Faculdade de Ciências da Universidade de Lisboa, Lisboa, Portugal.

3. **Fernanda Murtinheira**, Ana Sofia Boasinha, Luana Macedo, Patrícia Nascimento, Francisco Pinto, Vukosava Torres, Mário S. Rodrigues, Federico Herrera (2023). Biochemical and biophysical alterations in glial cell models of the Autosomal Recessive Spastic Ataxia of Charlevoix-Saguenay (ARSACS). 7th International ARSACS Symposium. Montereal, Canada.

4. **Fernanda Murtinheira**, Ana Sofia Boasinha, Luana Macedo, Patrícia Nascimento, Francisco Pinto, Vukosava Torres, Mário S. Rodrigues, Federico Herrera (2023). Glial cell models of the Autosomal Recessive Spastic Ataxia of Charlevoix- Saguenay (ARSACS): Biochemical and biophysical alterations. 13th EMBO Young Scientists' Forum. Instituto de Medicina Molecular João Lobo Antunes, Lisboa, Portugal.

5. **Fernanda Murtinheira**, Mafalda Miguéis, Ricardo Letra-Vilela R., Vanesa Martin, Carmen Rodriguez, Claúdia Valente, Cristina Duarte-Olivenza, Federico Herrera (2021). Ataxia-related protein sacsin regulates the intermediate filament network in glial cells. XVII Meeting of the Portuguese Society for Neuroscience. Coimbra, Portugal.

6. **Fernanda Murtinheira**, Cristina Duarte-Olivenza, Maria Beatriz Teixeira, Ricardo Letra- Vilela, Vanesa Martin, Carmen Rodriguez, Cláudia Valente, Abel Oliva and Federico Herrera. (2021). Deletion of the ataxia-related chaperone sacsin disrupts the intermediate filaments network in glial cells. Ciências Research Day, Faculty of Sciences of the University of Lisbon.

7. **Fernanda Murtinheira**, Cristina Duarte-Olivenza, Maria Beatriz Teixeira, Ricardo Letra- Vilela, Vanesa Martin, Carmen Rodriguez, Cláudia Valente, Abel Oliva and Federico Herrera (2021). Ataxia related protein sacsin knockout disrupts the intermediate filaments network in glial cells. IDPSeminars. Magnus Kjaergaard (Aarhus University) and Alex Holehouse (Washington University School of Medicine).

8. **Fernanda Murtinheira**, Cristina Duarte-Olivenza, Maria Beatriz Costa-Teixeira, Ricardo Letra-Vilela, Vanesa Martin, Carmen Rodriguez, Claúdia Valente, Abel Oliva, Federico Herrera (2021). Ataxia related protein sacsin knockout disrupts the intermediate filaments network in glial cells. XXI SPB National Congress of Biochemistry, Évora, Portugal.

9. **Fernanda Murtinheira**, Cristina Duarte-Olivenza, Maria Beatriz Costa-Teixeira, Ricardo Letra-Vilela, Vanesa Martin, Carmen Rodriguez, Claúdia Valente, Abel Oliva, Federico Herrera, (2020). Ataxia related protein sacsin knockout disrupts the intermediate filaments network in glial cells. BioISI Research Day, Lisboa, Portugal.

10. **Fernanda Murtinheira**, Cristina Duarte Olivenza, Ricardo Letra-Vilela, Beatriz Cardoso, Vanesa Martin, Carmen Rodriguez, Federico Herrera (2020). Towards a smaller but functional sacsin protein for ARSACS gene therapy. 10th ITQB NOVA PhDStudents' Meeting, Lisboa, Portugal.

11. **Fernanda Murtinheira**, Cristina Duarte Olivenza, Ricardo Letra-Vilela, Beatriz Cardoso, Vanesa Martin, Carmen Rodriguez, Federico Herrera (2019). Towards a smaller but functional sacsin protein for ARSACS gene therapy. XVI meeting of Portuguese Society for Neuroscience, Lisboa, Portugal.

12. **Fernanda Murtinheira**, Catarina Esteves, Catarina Silva-Almeida, Ricardo Letra-Vilela, Rita Delgado, Federico Herrera (2019). Dinuclear zinc complexes as specific inhibitors of stat3 phosphorylation at tyrosine 705. XVI meeting of Portuguese Society for Neuroscience, Lisboa, Portugal.

LIST OF ABBREVIATIONS

AD Alzheimer's disease

ALS Amyotrophic lateral sclerosis

ANOVA Analysis of Variance

ARSACS Autosomal Recessive Spastic Ataxia Charlevoix-Saguenay

ATM ataxia-telangiectasia

ATXN3 Ataxin 3

AxD Alexander disease

BG Bergmann's glia

CRISPR/Cas9 Clustered regularly interspaced short palindromic repeats/ CRISPR-associated protein 9

CF Climbing fibres

CMT Charcot-Marie-Tooth disease

CNS Central Nervous System

DAPI 4′,6-diamidino-2-phenylindole

DCFH-DA 2,7-dichlorodihydrofluorescein diacetate

DCN Deep Cerebellar Nuclei

DEPs Different Expressed Proteins

DHE Dihydroethidium

DMEM Dulbecco's Modified Eagle Medium

DMSO Dimethyl sulfoxide

EDTA Ethylenediamine tetraacetic acid

ER Endoplasmic reticulum

FA Friedreich's ataxia

FACS Fluorescence-activated cell sorting

FBS Fetal bovine serum

GAPDH Glyceraldehyde 3-phosphate dehydrogenase

GFAP Glial fibrillary acidic protein

GAN Giant Axonal Neuropathy

HD Huntington's disease (HD),

HDL High-density lipoprotein

HEK293T Human embryonic kidney 293T cells

HEPN Higher eukaryotes and prokaryotes nucleotide-binding

HSP70 Heat shock protein 70

IF Intermediate filaments

IL-6 Interleukin-6

IL-6R Interleukin-6 receptor

kDa Kilodalton

KER Human Keratinocytes

LC-MS/MS Liquid chromatography tandem mass spectrometry

LDH Lactate dehydrogenase

LIF Leukemia inhibitory factor

MF Mossy fibres

MTT 3-(4,5-Dimethylthiazol-2-yl)-2,5-Diphenyltetrazolium Bromide

NMR Nuclear magnetic resonance

PBS Phosphate-buffered saline

PCs Purkinje cells

PD Parkinson's disease

polyQ Polyglutamine

ROS Reactive oxygen species

SCA Spinocerebellar ataxia type

SIRPT Sacsin internal repeat

SMAD1 Mothers against decapentaplegic homolog 1

SPAX8 Spastic ataxia 8

STAT3 Signal transducer and activator of transcription 3

SDS-PAGE Sodium Dodecyl Sulphate-Polyacrylamide Gel Electrophoresis

SEM Standard error

TBS-T Tris Buffered Saline with Tween 20

UPS Ubiquitin–proteasome system

UbL Ubiquitin-like

XPCB Xeroderma Pigmentosum group C Binding Protein

LIST OF FIGURES

LIST OF SUPPLEMENTARY FIGURES

LIST OF TABLES

1. INTRODUCTION

1. CEREBELLUM AND CEREBELLAR DYSFUNCTION

1.1. Cerebellum anatomy and morphology

The cerebellum is an anatomical structure of the central nervous system (CNS) present in all vertebrates, located close to the brainstem and under the cerebral cortex in the hindbrain (Roostaei et al., 2014)(Fig. 1A). It has been long known to play crucial roles in motor performance, gait coordination, posture maintenance, muscle tone control, and voluntary muscle activity. However, the cerebellum has recently been also linked to cognition, emotion, memory, attention, social behaviour, and communication (Baumann et al., 2015).

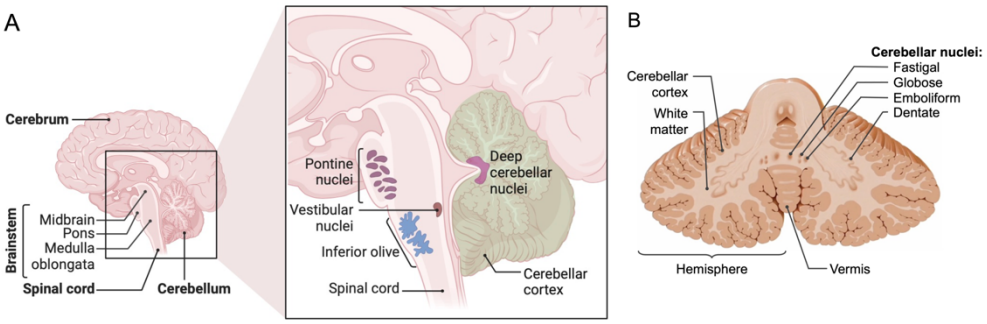

Figure 1: The cerebellum. (A) Mid-sagittal view shows the cerebellum, spinal cord and brainstem location and its structures related to the cerebellum. **(B)** Cross-section of the human cerebellum, showing the cerebellar nuclei and cross-section of the vermis. The figure was created with BioRender.

The cerebellum consists of a surface cortex of grey matter and a central core of white matter. Within the white matter, there are four deep cerebellar nuclei (DCN): dentate, globose, emboliform, and fastigial nuclei (Fig.1B). The DCN are the sole outputs of the cerebellum. The cerebellum receives inputs from other parts of the brain and nervous system, including the

cerebrum, brain stem, and spinal cord. First, these inputs arrive at the cerebellar cortex via two input pathways (the climbing and mossy fibres). Climbing fibres (CF) are derived entirely from inferior olive. Mossy fibres (MF) emerge from various brainstem nuclei and the spinal cord. Signals travel from the cerebellar cortex to the DCN output, sending axons to distant brain locations via the thalamus (Purves, 2004). The cerebellar cortex is densely packed with neurons, accounting for more than half of all neurons in the brain. It is organised into three distinct layers densely packed with neurons (granular cell layer (GCL), Purkinje cell layer (PCL), and molecular cell layer (MCL)) (Fig.2). According to their neurotransmitter profile, these neurons can be divided in GABAergic inhibitory neurons (Purkinje cells, Golgi cells, Lugaro cells, basket cells, stellate cells, and DCN interneurons) and glutamatergic excitatory neurons (granule cells, unipolar brush cells, and glutamatergic neurons of DCN). The proportion between glial cells and neurons in the cerebellum (1:21) is inverse to the proportion found in the rest of the brain (5:1), having less glia. However, these glial cells (Bergmann glia, Velate astrocytes, Fañanas cells and microglia) are very relevant for cerebellar biology and function (Amore et al., 2021; Hoshino, 2016; Peng et al., 2019; Van Essen et al., 2018; Von Bartheld et al., 2016).

1.1.1. Cellular composition of canonical cerebellar circuits

Purkinje cells (PCs) are the first neurons to form in the cerebellar cortex during early brain development and are considered the central regulators of cerebellar development(Apsley & Becker, 2022). The human brain has 15 million PCs, the CNS's largest and most complex neurons. They are highly specialized cells with a big pear-shaped cell body, extensive treelike branching dendrites, and a single long myelinated axon that generally bifurcates in the GCL and returns to the PCL and, sometimes, to the MCL. All PCs are aligned parallel with the cell body in the PCL, the dendritic tree

spreading in the MCL, and the axon extending along the GCL until the DCN (D'Angelo et al., 2013; Paul & Limaiem, 2021). They receive two unique excitatory inputs from PFs and CFs, and their axons provide the ultimate cortical output transmitted to the DCN. PCs are critical neurons in cerebellar circuitry as they relay information from varied inputs (Sotelo, 2015).

The cerebellum receives information via mossy and climbing fibers, which connect directly with granule cells. Activation of mossy fibers leads to the excitation of granule cells, subsequently exciting Purkinje cells and inhibiting the deep nuclei. Conversely, climbing fiber activation inhibits Purkinje cells and excites stellate cells, basket cells, and Golgi cells, causing lateral inhibition of Purkinje cells adjacent to the central excitation zone (Marzban et al., 2015).

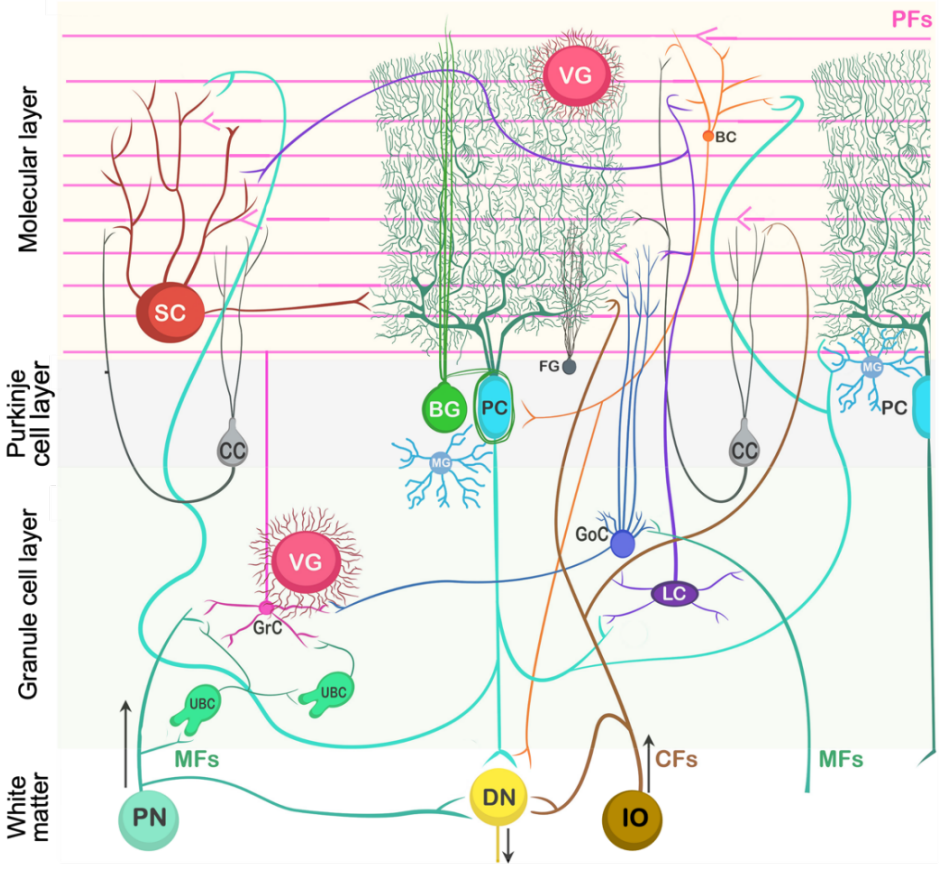

Figure 2: Cerebellar cytoarchitecture. The cerebellar cortex organization comprise three layers. The Granule cell layer contains excitatory granule cells surrounded by inhibitory interneurons such as Golgi and Lugaro cells, excitatory unipolar brush cells and velate astrocytes. The Purkinje cell layer comprises the cell bodies of Purkinje cells and Bergmann glia, and their dendrites and fibres span the entire Molecular layer. Granule cells' parallel fibres directly synapse onto Purkinje cell's dendrites and have contact points with molecular layer interneurons (Basket and Stellate cells). Cerebellar glial cells, including Bergmann, Velate, and Fañanas, help maintain homeostasis by regulating and recycling some neurotransmitters. Bergmann glia processes and microglia are closely connected with the whole dendritic tree and soma of Purkinje cells. The cerebellar cortex receives two distinct inputs (mossy fibres and climbing fibres) and provides a single output (deep cerebellar nuclei). PN – Pontine nuclei, DN - deep cerebellar nuclei, IO – Inferior olive, MFs - mossy fibers, CFs - climbing fibers, UBC - unipolar brush cell, GrC - granular cell, LC - Lugaro cell, GoC - Golgi cell,, CC - cell of candelabrum, PC - Purkinje cell, SC - stellate cell, BC - Basket cell, VG - Velate glia, BG - Bergmann glia, FG - Fañanas glia, MG – microglia, PFs - parallel fibers. Adapted from (Lara-Aparicio et al., 2022).

Golgi cells also receive inputs from parallel and mossy fibres, delivering inhibitory feedback to granule cells (Masoli et al., 2020). Brush cells receive afferent signals from mossy fibres and establish excitatory synapses with granule cell dendrites, other brush cells, and mossy fibres. Lugaro cells form connections with basket, stellate, and Golgi cells, being densely innervated by Purkinje cells. Candelabrum cells reside in the Purkinje layer, are excited by MFs and GCs and are inhibited by PCs. Additionally, they inhibit molecular layer interneurons, which causes PC disinhibition (Schilling et al., 2008).

Granule cells are the most prevalent cell type in the central nervous system. They have small, round soma with three to five short dendrites, and their axon extends upward to the molecular layer, where they split into a T-shaped structure called parallel fibres that activate PCs (Consalez et al., 2021; D'angelo, 2013). This process is regulated by the indirect activation of

stellate and basket cells through parallel fibres, allowing both cell types to inhibit Purkinje cells. Similarly, PCs inhibit deep nuclei and send recurrent axonal collaterals to neighbour cells, including stellate and basket cells, thereby exerting a similar inhibitory effect (Schilling et al., 2008). Therefore, PCs play a crucial role in the cerebellum, and their capacity to process and transmit signals is essential for the normal functioning of cerebellar activities. Thus, their optimal function is crucial to the cerebellum's overall function. PCs have considerable resistance to injury and special regenerative abilities in the CNS. Its response to cell injury differs from other neurons and involves regenerative, compensatory, and degenerative mechanisms (Kemp et al., 2016). Although PCs have a uniform appearance, they show great diversity in molecular phenotypes, physiological features, afferent and efferent connections, and susceptibility to injuries. The heterogeneity in the PCs population also occurs in the different cerebellar zones (Apsley & Becker, 2022; Magnus et al., 2023). For example, the anterior cerebellum has higher sensitivity and cell death, considering observations in mouse models, patients with ARSACS and Niemann-Pick type C disease (Ady et al., 2018; Fiorenza et al., 2022). The clinical manifestation of PCs loss is a progressive accumulation of dysfunction that might culminate in cerebellar ataxia (De Munter et al., 2016).

1.1.2. Cerebellar glial cells

There are approximately 16 billion glia to 69 billion neurons in the cerebellum (Von Bartheld et al., 2016). Glial cell organization reflects the three-layered structure of the cerebellar cortex's neuronal population. Astrocytes are a heterogeneous population of cerebellar glia, comprising four main distinct categories according to their morphology, layering, marker expression, and functions: fibrous astrocytes, velate astrocytes, Bergmann's

glia (BG), and Fañanas cells (a type of Bergmann's glia) (Stowell et al., 2018).

Fibrous astrocytes are found in white matter regions and are distributed in rows between axonal bundles. In the granule cell layer, velate astrocytes support granule cells and mossy fibre glomeruli. They control the flow of information towards the molecular layer through local interactions with neuronal synapses (Cerrato, 2020). BG are the predominant astroglia in the cerebellum, surpassing PCs by about eightfold. These astrocytes have polarized cell bodies in the PCL and extend long processes to reach the pial surface, where they enwrap Purkinje cells' dendrites and synapses within the MCL (De Zeeuw & Hoogland, 2015). BG play a critical role in neuroprotection, synaptic stability, and plasticity (Cerrato, 2020). Astrocytes are now being linked to various neurodevelopmental and neurodegenerative conditions, including Rett syndrome, fragile X syndrome, amyotrophic lateral sclerosis (ALS), Alzheimer’s disease (AD) and Alexander’s disease (AxD). Additional evidence supporting the involvement of cerebellar astroglia in neurodegenerative diseases can be found in ataxias such as SCA7 and SCA1 (Borgenheimer et al., 2022; M. Huang & Verbeek, 2018).

Microglia, the innate immune cells in the CNS, differ in embryonic origin from neurons, astroglia, and oligodendroglia, as they do not originate from neural precursor cells (endoderm) but from hematopoietic cells (mesoderm) (Buffo & Rossi, 2013; Ginhoux et al., 2013). In the cerebellum, microglia have a unique distribution and morphology compared to those in the cortex. Cerebellar microglia are distributed sparsely and display less intricate branching structures, in contrast to cortical microglia. The cerebellum microglia have similar functions to those found elsewhere in the central nervous system. They are involved in immune responses and play a critical role during brain development by engulfing and removing synapses to fine-

tune network connectivity as the brain matures (Stowell et al., 2018). Microglial activation in the cerebellum has been documented during *post-mortem* examination in various forms of ataxias, as well as in multiple rodent models of ataxia such as SCA6, SCA21, FA and ataxia-telangiectasia (AT) (Ferro et al., 2019).

Oligodendrocytes form myelin, which is crucial for nerve impulse conduction. In the cerebellum, oligodendrocytes are responsible for the myelination of mossy, climbing fibres and Purkinje axons. Consequently, they are typically located in the white matter and lower GCL. During the early postnatal development of the brain, the localization and function of ionotropic glutamate receptors in Purkinje neurons is impacted by the ablation of oligodendrocytes (Hashimoto et al., 2016). Unlike other glial cells, mature oligodendrocytes lack intermediate filaments, which is a feature especially relevant for this thesis. However, oligodendrocyte progenitor cells express the intermediate filament protein nestin (Almazán et al., 2001). The absence of intermediate filaments in mature oligodendrocytes may be linked to the lack of sacsin expression in these cells.

1.2. Cerebellar dysfunction

A large variety of neurological disorders are characterized by degeneration and atrophy of the cerebellum. Recent evidence indicates that there is cerebellar atrophy in common neurodegenerative disorders such as AD, ALS, FA, Parkinson's disease (PD), Huntington's disease (HD), spinal muscular atrophy, juvenile Batten's disease, and multiple sclerosis (Iskusnykh et al., 2024). However, there is a large family of disorders involving neurodegeneration linked specifically to the cerebellum that leads to ataxia, a movement disorder marked by impaired coordination, loss of balance, and additional symptoms such as vertigo, visual impairment,

slurred speech, swallowing difficulties, clumsiness, untidy handwriting, limited fine motor skills and tremors (Roberts et al., 2022).

The onset of some types of ataxias can be early after birth and in this case, there are doubts about the classification of the disorder as either neurodevelopmental or neurodegenerative. This is the case of ARSACS, spastic ataxia 8 (SAPX8) and other recessive hereditary ataxias. In other cases, ataxias have an adult onset, following an age-dependent profile more similar to typical brain neurodegenerative disorders. For example, spinocerebellar ataxias 1 and 3 (Machado Joseph disease) (Fogel, 2012; Khemani, 2022).

Cerebellar dysfunction can cause or impact a variety of CNS pathologies, including neuropsychiatric disorders and neurological symptoms such as ataxia (i.e. impaired coordination of voluntary muscle movement) (Schmahmann, 2004). Cerebellar ataxias are a clinically diverse group of disorders that includes acquired, sporadic and hereditary ataxias (Table. 1). The acquired cerebellar ataxias are chronic diseases of the cerebellum that are due to exogenous or endogenous nongenetic causes. Sporadic ataxia is a nongenetic neurodegenerative cerebellar condition characterized by progressive ataxia. Hereditary ataxias are neurological disorders that involve cerebellar degeneration, resulting in ataxia, as well as additional symptoms from impairment to other parts of the central or peripheral nervous system. They are classified into four types based on inheritance: autosomal dominant, autosomal recessive, X-linked and mitochondrial (Beaudin et al., 2020; Pilotto et al., 2024).

Table 1: Types of ataxias.

Type	Mechanisms
Acquired	Vascular and structural lesions
	Infectious, parainfectious (acute cerebelitis, inflammatory or immune mediated)
	Substrate deficiency (vitamin B1, B12, E or A)
	Toxin or drug induced
Sporadic	Idiopathic late-onset cerebellar ataxia
	Multiple system atrophy
Genetic	Autosomal dominant spinocerebellar ataxia (SCA)
	Autosomal recessive cerebellar ataxia (ARCA)
	Episodic ataxia
	Mitochondrial ataxia
	X- linked ataxia

Autosomal dominant ataxias (or spinocerebellar ataxias [SCA]) are neurodegenerative disorders caused by gene mutations that affect the cerebellum and brainstem. Over 48 SCA subtypes are caused by microsatellite repeat expansions or point mutations in critical genes. X-linked cerebellar ataxias are conditions caused by gene mutations or genomic imbalances on the X chromosome that lead to defective cerebellar development. Mitochondrial ataxias result from mutations in mitochondrial DNA. No specific features define mitochondrial ataxia except the common co-occurrence of neurological and non-neurological signs.

Autosomal recessive cerebellar ataxias are frequently characterized by a cerebellar motor syndrome of gait ataxia, dysmetria, adiadochokinesia, nystagmus, and dysarthria associated with neurodegeneration of the cerebellum (Beaudin et al., 2019). The onset is usually during childhood or adolescence but can also be in adulthood, with the age of onset influencing the progression and clinical signs of the disease (Paulus-Andres & Burnett,

2021). Friedreich ataxia is the most frequent recessive ataxia, followed by the worldwide reported Autosomal recessive spastic ataxia of Charlevoix-Saguenay (ARSACS) (Pilotto & Saxena, 2018; Synofzik et al., 2013).

Table 2: Most prevalent primary autosomal recessive cerebellar ataxias. Adapted from (Beaudin et al., 2020)

OMIM	Nomenclature	Gene (Locus)	Protein	Protein function
229300	Friedrich Ataxia (FRDA)	FRDA (9Q13)	Frataxin	Mitochondrial iron metabolism
270550	ARSACS	SACS (13q11)	Sacsin	Chaperone-mediated protein folding
208900	Ataxia telangiectasia (AT)	ATM (11q22.3)	Ataxia telangiectasia mutated	DNA double-strand break repair
208920	Ataxia with oculomotor apraxia type 1 (AOA1)	APTX (9p13)	Aprataxin	DNA single strand break repair
606002	Ataxia with oculomotor apraxia type 2 (AOA2)	SETX (9q34)	Senataxin	DNA and RNA repair
607459	Sensory ataxic neuropathy, dysarthria, and ophthalmoparesis (SANDO)	POLG(15q26.1)	DNA polymerase-gamma	Mitochondrial DNA maintenance
610743	Autosomal recessive spinocerebellar ataxia-8 (ARCA1/ SCAR8)	SYNE1 (6q25.2)	Nesprin-1	Nuclear–cytoskeletal connections
607259	Spastic paraplegia 7 (SPG7)	SPG7 (16q24.3)	Paraplegin	mitochondrial metalloprotease protein
612016	Autosomal recessive spinocerebellar ataxia-9 (ARCA2/ SCAR9)	ADCK3 (1q42.2)	ADCK3 (Mitochondrial protein)	Coenzyme Q10 biosynthesis
613728	Autosomal recessive spinocerebellar ataxia-10 (ARCA3/ SCAR10)	ANO10 (3p22.1)	Anoctamin 10	Endoplasmic Reticulum-resident calcium-regulated lipid scramblase
277460	Ataxia with vitamin E deficiency (AVED)	TTPA (8q12.3)	α-tocopherol transfer protein	α-tocopherol incorporation in VLDL
213700	Cerebrotendinous xanthomatosis (CTX)	CYP27A1 (2q33-ter)	Sterol 27-hydroxylase	Bile acid synthesis
248800	Marinesco-Sjögren syndrome (MSS)	SIL1 (5q31)	BiP associated protein	Stabilization and folding of newly synthesized polypeptides
271245	Infantile onset spinocerebellar ataxia (IOSCA)	C10orf2 (10q24)	Twinkle	Mitochondrial DNA repair and maintenance

The exact molecular pathways that govern the majority of cerebellar ataxias are still unidentified. However, they often display similar cellular and molecular hallmarks as neurodegenerative disorders affecting the brain.

This involves problems in gene expression, such as DNA repair defects and abnormal transcription, as well as protein-level issues like dysfunctional proteostasis, leading to protein misfolding and accumulation, oxidative stress, endoplasmic reticulum (ER) stress, autophagic impairment resulting in cell death (Manto & Marmolino, 2009; Smeets & Verbeek, 2014; Synofzik et al., 2019).

1.3. Autosomal recessive spastic ataxia of Charlevoix-Saguenay (ARSACS)

ARSACS (OMIM: #270550) is an inherited neurodegenerative disorder initially described in 1978 among the descendants of a small group of French immigrants from the 17th century, who settled in the Charlevoix-Saguenay-Lac-Saint-Jean region of North-Eastern Québec in Canada (Bouchard et al., 1998; Bouchard JP, Barbeau A, Bouchard R, 1978). However, ARSACS patients have been reported in all continents since then (Bagaria et al., 2022; Bchetnia et al., 2021; Pimenta et al., 2017; Silva et al., 2024; Vermeer, van de Warrenburg, & Kamsteeg, 1993). ARSACS worldwide incidence and prevalence remain unknown, but the carrier rate was estimated at 1 in 22 inhabitants in the Saguenay-Lac-St-Jean region (Quebec, Canada), and the estimated incidence at birth is 1 in 1,932 people. This incidence is now decreasing due to voluntary carrier screening (Vermeer, van de Warrenburg, & Kamsteeg, 1993). The onset of ARSACS usually occurs in early childhood: During gait initiation (around 12–18 months of age), toddlers present an unsteady gait with a tendency to fall (Bouchard et al., 1998). However, the onset of the disease can also occur later during adolescence or early adulthood (Baets et al., 2010).

1.3.1. ARSACS clinical features

ARSACS is clinically characterized by a typical triad of cerebellar ataxia, lower limb spasticity and peripheral neuropathy (Bouchard JP, Barbeau A, Bouchard R, 1978). However, not all characteristics of the triad may be present in patients, and there is also phenotypic overlap with other diseases, such as Charcot-Marie-Tooth disease (CMT), which makes diagnosis challenging and can lead to misdiagnosis. However, recently, a new approach to diagnosing ARSACS in patient blood samples based on the biochemical evaluation of sacsin protein reduction was presented (De Ritis et al., 2024). The variability in the phenotypic presentation of ARSACS has increased as the number of cases diagnosed outside of the Quebec region has risen, probably due to both genetic and environmental factors. The high phenotypic variability outside Canada demonstrates that cerebellar ataxia, spasticity and peripheral neuropathy cannot be considered mandatory symptoms of ARSACS (Synofzik et al., 2013). Early symptoms can include limb and gait ataxia, followed by spasticity, especially in the lower limbs. Children also develop speech problems due to spasticity and ataxia: speech is frequently slurred during childhood and becomes explosive in adulthood. Dysphagia, nystagmus and abnormal saccadic movements in ocular pursuit frequently complement the cerebellar signs (Bouchard JP, Barbeau A, Bouchard R, 1978; Duquette et al., 2013; Takiyama, 2007; Vogel et al., 2018). Early symptoms include bilateral abnormal plantar response and increased deep tendon reflexes, which may diminish or disappear by adulthood due to progressive neuropathy (Bouchard JP, Barbeau A, Bouchard R, 1978). Peripheral neuropathy usually appears later in life and is characterized by the absence of the Achilles tendon reflex, profound sensory disturbances (e.g. impaired vibration sense) and progressive distal amyotrophy. Early spasticity combined with progressive neuropathy frequently results in skeletal deformities of the foot, including *pes cavus*

(Bouchard JP, Barbeau A, Bouchard R, 1978; De Braekeleer et al., 1993; Heyer, 1995; Tzoulis et al., 2013). Hand deformity has been reported, with dystonia occasionally causing abnormal posturing of the hands and neck (De Braekeleer et al., 1993; Heyer, 1995; Tzoulis et al., 2013). Less common manifestations of ARSACS are intellectual disability, epileptic seizures, hearing loss, mitral valve prolapse, and bowel and bladder dysfunction (Bouchard JP, Barbeau A, Bouchard R, 1978; De Braekeleer et al., 1993; Prodi et al., 2013; Stevens et al., 2013; Synofzik et al., 2013; Takiyama, 2006; Vermeer et al., 2008). The disease progresses slower than other types of ataxias, and the symptoms can remain stable for a long time. However, ARSACS can advance swiftly in early adulthood, and patients may lose their ability to walk by the time they are 40 years old, with a life expectancy of about sixty years (Bouchard et al., 1998; Dupré et al., 2006).

1.3.2. ARSACS histopathological features

ARSACS causes distinct retinal anomalies, such as hypermyelination of retinal nerve fibres or thickening of peripapillar retinal fibres, pointing to retinal hyperplasia caused by abnormal retinal development (Bouchard JP, Barbeau A, Bouchard R, 1978; Garcia-Martin et al., 2013; Rezende Filho et al., 2021). Patients may also exhibit biochemical issues such as impaired pyruvate oxidation, hyperbilirubinemia, and low serum levels of beta- or HDL lipoproteins (Bouchard JP, Barbeau A, Bouchard R, 1978). ARSACS patients' nerve biopsies show a significant reduction in large myelinated fibres, axonal degeneration with axoplasmic condensation, increased collagen pockets, and mitochondrial and vesicular body accumulation. These findings are indicative of axonal neuropathy associated with demyelination. Axonal regeneration and myelin sheath thinning with rare onion bulbs can sometimes be observed (El Euch-Fayache et al., 2003; Peyronnard et al., 1979; Takiyama, 2006). Muscle biopsies are consistent

with neurogenic atrophy (Parkinson et al., 2014). *Post-mortem* examinations were performed on two ARSACS patients, one a young adult (21 years old) and the other a middle-aged patient (59 years old). Atrophy of the superior cerebellar vermis, notably in the anterior structures, was observed in the young patient. Purkinje cell loss and thinned molecular and granular cell layers were observed in this cerebellum region. Demyelination was found in the lateral and anterior corticospinal tracts, posterior spinocerebellar tracts, and pyramidal tract, but it was more pronounced in the lateral corticospinal tracts. Similar features were observed in the older patient, albeit to a greater extent. Swollen thalamic and cerebellar cortical neurons were identified, and most of these neurons had dense lipofuscin-like granules within the lysosomes, indicative of ageing or sick cells (Bouchard et al., 1998). Notably, a patient with ARSACS had lipofuscin deposits in a skin biopsy, suggesting that the pathology could be systemic, and not only cerebellar (Stevens et al., 2013).

1.3.3. ARSACS molecular genetics

Loss-of-function mutations in the *SACS* gene (OMIM: 604490), discovered in the 2000s, are responsible for ARSACS (Engert et al., 2000). The *SACS* gene is located on the long arm of chromosome 13 (13q12.12: chr13:23,288,689-23,433,763, GRCh38/hg38) and has ten exons. The first exon is a non-coding component, while the 10th exon, which has 11,487 base pairs, is the longest in vertebrates (Parfitt et al., 2009; Takiyama, 2006). The *SACS* gene encodes sacsin (Q9NZJ4 SACS_HUMAN), one of the biggest proteins in the human genome, with 4,579 amino acids and a molecular weight of about 520 kDa (Parfitt et al., 2009). This extremely large size makes it very difficult to study and manipulate the gene and the protein.

Over 200 mutations associated with ARSACS have been identified globally, most located in exon 10. There are registers of missense,

nonsense, and frameshift variants (Fig.3) (Romano, et al., 2013). Regardless of the nature or position of the mutation, sacsin is practically absent in ARSACS patients. Additionally, evidence indicates nonsense-mediated mRNA decay in some frameshift and nonsense mutations and co-translational folding and degradation in some missense mutations (Longo et al., 2021). Many of the mutations originate truncated forms of the protein, and sacsin is either absent or expressed at low levels. These observations support the idea that sacsin loss-of-function is the molecular mechanism of ARSACS (Baets et al., 2010; Bouhlal et al., 2011; Romano, Tessa, Barca, Fattori, Fulvia de Leva, et al., 2013; Synofzik et al., 2013). Sacsin knockout animal models further support this idea.

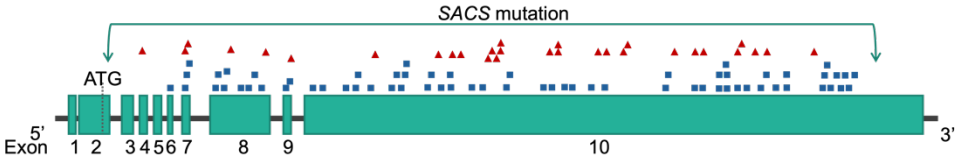

Figure 3: *SACS* mutations in various exons. Graphical representation of *SACS* mutations associated with ARSACS. ■ missense mutations; ▲ insertions/duplications/deletions. Adapted from (Aly et al., 2022).

1.3.4. Sacsin

Sacsin is a protein conserved among vertebrates, including mammals, birds, reptiles, and fish (A. Romano, Tessa, Barca, Fattori, de Leva, et al., 2013). Several different tissues express sacsin, including the immune system (blood, white blood cells, spleen, and lymph nodes); the nervous system (brain, cortex, cerebellum, spinal cord, and tibial nerve); muscle (heart, artery, and skeletal muscle); the digestive and excretion systems (small intestine, colon, adipocyte, kidney, liver, stomach, oesophagus, and bladder); several glands (pancreas, thyroid, salivary gland, adrenal gland, pituitary, breast); the skin; and the reproductive system (ovary, uterus,

prostate, and testis) (GeneCards – The Human Gene Database, SACS Gene, GCID: GC13M023288). Protein expression in normal tissues and cell lines correlates well with mRNA levels in most of these tissues, particularly the immune and nervous systems (GeneCards – The Human Gene Database, SACS Gene, GCID: GC13M023288). However, sacsin expression is especially higher in the central nervous system. In the brain, sacsin expression is highest in the motor system, including the cerebellum, granular system, and Purkinje cells (Parfitt et al., 2009). In cells, sacsin localises in the cytoplasm and mitochondria of cells, but it is also found at lower levels in the nucleus, plasma membrane, peroxisomes, endoplasmic reticulum (ER), endosomes, and lysosomes, as well as in the extracellular medium (GeneCards – The Human Gene Database, SACS Gene, GCID: GC13M023288; Parfitt et al., 2009).

1.3.5. Sacsin domains

According to *in silico* analysis, based on sequence homologies with other proteins, sacsin has multiple functional domains. These domains include a ubiquitin-like (UbL) domain at the N-terminus, three sacsin internal repeats (SIRPT1, SIRPT2, SIRPT3), a xeroderma pigmentosum group C binding domain (XPCB), a J-domain, and a higher eukaryotes and prokaryotes nucleotide-binding (HEPN) domain (Fig.4).

According to the atomic structure analysis, sacsin's UbL domain has the β-grasp fold typical of ubiquitin-like domains. However, the surface composition is different: it is less hydrophobic and has a less pronounced positive charge than ubiquitin (Ménade et al., 2018). Co-immunoprecipitation experiments showed that the N-terminal region of sacsin (residues 1-124) including the UbL domain interacts with a subunit of the 20S proteasomal alpha subunit C8, linking sacsin to protein quality control function (Parfitt et al., 2009).

The three SIRPT domains have high homology in domain organization and account for more than 80% of the human sacsin protein. Each SIRPT contains three sub-repeats: sr1, sr2, and sr3. SIRPT1 and SIRPT3 also have the srX sub-repeat. Part of sr1 shares sequence homology with the Histidine kinase-like ATPase (HATPase)_c domain of heat shock protein 90 (HSP90) (A. Romano, Tessa, Barca, Fattori, de Leva, et al., 2013). The SIRPT1 sr1 structure has a Bergerat protein fold with a nucleotide-binding pocket, characteristic of nucleotide-binding domains (NBD) involved in ATPase activity, particularly in the Hsp90 family proteins. While sacsin binds nucleotides with very low affinity (Ménade et al., 2018), there is experimental evidence supporting SIRPTs ATPase and chaperone-like activities (Anderson et al., 2010, 2011).

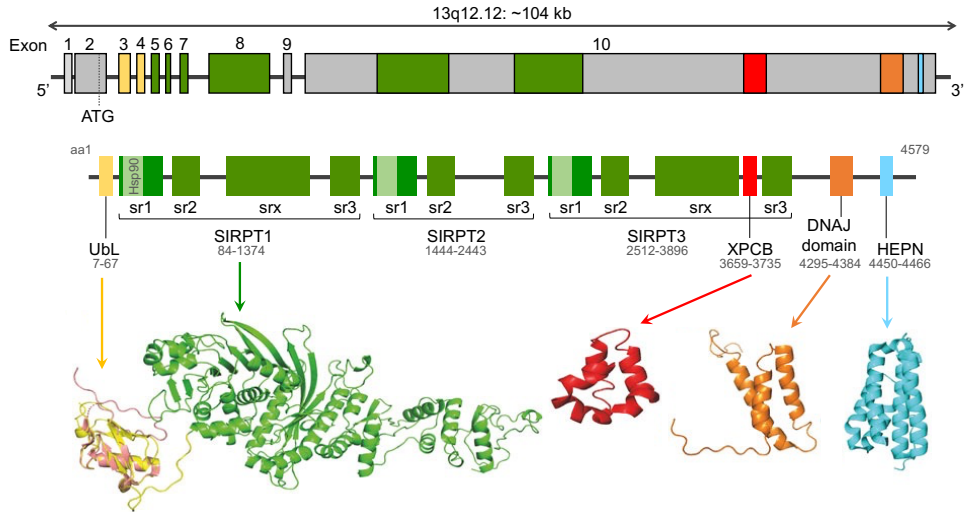

Figure 4: Schematic representation of sacsin domain structure. Schematic representation of the sacsin protein, indicating regions with homology to functional domains found in other proteins. The numbers shown correspond to the amino acid positions of each domain. The figure includes the respective structural motifs. Adapted from (Longo et al., 2021; Perna et al., 2023)

The Sr1 and Hsp90 proteins share a higher similarity in the nucleotide-binding site of the NBD. The three sr1 domains in sacsin conserve many of the residues involved in ATP binding and hydrolysis in Hsp90 proteins. Sr1

domains have a high frequency of ARSACS-causing missense mutations, highlighting their function's significance (Ménade et al., 2018).

A xeroderma pigmentosum group C binding domain (XPCB) upstream of SIRPT3 has 35% similarity to the XPCB domain of hHR23A/B, the human homologs of yeast protein Rad23 (Kamionka & Feigon, 2004). Rad23 is a protein involved in the nucleotide excision repair pathway. Sacsin´s XPCB domain is a potential substrate for the E3 ubiquitin ligase UBE3A (an interactor of Rad23). *Ube3A* knockout mice had significantly lower levels of ubiquitinated sacsin, indicating a possible role of Ube3A via XPCB binding in sacsin ubiquitination (Greer et al., 2010; Jana, 2012). According to this data, it is possible that Angelman Syndrome (AS), a rare early-onset neurodevelopmental disorder that occurs due to UBE3A loss of function mutations, could be caused by impaired Ube3A-mediated ubiquitination of sacsin. AS is characterized by cerebellar atrophy, with loss of Purkinje cells and ataxia, similar to ARSACS. Bioinformatic analysis suggests that sacsin has two ubiquitin-interaction motifs (UIM) on either side of the XPCB domain, which interact directly with ubiquitin (Duncan et al., 2015). The UbL domain, XPCB domain, and potential UIM motifs suggest that sacsin could participate in ubiquitin-mediated degradation pathways (Duncan et al., 2015).

The C-terminal J-domain shares 60% homology with Hsp40 and includes the highly conserved His-Pro-Asp (HPD) motif required to stimulate HSP70 ATPase activity (Engert et al., 2000; Parfitt et al., 2009). Sacsin's J-domain is functional as shown in an *in vivo* bacterial complementation assay. The sacsin J-domain was able to replace the lack of chromosomally expressed J-domain and CbpA in *E. coli* OD259, allowing growth at 37°C (Parfitt et al., 2009). Recombinant J-domain from mouse sacsin enhanced HSP70's ATPase activity (Anderson et al., 2010). These analyses demonstrating the

functionality of the J-domain, and its structure determined by nuclear magnetic resonance (NMR) spectroscopy (available as Protein Data Bank (PDB) code 1IUR) strongly suggest that sacsin is a type III HSP40 protein.

The higher eukaryotes and prokaryotes nucleotide-binding (HEPN) domain is a 110-residue region at the C-terminus of sacsin. In humans, the HEPN domain is found only in sacsin (Grynberg et al., 2003). Isothermal titration calorimetry (ITC) and NMR spectroscopy revealed that the HEPN domain binds with low-micromolar affinity to nucleotides, including ATP, ADP and GTP, but lacks GTPase and ATPase activity (Kozlov et al., 2011). A fluorescence polarization (FP) assay confirmed that HEPN binds to nucleotides and nucleotide analogues, with preference for nucleotides with more phosphate groups, implying that the binding is due to electrostatic interactions (X. Li et al., 2015). In addition, a high-resolution crystal structure of the human HEPN domain indicated that it forms a stable dimer that it could mediate sacsin dimerization. The proximity of the J-domain and the HEPN domain may be crucial for sacsin's proposed function as a co-chaperone. The HEPN domain may promote nucleotide exchange onto HSP70 by increasing the local concentration of GTP or ATP, for example (Kozlov et al., 2011). Furthermore, HEPN may stabilise the interaction between the J-domain, ATP, and Hsp70 (Grynberg et al., 2003). The HEPN domain could also support sacsin's chaperone activity by binding to mRNA or tRNA in the cell and mediating their degradation (Anantharaman et al., 2013).

1.3.6. Sacsin knockout models

Sacsin's domain architecture associates it with the ubiquitin-proteasome system and molecular chaperones, indicating that it might participate in protein quality control mechanisms. However, its exact role still needs clarification despite evidence pointing to its contribution to these mechanisms. Research involving sacsin deletion has led to the development

of various cellular and animal models. These models have unveiled a complex phenotype, impacting multiple cellular mechanisms, including mitochondrial function and cytoskeletal organisation.

Sacsin knockout mice display the three main features of ARSACS: cerebellar ataxia with the loss of PCs, axonopathy of upper motor neurons, and peripheral neuropathy. These mice also show a progressive degeneration of PCs, mirroring the clinical phenotype seen in ARSACS patients (Girard et al., 2012; Prodi et al., 2013). Similarly, the zebrafish model exhibits the main characteristics of ARSACS, including motor impairments, hindbrain atrophy, mitochondrial dysfunction, and accumulation of reactive oxygen species (Naef et al., 2021).

Sacsin deficiency disrupts the cytoskeletal network within neuronal cells, significantly affecting the organisation of intermediate filaments, particularly neurofilaments. Induced pluripotent stem cells derived from motor neurones and Purkinje cells of ARSACS patients display reduced sacsin levels and exhibit the formation of neurofilament aggregates (Louit et al., 2023). In human dermal fibroblasts from ARSACS patients, vimentin accumulation was seen in the perinuclear region, and it was observable even in patients with low sacsin levels. This phenotype can be reproduced by knocking out sacsin in fibroblasts and human cell lines, such as HEK293 and SHSY5Y. Remarkably, reintroducing sacsin into these cells restores their normal phenotype (Duncan et al., 2017). In $SW13^{Vim-/-}$ cells lacking endogenous vimentin, co-expression of plasmids encoding the J-domain and UbL domains with NFL and NFH prevented the formation of NF networks. Among Sacs-/- neurones, the UbL, SIRPT1, and J-domain consistently showed the highest efficacy in resolving vimentin and neurofilament bundles. Notably, the expression of both SIRPT1 or J-domain reduced the proportion of ARSACS fibroblasts that exhibited juxtanuclear intermediate filament

bundles. These findings indicate that sacsin is essential for the organisation and dynamics of intermediate filaments (Gentil et al., 2018).

When sacsin was knocked out in SH-SY5Y human neuroblastoma cells, there was no formation of aggresome-like inclusions. In ARSACS fibroblasts, HSP70 and ubiquitin were redistributed to areas where vimentin was accumulating, yet there was no increase in the expression levels of HSPA8 or HSPA1. These observations indicate that in the absence of sacsin, the ubiquitin-proteasome system remains intact while proteostasis-related proteins are relocated. Notably, the absence of protein amyloid structures in these conditions suggests that sacsin may not be directly involved in forming these structures. In Sacs-/- motor neurons, the upregulation of molecular chaperones like HSPA1A partially compensates for the loss of sacsin in neurofilaments organisation. Additionally, transcriptomic analysis of Sacs-/- cells showed enrichment of differentially expressed genes associated with protein folding, autophagy and programmed cell death (Morani et al., 2019).

In the transcriptomic analysis of sacsin knockout cells, notable changes were observed in genes associated with mitochondrial organisation, cellular respiration, and oxidative phosphorylation (Morani et al., 2019). Neurones from sacsin knockout mice showed an increased vulnerability to stress, accompanied by decreased mitochondrial transport into dendrites (Larivière et al., 2015). SH-SY5Y$^{Sacs-/-}$ cells showed reduced mitochondrial membrane potential (Δψm) and increased reactive oxygen species (ROS) levels, indicating impaired mitochondrial function (Morani et al., 2019). In fibroblasts from ARSACS patients, mitochondria were displaced to the periphery of vimentin aggregates, suggesting that sacsin plays a crucial role in maintaining mitochondria's normal distribution and function. Interestingly, transient siRNA-mediated sacsin knockdown did not seem to influence

mitochondrial dynamics in wildtype human fibroblasts, indicating that a short-term or partial reduction in sacsin levels may not sufficiently mimic the mitochondrial alterations characteristic of ARSACS (Duncan et al., 2017). On a positive note, recent research has shown that chronic treatment with the mitochondrial-targeted antioxidant ubiquinone MitoQ can improve motor coordination by increasing the mitochondrial activity of cerebellar Purkinje cells and reducing cell death in these neurons (Márquez et al., 2023).

In ARSACS fibroblasts, researchers observed elevated levels of LAMP2 (lysosomal-associated membrane protein 2) and decreased levels of protein 62 (a ubiquitin-binding autophagic adaptor). These essential autophagy proteins were redistributed to areas where vimentin accumulated (Duncan et al., 2017). Additionally, SH-SY5Y$^{Sacs-/-}$ cells showed decreased autophagosome accumulation and disrupted autophagosome-lysosome fusion, suggesting that sacsin is involved in autophagy regulation. In the zebrafish model of ARSACS, there was an increase in LC3 levels accompanied by a decrease in p62 levels, further corroborating autophagy dysfunction (Naef et al., 2021). On the other hand, the autophagic flux was elevated in ARSACS fibroblasts subjected to starvation and in SH-SY5Y$^{Sacs-/-}$ cells treated with rapamycin (Duncan et al., 2017; Morani et al., 2019). Another study revealed that mTOR-dependent autophagy, induced by the mitochondrial uncoupler carbonyl cyanide-p-trifluoromethoxyphenylhydrazone (FCCP), is compromised in Sacs-/- cells (Morani et al., 2019, 2022). Although the lysosomal distribution in motor neurons from Sacs-/- mice remained unchanged, they did exhibit reduced motility. These findings suggest that sacsin is key in lysosomal positioning and trafficking (Francis et al., 2022).

The sacsin loss also affects other organelles and proteins linked to the cytoskeleton. Notably, the Golgi apparatus becomes fragmented, with its

cisternae scattered throughout the cytoplasm in areas devoid of mitochondria (Duncan et al., 2017). Additionally, the endoplasmic reticulum (ER) distribution in the dendrites of sacsin knockout primary Purkinje cells changes closely, corresponding with the mitochondria. This alteration and significant downregulation of crucial Ca^{2+} buffer proteins lead to a pathological increase in Ca^{2+}-induced responses (Bondio et al., 2023). Ceftriaxone, a drug that reduces glutamatergic stimulation and Ca^{2+} influx in neurones, improves motor symptoms and prevents PCs degeneration in the Sacs-/- mouse model. This beneficial effect is likely achieved through restoring Ca^{2+} homeostasis in PCs and reduced neuroinflammation in the cerebellum (Bondio et al., 2023).

Sacsin also participate in microtubule-dependent trafficking and dynamics. Its absence in fibroblasts from patients with ARSACS and in SH-SY5Y cells disrupts microtubule dynamics and the phosphorylation of the microtubule-associated protein TAU. Additionally, sacsin interacts with JIP3, an adapter for microtubule-motors, and binds to microtubules (Francis et al., 2022; L. E. L. Romano et al., 2022). Interestingly, plectin, a cytolinker protein that connects intermediate filaments to various cellular components, has been identified as an interactor of sacsin. Plectin accumulation was observed in the cerebellar insoluble fractions of Sacs-/- mice, with an increased plectin signal in the somatodendritic regions of Sacs-/- Purkinje cells, coinciding with the presence of neurofilament bundles (Bondio et al., 2023).

The expression of various proteins on the cell surface, including those necessary for focal adhesion formation, is altered in Sacs-/- cellular models. These findings suggest that the absence of sacsin dislocates some integrins and synaptic proteins, likely leading to the impairment of Purkinje cell synapses in the brains of Sacs-/- mice. Evidence also indicates that sacsin

interacts with intermediate filaments and focal adhesion proteins and is essential for the interaction between vimentin and vinculin (L. E. L. Romano et al., 2022). All these observations suggest that sacsin may be a cytoskeletal cytolinker or scaffold required for assembling complexes.

1.4. General features of neurodegenerative disorders and their relation to ataxias

Neurodegenerative disorders have several common features that have been mostly studied in relatively frequent pathologies, such as Alzheimer´s and Parkinson´s diseases, but are only beginning to be understood in rarer ataxias (Fig.5).

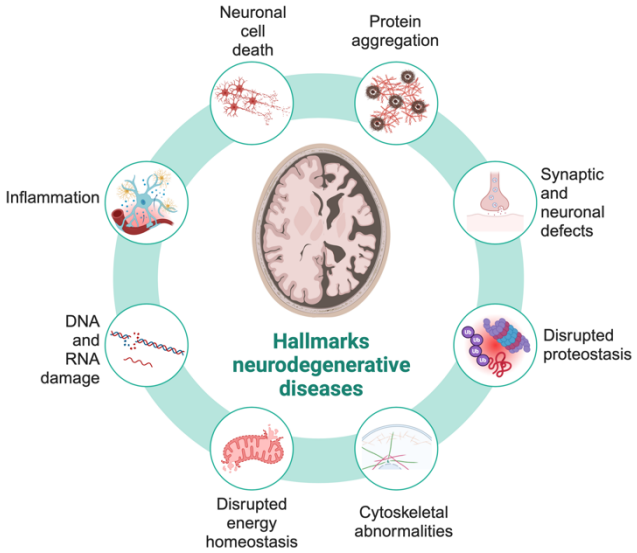

Figure 5: Hallmarks of neurodegenerative diseases. Adapted from (Wilson et al., 2023). The figure was created with BioRender.

1.4.1. Protein aggregation

Various studies have identified protein misfolding and aggregation as central pathological features in neurodegenerative conditions, including autosomal recessive cerebellar ataxias (ARCAs). Misfolded proteins lose their functional roles, forming harmful oligomers that aggregate into fibrils,

disrupting cellular homeostasis. Aggregation begins with nucleation, where improperly folded proteins form a core structure that recruits additional monomers, accumulating non-functional protein complexes. While cellular defence mechanisms, such as the ubiquitin-proteasome system and autophagy, work to degrade these aggregates, failure in these systems often results in cytotoxicity, inflammation, and eventually neuronal death (Bloomingdale et al., 2022; Koszła & Sołek, 2024; Ruffini et al., 2022; P. Sweeney et al., 2017).

Protein aggregation is a shared feature among ARCAs frequently linked to specific gene mutations. These mutations play an essential role in the development of the disease. For example, mutations in the *SYNE1* gene, responsible for autosomal recessive cerebellar ataxia type 1 (ARCA1), produce a truncated Syne-1 protein that disrupts neuronal integrity, leading to protein misfolding and aggregation (Klockgether & Paulson, 2011; Qian et al., 2022). Similarly, mutations in the *APTX* gene, associated with ataxia with oculomotor apraxia type 1 (AOA1), compromise DNA repair pathways, indirectly contributing to protein homeostasis failure and aggregation (Ababneh et al., 2020; Synofzik et al., 2019). Beyond these examples, loss-of-function variants in the *MTCL1* gene, essential for Purkinje cell maintenance, contribute to protein aggregation and neurodegeneration (Krygier et al., 2019).

The pathological consequences of protein aggregation are not restricted to specific genes but represent a broader phenomenon across multiple ARCA subtypes. In spinocerebellar ataxia type 3 (SCA3), expanded ataxin-3 proteins form insoluble aggregates, which appear in early disease stages and are thought to precede clinical symptoms (Robinson et al., 2021). Likewise, in ataxia-telangiectasia (AT), poly-ADP-ribosylation is implicated in protein misfolding, contributing to the aggregation process (Lee et al.,

2020; Synofzik et al., 2019). Even in Friedreich's ataxia and ARSACS, two of the most prevalent ARCAs, protein aggregation is a hallmark feature, underscoring its central role in disease progression (Salem et al., 2020). With over 100 genes implicated in ARCAs, the genetic landscape highlights significant heterogeneity, yet protein aggregation emerges as a unifying pathological process. Understanding the molecular link between genetic mutations, protein misfolding, and cellular stress responses is essential to mitigate the deleterious effects of protein aggregation in ARCAs.

1.4.2. Mitochondrial dysfunction

Mitochondria play a central role in whole-body energy homeostasis. Neurons are highly energy-consuming cells with a complex structure. The normal functionality of neurons relies on mitochondria's structure and functional integrity. In addition to their role as the primary energy suppliers, mitochondria also play crucial roles in regulating cellular activities, including calcium balance, oxidative stress management, metabolism of amino acids and lipids, and cell proliferation (X. Li et al., 2024). Mitochondrial dysfunction can cause disruptions in calcium balance, leading to increased levels of intracellular calcium and disturbed activities of calcium-dependent enzymes, release of lysosomal enzymes, and degradation of cytoskeletal proteins, lipids, and DNA (Baev et al., 2022). A decline in mitochondrial function and ATP production is also connected to reduced generation of the antioxidant glutathione, which may exacerbate the cell's oxidative environment (Marí et al., 2009). Mitochondrial dysfunction is a common pathogenic mechanism underlying neurodegeneration in various ARCAs (Beaudin et al., 2017; Salem et al., 2020). Different studies have revealed that various ARCAs exhibit significant alterations in mitochondrial dynamics, bioenergetics, and quality control mechanisms, highlighting the central role of mitochondrial homeostasis in cerebellar function and survival (Synofzik et al., 2019). In

Friedreich's ataxia (FA), frataxin deficiency disrupts iron-sulfur cluster formation, leading to compromised electron transport chain function, particularly affecting complexes I and II (Ocana-Santero et al., 2021). ARSACS, caused by mutations in the *SACS* gene, exhibits marked abnormalities in mitochondrial network organization and motility (Girard, Larivière, et al., 2012; Salem et al., 2020), while SCAR16 shows disrupted PINK1/Parkin-mediated mitophagy and altered membrane potential (Synofzik et al., 2019; Yoo & Chung, 2018). Ataxias associated with *SPG7* and *ADCK3* exhibit disrupted mitochondrial networks and compromised mitochondrial proteostasis (Salem et al., 2020). These mitochondrial alterations manifest through various cellular mechanisms, including disrupted fusion-fission balance, compromised mitochondrial trafficking, altered mitochondrial-ER contact sites, and impaired mitochondrial biogenesis (Synofzik et al., 2019).

1.4.3. Cytoskeletal abnormalities

Alterations in the three main components of the cytoskeleton (actin microfibers, tubulin microtubules and intermediate filaments) have been described in many neurodegenerative disorders. Intermediate filaments are a diverse set of proteins which, together with microfilaments (MFs), and microtubules (MTs), form the main fibrous components constituting the cytoskeleton. One key distinction between IFs and other filaments lies in their lack of polarization. IFs have the ability to grow in both directions, unlike MTs and MFs which grow from a negative pole (where monomers are removed) to a positive pole (where monomers are attached to the fibril). In comparison to actin filaments and microtubules, the protein composition of intermediate filaments differs significantly across various tissues, organs, and cell types both during development and in disease states. Intermediate filaments can be grouped into six main categories using similarities in amino

acid sequence, protein structure predictions, and assembly properties (Table. 3) (Brandt & Götz, 2023; Didonna & Opal, 2019; Sen et al., 2022).

All intermediate filaments have a common tripartite structure, which includes a highly conserved α-helical central domain (rod domain). The rod domain is flanked by an amino (N)-terminal head domain and a carboxy (C)-terminal tail domain (Fig. 6). It comprises four hydrophobic alpha-helical segments of conserved length (1A, 1B, 2A, and 2B) connected by three linkers (L1, L12, and L2). The initial and terminal parts of the rod domain are preserved in all intermediate filaments. Both preserved areas have an impact on dimer interactions, and mutations in these regions are deleterious to the organization and dynamics of intermediate filaments. On the other hand, the head and tail regions exhibit minimal secondary structure and show significant variations in length and sequence across various IF protein (Muñoz-Lasso et al., 2020).

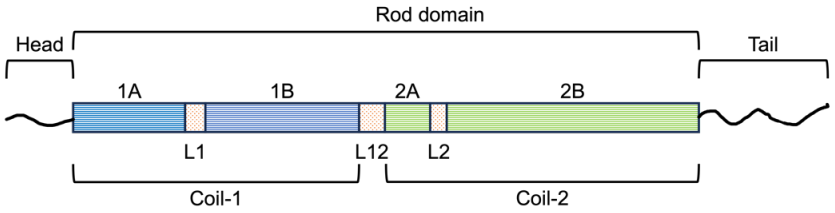

Figure 6: Schematic representation of IF protein structure. All IFs share a common tripartite structure with a conserved central rod domain flanked by a N-terminal head domain and a C-terminal tail domain.

Several established and emerging functions for IFs include cell-specific roles, such as the role of neurofilaments in axonal transport, as well as generalized functions like cytoprotection from various forms of stress. IFs can interact with cellular organelles by enclosing them in cage-like structures around the nucleus, thus influencing their shape, position, and mobility. They also serve as anchoring structures for mitochondria, positioning them near high-energy-demanding sites (Hohmann & Dehghani, 2019; Schwarz &

Leube, 2016). Additionally, considerable evidence supports a crucial role for IFs in protein targeting and synthesis, cell signalling, division and migration (Pradeau-Phélut & Etienne-Manneville, 2024; Schwarz & Leube, 2016). Mutations or changes in IF networks are implicated in over 80 human diseases, often presenting with distinct cytoplasmic inclusions (Table 3) (Lowery et al., 2015; Omary et al., 2004). Neuronal changes in the cytoskeleton can result in the inability to effectively transmit information and essential components, such as mitochondria for energy supply, between the cell body and synaptic endings (Yuan et al., 2017).

Cytoskeletal disruption is one of the pathogenic mechanisms underlying many forms of ARCA (Anheim et al., 2012; Beaudin et al., 2019). These cytoskeletal alterations manifest through various cellular pathways, affecting neuronal morphology, transport, and function (Synofzik et al., 2019). In ARSACS, mutations in the sacsin gene lead to abnormal neurofilament accumulation and disrupted intermediate filament organization, significantly affecting axonal transport (Y. Chen et al., 2022; Shimazaki & Takiyam, 2012). Friedreich's ataxia exhibits, abnormal distribution of phosphorylated neurofilaments (Sparaco et al., 2009). These cytoskeletal alterations manifest through various cellular mechanisms, including disrupted microtubule stability, compromised axonal transport, altered dendritic spine morphology, and impaired synaptic vesicle trafficking (Omary et al., 2004; Pérez-Sala & Quinlan, 2024; Sen et al., 2022). The widespread impact of cytoskeletal dysfunction on cellular processes has led to an increased focus on therapeutic strategies targeting cytoskeletal stability and function, including compounds to improve microtubule stability and enhance axonal transport (Cyske et al., 2023; Theunissen et al., 2021). Take into account this is evident the importance of cytoskeletal regulation as a potential

therapeutic target in the treatment of ARCAs, highlighting its significance in the development of effective treatments (Synofzik et al., 2019).

Table 3: Classification of Intermediate filaments, characteristic cell subsets, main function and associated pathologies. Adapted from (Bernal & Arranz, 2018).

Class	Proteins	Cell Subsets	Function	Example of diseases
I	Keratins (acidic)	Soft epithelia, hard epithelia	Structural integrity, mechanical resistance, adhesion, signal transduction, inflammation, proliferation, apoptosis, motility	Epidermolysis bullosa simplex, epidermolytic hyperkeratosis, monilethrix, keratodermas
II	Keratins (basic)	Soft epithelia,hard epithelia, inner root sheath		
III	Vimentin	Mesenchymal cells, developing neurons, astrocytes, endothelial cells, leukocytes	Structural maintenance, cell shape, motility, focal adhesion	Dominant cataracts
	GFAP	Neural stem cells, radial glia-like precursors, astrocytes, regenerative glia, mature glia in CNS and PNS	Structural maintenance, cell shape, motility	Alexander disease
	Desmin	Satellite stem cells, striated muscle, replicating myoblasts, fibroblastic reticular cells of lymphoid organs	Contraction	Desmin-related myopathy
	Peripherin	Mature neurons in PNS	Neurite elongation	Amyotrophic lateral sclerosis 1
	Syncoilin	Skeletal and cardiac muscle, nervous system	Structural maintenance	Desminopathy; muscular dystrophy
IV	NF light	Maturing neurons in CNS, mature neurons in PNS and CNS	Functional maintenance, intracellular transport, morphogenesis of neurons	Various Charcot-Marie-Tooth diseases, Parkinson disease
	NF medium			
	NF heavy			
	α-Internexin	Postnatal, maturing and mature neurons		Amyotrophic lateral sclerosis, dementia
	Nestin	Neural stem and progenitor cells, neurogenic cells, radial glia-like precursors, regenerative glia, mesenchymal stromal cells, subsets of endothelial cells, Schwann cell precursors in PNS	Self-renewal, proliferation, survival, differentiation, migration	
	Synemin	Mature neurons in PNS, glia, skeletal and cardiac muscle	Structural maintenance	Various cancers
V	Lamin A/C	Nucleus	Nuclear shape, chromatin scaffold, gene expression, differentiation, migration	Emery-Dreifuss muscular dystrophy, Dunnigan-type familial partial lipodystrophy, Hutchinson-Gilford progeria syndrome
	Lamin B1			Microcephaly, Neural Tube Closure defects
	Lamin B2			Lipodystrophy,Epilepsy, ataxia
Orphans (VI)	Bfsp1 (filensin)	Lens cells	Maintenance of fiber cell morphology and structure, optical properties of the lens	Autosomal-dominant cataract
	Bfsp2 (phakinin)			Autosomal-recessive cataract

1.4.4. Oxidative stress

Oxidative stress in the brain (lipid peroxidation, decrease in neuronal nitric oxide synthase activity) arises from the accumulation of free radicals due to environmental factors like chronic inflammation and mitochondrial dysfunction. Reactive oxygen species (ROS) are key free radicals that can contribute to tissue dysfunction and worsen oxidative stress. Reactive oxygen species (ROS) are unstable, highly reactive molecules and radicals which are derived from molecular oxygen. ROS production takes place in aerobic organisms that utilize mitochondrial electron transport for respiration or undergo oxidation catalysed by metals and intracellular enzymes. Normally, there exists a delicate balance between ROS generation and elimination in the cells. Controlled levels of ROS play a role in activating specific signalling pathways (such as AMPK/Ras pathway, epidermal growth factor receptor pathway, and protein kinase C pathway), modulating cell metabolism, as well as inducing cell proliferation. However, when the capability to eliminate ROS falls short of its production rate, it leads to accumulation affecting cells by causing instability in chromosomes, damage to DNA (both nuclear and mitochondrial DNA), detrimental alterations to proteins, and lipids (Abdelazim & Abomughaid, 2024; Chiurchiù et al., 2016; Di Meo et al., 2016; R. Huang et al., 2021; Lennicke & Cochemé, 2021; Lew et al., 2022; Singh et al., 2019; Tumilaar et al., 2024).

In Friedreich's ataxia (FA), the decreased expression of frataxin, a mitochondrial protein essential for iron homeostasis, leads to iron accumulation within the mitochondria. This leads to enhanced ROS production that damages cellular components, including DNA, proteins, and lipids, thereby significantly contributing to oxidative stress linked to the progressive neurological symptoms typical of the FA (Dash et al., 2024; Sparaco et al., 2009).

Ataxia-telangiectasia (AT) results from the dysfunction of DNA repair mechanisms caused by mutations in the *ATM* gene, which plays a critical role in preserving DNA integrity. The absence of ATM protein leads to mitochondrial dysfunction, potentially resulting in DNA double-strand breaks and oxidative stress-related damage to DNA. Changes in mitochondrial dynamics - such as reduced mitochondrial membrane potential and increased expression of genes related to mitochondrial DNA repair and ROS scavenging - signal a response to oxidative stress in AT cells. Key genes involved in these processes include polymerase gamma (POLG), mitochondrial-targeted topoisomerase 1 (TOP1mt), peroxiredoxin 3 (Prx3), and superoxide dismutase 2 (SOD2). These alterations reflect compensatory mechanisms aimed at combating mitochondrial dysfunction (Abdelazim & Abomughaid, 2024; Lew et al., 2022).

In AOA1, aprataxin deficiency impairs mitochondrial structure and function. Without aprataxin, cells undergo mitochondrial stress, resulting in altered expression of the mitochondrial inner membrane fusion protein optic atrophy type 1 (OPA1) and components of the oxidative phosphorylation complexes, specifically complexes I to IV. The impaired removal of damaged mitochondria via autophagy enhances the production of ROS within the mitochondria, disrupting the cellular redox balance (Lew et al., 2022).

Fibroblasts derived from ARSACS patients show increased oxidative stress and mitochondrial dysfunction, resulting in reduced basal respiration rates, respiratory chain activities and mitochondrial ATP synthesis (Battaglini et al., 2022).

Current insights indicate that antioxidant therapies may enhance or prevent the progression of ARCAs. Customising these therapies to fit with different phases of the disease may improve the management of ARCAs.

1.4.5. Ubiquitin-proteasome system

The ubiquitin-proteasome system (UPS) is a major intracellular pathway for degradation of proteins. It is crucial for preserving protein homeostasis, regulating various cellular processes (e.g., signal transduction, cell cycle progression, protein trafficking, translation, DNA repair, and immune and inflammatory responses), and removing abnormal or damaged proteins. The UPS is responsible for the targeted degradation of proteins. It comprises a group of enzymes (E1 ubiquitin-activating enzymes, E2 ubiquitin-conjugating enzymes, and E3 ubiquitin ligases) that successively attach Ub protein tags to target proteins in an ATP-dependent way, guiding them for degradation by the proteasome, a multi-subunit protease complex (Verheijen, 2023). Protein aggregates often consist of ubiquitin and the enzymes that facilitate its attachment to substrates. This suggests that these protein aggregates may serve as a protective reaction to harmful misfolded proteins or as a sign of disrupted ubiquitin-mediated degradation leading to toxic aggregation (Kandel et al., 2024; Y. Li, Li, et al., 2022; Ronnebaum et al., 2014).

A significant contribution to ARCAs pathophysiology is the dysregulation of the UPS. These disorders demonstrate UPS dysregulation via both primary and secondary mechanisms. Primary dysregulation arises from mutations that directly affect the components of the UPS. In spinocerebellar ataxia autosomal recessive 16 (SCAR16), mutations in the *STUB1* gene disrupt the function of the CHIP ubiquitin ligase, accumulating misfolded proteins (Ronnebaum et al., 2014; Shi et al., 2018; Türkgenç et al., 2018). Similarly, in ARSACS, mutations in *SACS* impair sacsin, a multifunctional protein thought to assist in protein quality control via its interaction with the UPS (Girard, Larivière, et al., 2012). Mutations in the *UCHL1* gene impair

the recycling of ubiquitin, reducing the pool of free ubiquitin and limiting the clearance of damaged proteins (Ronnebaum et al., 2014).

Secondary UPS dysregulation, on the other hand, is caused by different cellular stresses instead of direct mutations in genes related to UPS. For example, *FXN* deficiency in FA causes mitochondrial dysfunction and oxidative stress, which crowds the UPS with oxidised and misfolded proteins (Ocana-Santero et al., 2021; Sparaco et al., 2009). Likewise, AT and AOA1 indirectly affect the UPS. These conditions stem from disrupted DNA damage response pathways that create chronic oxidative and proteotoxic stress (Beaudin et al., 2022; Synofzik et al., 2019). Mutations in the *VPS13D* gene (SCAR4) show the connection between mitochondrial malfunction and UPS dysfunction. *VPS13D* is mainly involved in mitochondrial dynamics, but when mutations occur, it stresses the UPS by increasing the production of ROS. This fact causes proteostasis to collapse due to mitochondria and oxidised protein accumulation (Sultan et al., 2024). Understand how cellular pathways converge to disrupt the UPS in ARCAs, highlight potential therapeutic strategies to restore proteostasis and mitigate disease progression.

1.4.6. Autophagy -lysosomal pathway disruption

Autophagy is a major player in removing misfolded aggregated proteins. It is a cellular process where proteins and organelles are degraded through lysosomes to maintain cellular homeostasis. In mammals, there are three types of autophagy pathways: macroautophagy, microautophagy, and chaperone-mediated autophagy (CMA) (Fig.7) (Cui et al., 2022; Fassio et al., 2020; Finkbeiner, 2020). Macroautophagy and CMA, along with the proteasome, help recycle cellular proteins, including those that may disrupt

normal cell function by forming abnormal folded structures leading to aggregate or inclusion formation.

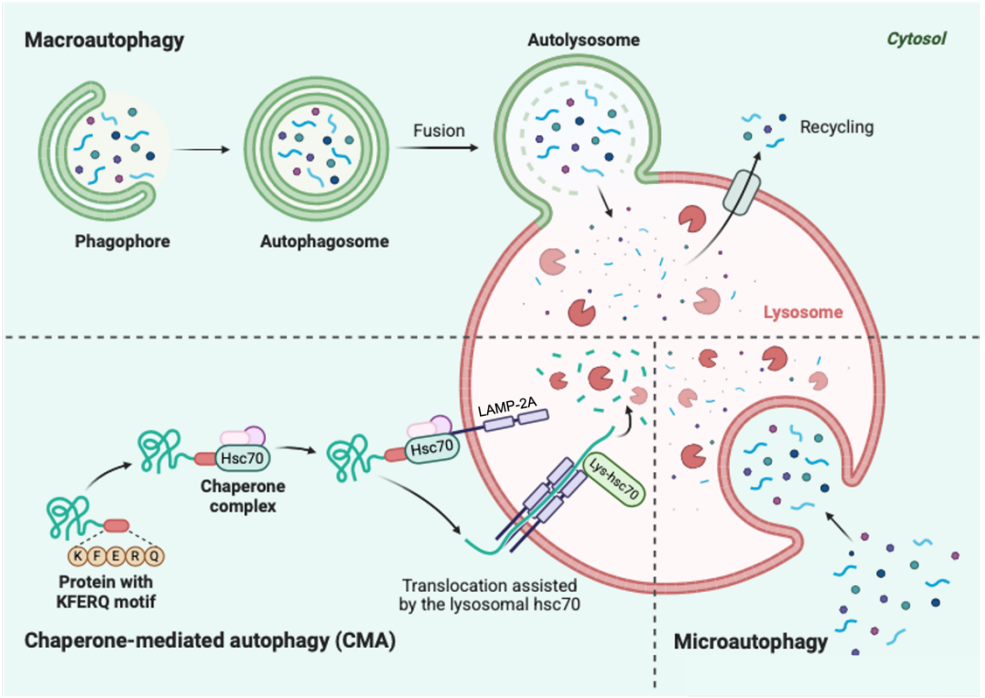

Figure 7: Three main types of autophagy. Three main types of autophagy. Macroautophagy involves a sequence of events that starts with the formation of a phagophore, which then enlarges and closes off to form an autophagosome. The autophagosome then fuses with a lysosome, forming an autolysosome, where intracellular components are degraded and recycled. Chaperone-mediated autophagy (CMA) is a process in which chaperones, such as Hsc70 recognize specific proteins containing KFERQ-like motifs, transport them to lysosomal membrane, and facilitate their internalization through interaction with lysosomal receptor LAMP-2A for degradation. Microautophagy, mediates a non-selective up-take of intracellular components through lysosomal membrane invagination, and internalization into the lysosome for degradation. The figure was created with BioRender.

Macroautophagy is a complex process that begins with the creation of an autophagosome, a double membrane vesicular structure that includes the cargo to be degraded. Autophagosome formation requires various factors including the Atg protein family, LC3-II, p62, Beclin, among others. Upon formation, the autophagosome merges with the lysosome to release its

proteolytic content, forming an autolysosome structure that ultimately degrades the cargo. In addition to proteins, macroautophagy can also target impaired and/or oxidized cell components like mitochondria, endoplasmic reticulum, peroxisomes and lipid droplets (Dupont et al., 2024).

Microautophagy involves the direct engulfment of proteins and organelles by the lysosome for degradation. While some proteins are incorporated into the lysosome in an unspecific manner, others, such as those in CMA, require interaction with the Hsc70 chaperone (Fassio et al., 2020; Finkbeiner, 2020; Y. Li, Li, et al., 2022; Yim & Mizushima, 2020).

Chaperone-mediated autophagy (CMA) is a distinct mechanism for degrading proteins that depends on lysosomes. Unlike macroautophagy, it does not require the creation of autophagosomes and autolysosomes, its focus is on cellular proteins rather than organelles, and the protein cargo is directly transported into the lysosomal lumen through interaction with HSC70 and LAMP-2A. HSC70 in the cell cytoplasm identifies the KFERQ pattern in target proteins, leading to the formation of the HSC70-substrate complex. This complex then associates with the cytosolic tail of LAMP-2A, which subsequently facilitates the movement of the target protein into the lysosome interior. All cells possess a basic CMA function that contributes to the upkeep of cellular protein homeostasis. However, in response to specific stimuli such as nutrient deprivation, serum starvation, or cellular stress (e.g., protein aggregation), CMA activity is increased (Yim & Mizushima, 2020).

When autophagy malfunctions, unfolded and misfolded proteins accumulate in the endoplasmic reticulum (ER) and other cellular compartments.

1.4.7. Endoplasmic Reticulum Stress

Damaged, misfolded, and unfolded proteins contribute to the storage and conformational anomalies within the ER (Ellgaard et al., 1999; Fewell et al., 2001). The ER, being a membranous compartment, is highly sensitive to changes that impact its structure, integrity and function which can disrupt protein folding (Rao & Bredesen, 2004). If the final tertiary structure cannot be attained, unfolded proteins are moved to the cytosol where they undergo ubiquitination and proteasome-dependent degradation known as ER-associated degradation (ERAD).

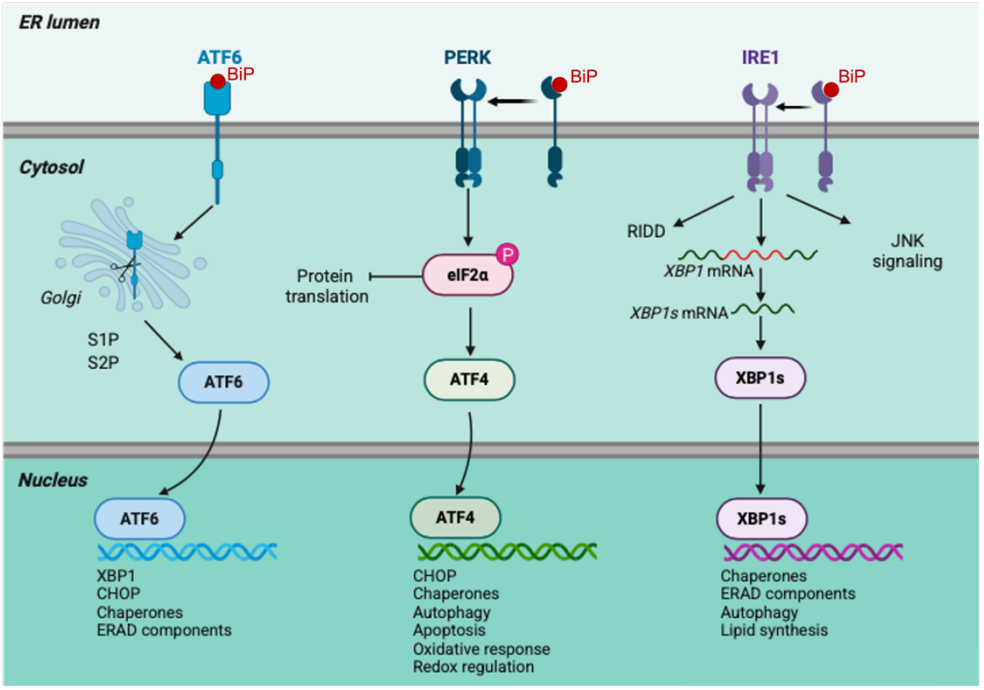

Figure 8: General unfolded protein response pathway during ER stress. The UPR is controlled by three major branches, ATF6, PERK and IRE1α, which bind to BiP in the ER. Upon ER stress or misfolded protein accumulation, BiP dissociates from all these UPR transducers and permits stress sensors to activate downstream signalling. Adapted from (Bhattarai et al., 2021). The figure was created with BioRender.

When there is an accumulation of misfolded or unfolded proteins within the cell, it results in ER stress due to failure of coping with excessive protein

load. Cells respond by reducing the rate of protein synthesis and increasing expression of genes encoding chaperones along with other protective proteins that prevent polypeptide aggregation while degrading accumulated misfolded proteins (Han et al., 2013; Hughes & Mallucci, 2019; Kettel & Elif Karagöz, 2024). This cellular response is activated through an integrated intracellular signalling cascade called Unfolded Protein Response (UPR). UPR is controlled by three sensor proteins: PERK (PKR-like ER kinase), IRE1α (inositol-requiring transmembrane kinase/endoribonuclease 1α) and ATF6 (activating transcription factor 6) (Fig.8) (Dombroski et al., 2010; M. Wang & Kaufman, 2016). These sensor proteins remain inactive when associated with BiP under normal conditions; upon ER stress however BiP is released from these sensor proteins, leading to the activation of the UPR (Bertolotti et al., 2000). This activates a cascade involving PERK and IRE1α through dimerization and autophosphorylation (Harding et al., 1999; Y. Li, Huang, et al., 2022). ATF6 undergoes regulated intramembrane proteolysis. Activation of PERK results in eIF2α phosphorylation, which reduces global protein synthesis but promotes the translation of the activating transcription factor 4 (ATF4) which upregulates the genes related to apoptosis (Harding et al., 1999; Vattem & Wek, 2004). The endoribonuclease activity of IRE1α is activated enabling the splicing of the unspliced X-box binding protein 1 (XBP1) to produce a mature and active XBP-1 protein (XBP1s). XBP1s then upregulates gene transcription involved in UPR and ERAD (Adams et al., 2019). Under ER stress, ATF6 translocates from the ER to the Golgi, where it is cleaved sequentially by enzymes. The activated ATF6 is translocated into the nucleus, where it binds promoters of various genes involved in UPR such as (C/EBP homologous protein (CHOP), BiP, and XBP-1) inducing target-gene transcription (Shen et al., 2002; Yoshida et al., 2001). UPR mediators play a role in preserving ER homeostasis (Almanza et al., 2018; Bhattarai et al., 2021; X. Chen et al., 2023). Prolonged or excessive

accumulation of misfolded proteins can disrupt the adaptive reactions of UPR, trigger regulated cell death and inflammation.

The aetiology of ARCAs is varied and involves mutations that affect distinct organelles in different neuronal populations in the cerebellum that disrupt cellular stress response mechanisms (Wilson et al., 2023). Genes associated with different forms of ataxia interact in these processes, showing common biological mechanisms across varied mutations and inheritance patterns (Fig.9) (Beaudin et al., 2022). Developing therapeutic strategies targeting or mitigating the detrimental downstream effects of dysregulated pathways could benefit a wide range of ataxia patients with diverse genetic causes.

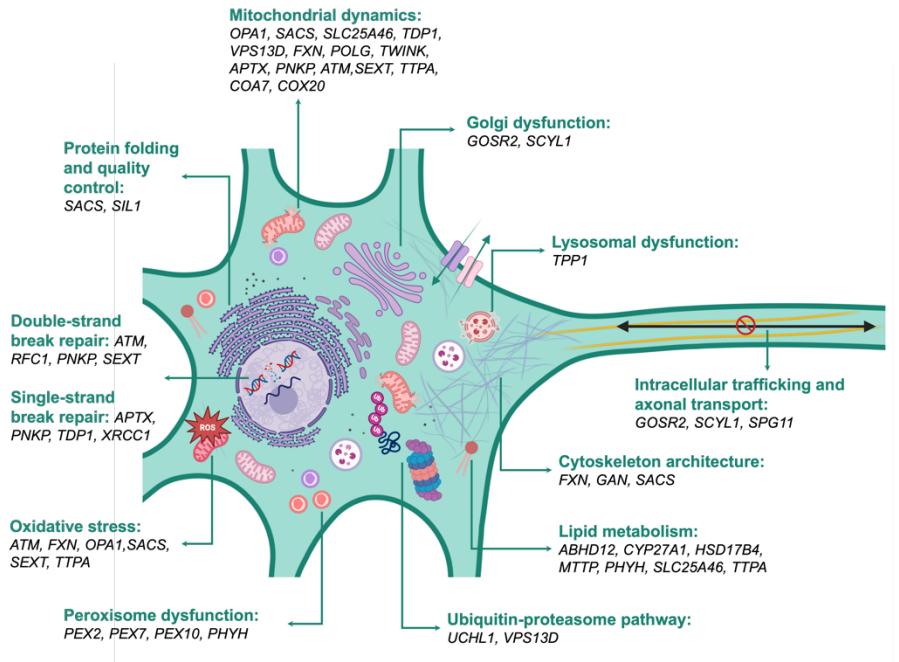

Figure 9: Cellular pathways involved in recessive cerebellar ataxias. Adapted from (Beaudin et al., 2022). The figure was created with BioRender.

1.4.8. Neuroinflammation

Neuroinflammation is a central feature of many neurodegenerative disorders, playing a dual role in both protecting and damaging the central nervous system (CNS). At its core, neuroinflammation is regulated by glial cells, particularly microglia and astrocytes, which mediate the brain's immune response (Fig. 10) (Wyss-Coray & Mucke, 2002). In neurodegenerative diseases such as Alzheimer's disease (AD), Parkinson's disease (PD), and amyotrophic lateral sclerosis (ALS), chronic activation of these glial cells contributes to a sustained inflammatory environment that exacerbates neuronal damage and accelerates disease progression (Ginhoux et al., 2013; Giri et al., 2024; Lee et al., 2022; Lull & Block, 2010).

Microglia, the resident immune cells of the CNS, are the first responders to injury or pathological stimuli such as protein aggregates, including amyloid-β in AD or α-synuclein in PD. Upon activation, microglia undergo phenotypic changes and can adopt either a pro-inflammatory (M1) or anti-inflammatory (M2) state. The M1 phenotype is associated with the release of inflammatory mediators such as interleukin-6 (IL-6), tumour necrosis factor-alpha (TNF-α), and reactive oxygen species (ROS), which amplify inflammation and contribute to neuronal toxicity. Conversely, the M2 phenotype promotes tissue repair and resolution of inflammation. In neurodegenerative disorders, microglia often become persistently activated in the M1 state, perpetuating a cycle of inflammation and neurodegeneration (Colonna & Butovsky, 2017; Hyuk Sung Kwon, 2020; Mohamed et al., 2023; Y. Tang & Le, 2016).

Astrocytes also play a pivotal role in neuroinflammation and interact closely with microglia to regulate the CNS environment. In response to injury or pathological changes, astrocytes undergo reactive gliosis, characterized by hypertrophy, proliferation, and changes in gene expression. Reactive

astrocytes can adopt neurotoxic ("A1") or neuroprotective ("A2") phenotypes, depending on the context and signalling cues from their environment. While reactive gliosis initially serves to contain damage and maintain homeostasis, prolonged activation or breakage of the blood-brain-barrier often leads to the formation of a glial scar. This scar isolates damaged tissue but also impedes axonal regeneration and repair, contributing to chronic dysfunction in neurodegenerative diseases (Liddelow et al., 2017; Liddelow & Barres, 2017; Mohamed et al., 2023; Nedergaard et al., 2003; Phatnani & Maniatis, 2015).

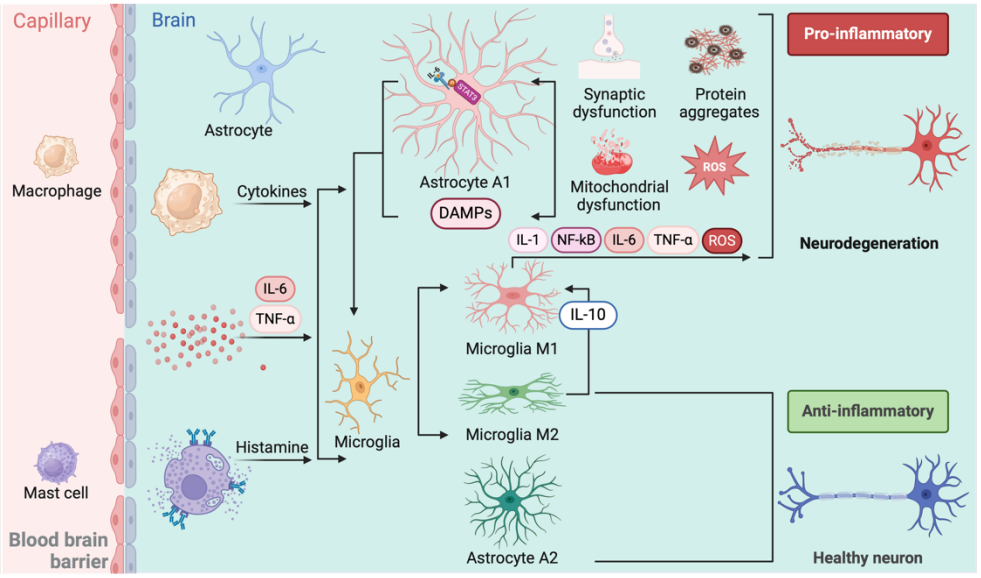

Figure 10: Role of glial cells in neuroinflammation. Pro-inflammatory molecules such as Il-6 and TNF can cross BBB and reach the CNS parenchymal tissue. Mast cells secrete abundant pro-inflammatory cytokines like histamine that can induce some changes in microglia. Resting microglia can then be activated into two classical subtypes. M1 and M2 microglia transform make their action through some secretions. M1 microglia can produce pro-inflammatory cytokines that contribute to dopaminergic neurons dysfunction. Degenerated neurons can produce protein aggregates and reactive oxygen species (ROS) cross talking with microglia and astrocytes in a non-terminating loop of neuroinflammation. Protein aggregates and ROS cause mitochondrial and synaptic dysfunction due to the accumulation of misfolded tangles and oligomers. Contrary, activation of M2 microglia that downregulates M1 function by releasing Il-10 cytokines thus maintain healthy neurons and anti-inflammatory state. The figure was created with BioRender.

At the molecular level, several signalling pathways drive the inflammatory responses of microglia and astrocytes. One key pathway is the Janus kinase/signal transducer and activator of transcription 3 (JAK/STAT3) pathway, which is particularly relevant in astrocytic function during neuroinflammation. IL-6, a cytokine secreted by both activated microglia and astrocytes, binds to its receptor on glial cells and activates JAK kinases. These kinases phosphorylate STAT3, enabling it to dimerize and translocate into the nucleus where it regulates the expression of genes involved in inflammation, cell survival, and proliferation. In reactive astrocytes, persistent activation of the JAK/STAT3 pathway has been implicated in glial scar formation and chronic neuroinflammation. While this pathway can promote protective functions under acute conditions, its dysregulation in chronic disease states exacerbates inflammation and contributes to neuronal dysfunction (Jain et al., 2022; Mohamed et al., 2023; W. Y. Wang et al., 2015).

In neurodegenerative disorders, persistent activation of microglia and astrocytes transforms an initially protective response into a chronic pathological state. Protein aggregates such as amyloid-β or misfolded tau proteins act as damage-associated molecular patterns (DAMPs), perpetually activating glial cells through toll-like receptors (TLRs) or other pattern recognition receptors. This chronic activation not only sustains inflammation but also disrupts neuronal-glial interactions critical for maintaining CNS homeostasis. Understanding these cellular mechanisms underlying neuroinflammation - particularly the roles of microglia and astrocytes - and targeting key signalling pathways like JAK/STAT3 offers promising avenues for therapeutic intervention aimed at mitigating inflammation-driven neurodegeneration (Jain et al., 2022; L. Li et al., 2021; Rahman et al., 2022; W. Y. Wang et al., 2015).

Not surprisingly, neuroinflammation has emerged as a significant factor in the pathogenesis of various ataxias, including Friedreich's ataxia (FA) and spinocerebellar ataxias (SCAs) (Apolloni et al., 2022; Cerrato, 2020; Edamakanti et al., 2023). In FA, recent findings suggest that inflammatory responses in the cerebellum and spinal cord play a critical role in disease progression. The genetically decreased expression of frataxin leads to disturbances in iron metabolism, resulting in increased iron levels in reactive microglia and astrocytes, along with mitochondrial dysfunction (Apolloni et al., 2022). FA microglia exhibit elevated oxidative damage, increased expression of DNA repair proteins MUTYH and PARP-1, and higher levels of ROS. These changes contribute to the activation of inflammatory pathways involving activator protein 1 (AP1) and cAMP response element-binding protein (CREB), which drive cyclooxygenase 2 (COX2) expression (Apolloni et al., 2022). In SCAs, particularly SCA1, Bergmann glia (BG) inflammation has been identified as a key contributor to cerebellar degeneration. BG, the radial glia of the cerebellum, display inflammatory JNK-dependent c-Jun phosphorylation, which is not observed in other activated glial populations. Studies using SCA1 mouse models have demonstrated that inhibiting the JNK pathway reduces BG inflammation, leading to improvements in both behavioural and pathological aspects of the disease (Edamakanti et al., 2023; Nanclares et al., 2023). Additionally, neuroimaging studies in FA patients have revealed increased [18 F]-FEMPA binding, indicative of neuroinflammation, in the dentate nuclei, superior cerebellar peduncles, and midbrain. This increased neuroimmune activity correlates with earlier disease onset and may attenuate over the course of the illness (Khan et al., 2022). These findings collectively suggest that targeting neuroinflammation, particularly glial-mediated inflammation, could be a promising therapeutic strategy for various ataxias. However, little is still known about the role of glial cells in other, rarer ataxias, such as ARSACS or Spastic ataxia 8.

When we started this PhD thesis, there were no studies on neuroinflammation in ARSACS brains, and the scarce research in the field focused on Purkinje cell neurodegeneration. The role of sacsin loss-of-function was in ARSACS was discovered only in 2015, with the development of the first animal models (Larivière et al., 2015). The alterations in IF and mitochondrial networks caused by sacsin loss were demonstrated in a series of works between 2017 and 2019, but always disregarding glial cells (Duncan et al., 2017). No signs of neuroinflammation in ARSACS mice were described until 2023 (Bondio et al., 2023). Our work on the development of glial cell models of ARSACS was therefore an original and fresh perspective in the field and could contribute to unravelling the possible role of glial cells and neuroinflammation in ARSACS in the future.

2. OBJECTIVES

ARSACS is an early-onset neurodevelopmental disorder characterized by progressive cerebellar ataxia, spasticity, axonal demyelination, and Purkinje cell loss. ARSACS is caused by loss-of-function mutations in the SACS gene, which encodes the protein sacsin. Current evidence points to the involvement of sacsin in protein homeostasis, cytoskeleton organization and mitochondrial dynamics. The scientific literature on sacsin function and dysfunction has focused mainly on neuronal cells, but glial cells also play critical roles in neurodegenerative disorders. Indeed, the histopathological features of ARSACS (e.g. hypomyelination and leukodystrophy) suggest a glial contribution. In this thesis, we focused on the effects of sacsin depletion in glial cells as well as their putative involvement in ARSACS pathology. Our specific objectives are:

1) to generate glial cell models of ARSACS;

2) to unravel the cellular and molecular consequences of sacsin loss-of-function; and

3) to advance our understanding of the basic biological functions of sacsin through the analysis of its interactome.

3. MATERIALS AND METHODS

3.1. Reagents

Dulbecco's modified Eagle's medium (DMEM) was purchased from Biowest (Nuaillé, France); Fetal bovine serum (FBS), rotenone, dimethylsulfoxide (DMSO), 2′,7′-dichlorodihydrofluorescein diacetate (DCFH-DA) and 3-4,5-dimethylthiazol-2-yl-2,5-diphenyltetrazolium bromide (MTT) were acquired from Sigma-Aldrich (St. Louis, MO, USA). Penicillin-Streptomycin (Pen/Strep), dihydroethidium (DHE), 4',6-Diamidino-2-Phenylindole, Dihydrochloride (DAPI), Pierce ECL Plus Western Blotting Substrate, MitoTracker Red CMXRos and Hoechst 33,342 were purchased from Invitrogen, Life Technologies (Carlsbad, CA, USA). Protease inhibitor cocktail was purchased from Abcam. Phosphatase inhibitor cocktail was purchased from NZYTech (Lisboa, Portugal). Mouse anti-Sacsin (N-terminal), anti-GFAP, anti-Nestin, anti-Vimentin and anti-GAPDH antibodies were purchased from Santa Cruz Biotechnology Inc. (Dallas, TX, USA). Anti-Sacsin (C-terminal) and anti-GFAP rabbit polyclonal antibodies were purchased from Millipore-Sigma™ (St. Louis, MO, USA). Anti-vimentin rabbit polyclonal antibody, horseradish peroxidase-conjugated secondary antibodies—goat anti-rabbit IgG (H + L) and goat anti-mouse IgG (H+L)—and goat anti-mouse or anti-rabbit secondary antibodies conjugated to AlexaFluor 488 or AlexaFluor 594 fluorophores were purchased from Invitrogen, Life Technologies (Carlsbad, CA, USA). Leukemia inhibitory factor (LIF) was purchased from Rockland Immunochemicals (Pottstown, PA, USA). Interleukin-6 (IL-6) and the soluble IL-6 receptor (IL-6R) were obtained from R&D Systems (Minneapolis, MN, USA). Protein extracts from the murine microglial cell line N9 were a kind gift from Dr. Adelaide Fernandes (Faculdade de Farmácia, Universidade de Lisboa, Portugal).

Protein extracts from a mouse embryonic frontal cortex neural precursor cell line and adult precursor cells from the rat dentate gyrus and subgranular zone were kindly provided by Drs. Susana Solá (Faculdade de Farmácia, Universidade de Lisboa, Portugal) and Sara Xapelli (Instituto de Medicina Molecular João Lobo Antunes, Lisboa, Portugal), respectively.

3.2. Cell Cultures and Treatments

C6 rat glioma cells, HeLa human cervix adenocarcinoma cells, HEK293T human embryonic kidney cells and HMC3 human microglial clone 3 cells were acquired from ATCC (references CCL-107TM, CRM-CCL-2, CRL-1573 and CRL-3304, respectively). Human Dermal Fibroblasts (HDFn) were obtained from Innoprot (Derio, Spain) (P10857), and Human Keratinocytes (KER) from Gibco (Waltham, MA, USA) (C-100-5C). These cell lines were grown in DMEM, supplemented with 10% (*v*/*v*) FBS, 1% (*v*/*v*) Penicillin/Streptomycin and maintained at 37 °C in a humidified atmosphere containing 5% CO_2, except for KER, which were cultured in Epilife medium (Gibco®) (Waltham, MA, USA), 1% Pen/Strep, 1% HKGS (Gibco®) (Waltham, MA, USA), with 0.6 mM $CaCl_2$. All cell lines were periodically tested for mycoplasma contamination by means of a commercial test (Biontex Laboratories, Munich, Germany).

For experiments, cells were plated on sterile plastic dishes or on sterile glass coverslips and allowed to adhere for 16–24 h before experiments or sample preparation. When applicable, C6 and $C6^{Sacs-/-}$ cells were incubated with rotenone (5 µM) for 4 h or its vehicle (DMSO 0.1% *v*/*v*). For cytokine experiments, complete medium was removed, cells were washed with PBS and incubated in serum-free medium for 2 h before adding LIF (200 ng/mL), IL-6 (30 ng/mL) and the soluble IL-6 receptor (IL-6R, 60 ng/mL). Cells were then incubated for 2 h with the cytokines in the absence of serum before

sample preparation. For serum starvation experiments, complete medium was removed, cells were washed twice with PBS, and serum-free medium added. Both serum-deprived and control (10% FBS) cells were grown for 48 h before sample preparation.

3.3. Generation of Sacsin knockout Cell Lines Using the CRISPR/Cas9 System

Sacsin knockout strains from C6 rat glioma cells ($C6^{Sacs-/-}$) and HMC3 human microglial cells ($HMC3^{Sacs-/-}$) were generated using a commercial Sacsin CRISPR/Cas9 knockout plasmid set (sc-404592, Santa Cruz Biotechnologies, Dallas, TX, USA), following manufacturers' instructions. Transfected cells were isolated by fluorescence-activated cell sorting (FACS) and single cells were plated in 96-well plates for clonal expansion. The resulting clones were probed for sacsin expression by Western blot.

Genomic DNA was extracted from C6 and $C6^{Sacs-/-}$ cells using a DNA extraction kit following the manufacturer´s instructions (QuickDNA miniprep kit, Zymo Research), and the concentration of DNA was measured by means of a NanoDrop spectrophotometer (Thermo Fisher Scientific). A pair of primers was designed to amplify a 900-bp region spanning the expected gene deletion/insertion area using NCBI primer design tool (https://www.ncbi.nlm.nih.gov/tools/primer-blast/):

5' GAATTAATTCAGAATGCAGAAGATGCTGGG 3'

5' AACTGAACATGATTGCAGGAGGC 3'

PCR products for the targeted genomic region were obtained by amplification of 50 ng of genomic DNA with Phusion High-Fidelity DNA Polymerase (Thermo Fisher Scientific). PCR was performed using a thermocycler (Multigene OptiMAX Labnet) with the following conditions:

Initial denaturation at 98 °C for 5 min, followed by 30 cycles of denaturation (98 °C for 30 secs), annealing (60 °C for 30 secs) and extension (72 °C for 30 secs), and a final extension at 72 °C for 15 min. PCR products were mixed with loading buffer 4X and loaded on a 1% agarose gel. The target DNA bands were gel-extracted under UV light and purified with a DNA Purification Kit (NZY GelPure, NZYTech) according to the vendor's protocol. Ten ng of the purified PCR product were used as template for 30 cycles of PCR in the same conditions. To identify the exact nature of CRISPR-induced mutations, purified PCR products were subjected to Sanger sequencing. Raw sequencing chromatograms were analysed using ApE, a Plasmid Editor free software (https://jorgensen.biology.utah.edu/wayned/ape/).

3.4. Primary Cultures of Astrocytes

Cultures were prepared as described elsewhere. Briefly, astrocyte-enriched cultures were prepared from neonatal Sprague Dawley rat pups' cerebral cortexes (0–2 days). Animals were sacrificed by decapitation and the brains were dissected in ice-cold PBS (NaCl 137 mM, KCl 2.7 mM, $Na_2HPO_4.2H_2O$ 8 mM and KH_2PO_4 1.5 mM, pH 7.4). Cortexes were isolated, placed in 10 mL of 4.5 g/L glucose DMEM, supplemented with 10% FBS and 1% antibiotic/antimycotic, and dissociated mechanically through up-and-down movements with a serological pipette until no cell clumps were observed. Cell suspension was filtered successively through 230 µm and 70 µm (BD Falcon, NJ, United States) cell strainers and centrifuged at room temperature (RT) at 200× *g* for 10 min. The final pellet was resuspended in 4.5 g/L glucose DMEM, and cells were seeded according to the required assay. Cultures were kept at 37 °C in a humidified atmosphere (5% CO_2) and medium was changed twice a week. At 10 days *in vitro* (DIV), plates were shaken for 6 h in an orbital shaker at 300 rpm to remove any contaminating microglial cells and obtain astrocytic-enriched cultures.

3.5. Cell Viability and Migration Assays

For MTT assays, C6 and C6$^{Sacs-/-}$ cells were seeded onto 96-well plates at a concentration of 10^4 cells/well. After the corresponding treatments, cells were incubated with MTT (0.5 mg/mL) for 2 h. The medium was then replaced with DMSO (100% *v*/*v*) and, after15 min of incubation in the dark at RT, absorbance was determined using an automatic microplate reader (Tecan Sunrise Microplate Reader) (Tecan, Männedorf, Switzerland) at 570 nm. For LDH assays, cells were seeded in 24-well plates at a concentration of 10^5 cells/well, and the determination of released and total LDH was carried out by means of the LDH cytotoxicity detection kit (Takara), following manufacturer's instructions. DAPI exclusion assay was also used as a complementary cytotoxicity assay by flow cytometry, as described below.

For wound healing assay C6 and C6$^{Sacs-/-}$ cells were seeded into 35 mm glass bottom dishes in a standard growth medium. Cells were allowed to adhere for 16–24h, and then the confluent monolayer was gently scratched across the centre of the dish with a sterile pipette tip (Ø = 0.1 mm) and washed with PBS. The scratch-injured cells were incubated at 37 °C and 5% CO_2. The wound healing was evaluated using phase-contrast images acquired at 0, 5 and 24h post-scratch with a Leica DMI6000 B widefield Microscope equipped with a x20 objective HC PL FLUOTAR and a Monochrome CMOS camera 4.0 MP (2048 x 2048 pixels). We determined the scratch area with the Wound_healing_size_tool plugin of ImageJ*TM* software. We calculated the percentage of wound closure according to the equation:

$$Wound\ Closure\% = \left(\frac{A_{t=0} - A_{t=\Delta t}}{A_{t=0}}\right) x100\%$$

Where $A_{t=0}$ is the initial wound area, $A_{t=\Delta t}$ is the wound area after n hours of the initial scratch, both in μm^2.

3.6. Myelin Debris Phagocytosis Assay

Microglial phagocytosis of BASHY-labelled myelin debris was assayed according to a previously published protocol with minor modifications (Rolfe et al., 2017). HMC3 and HMC3$^{Sacs-/-}$ cells were incubated with 1 mg/ml of myelin debris previously stained with BASHY probe or 1 h to mimic microglia neuroprotective ability to remove debris; or with 0.0025 % (*v*/v) 1 mm zymogen-coated fluorescent latex beads (Sigma Chemical) for 75 min to mimic microglia reactivity against infections (innate immune response). Then, non-phagocytosed myelin debris were washed out three times with PBS. Cells were fixed with 4% (*w*/*v*) PFA in PBS for 30 min at RT to perform future immunocytochemistry.

3.7. Flow Cytometry

Cells were seeded in 6-well plates (5 × 10^5 cells/well). After treatments, cells were detached by trypsinization (0.05% *w/v*), collected, resuspended in PBS, and incubated with 10 µM DCFH-DA (to detect all reactive oxygen species) or DHE (to detect superoxide radicals) in serum-free DMEM medium for 20 min at 37 ˚C in the dark. After washing cells twice with PBS, pellets were resuspended in PBS with DAPI (1 µg/mL) to discriminate between live and dead cells, and fluorescence was immediately analysed by means of a BD LSRFortessa X-20 cell analyser (BD Biosciences, San Jose, CA, USA). Ten thousand events were recorded for analysis with FLOWJO software Version 9 (Emerald Biotech Co., Ltd., Córdoba, Spain).

For cell cycle analysis, both floating and adherent cells were collected by centrifugation and fixed in ice-cold 70% ethanol overnight at 4ºC. Cells were then centrifuged at 500x*g* for 5 min, washed twice with PBS, and resuspended in a propidium iodide solution (50 µg/ml in PBS) containing RNase A (100µg/ml). After 20 min of incubation at 37°C, cells were analysed

using a FACSCalibur flow cytometer (BD Biosciences, Franklin Lakes, NJ, USA). Ten thousand events were recorded for cell cycle analysis with FLOWJO software Version 9 (Emerald Biotech Co., Ltd., Córdoba, Spain).

3.8. Western Blot

Western blot analysis was performed as previously described (Letra-Vilela et al., 2020). Briefly, cells were lysed using an NP-40 lysis buffer (150 mM NaCl, 50 mM Tris-HCl pH 7.4/7.5, 1% NP- 40 *v/v*) supplemented with protease inhibitors (NZYTech) (Lisboa, Portugal) and phosphatase inhibitors (Halt Phosphatase Inhibitor Single-use Cocktail, Thermo Fisher Scientific, Waltham, MA, USA). Samples were sonicated in a UP200s sonicator (Hielscher Ultrasonics GmbH, Teltow, Germany) for 8 s. Cell suspension was then centrifuged at 10,000×*g* for 10 min at 4 °C, and the soluble protein fraction was collected and quantified by the Bradford method. One µL of protein sample was incubated with 200 µL of Bradford solution (Alfa Aesar, Ward Hill, MA, USA) for 5 min and the absorbance was determined at 595 nm. Thirty micrograms of total protein were separated by SDS-PAGE on 10% (*w/v*) polyacrylamide gels or gradient gels 6% + 15% (*w/v*) and transferred to a nitrocellulose membrane. Protein transfer quality was assessed by Ponceau S staining. Membranes were blocked with 5% (*w/v*) milk in TBS-T (TBS supplemented with 0.1% Tween-20) and probed with primary antibodies in 5% (*w/v*) Bovine Serum Albumin (BSA) in PBS overnight at 4 °C. Primary antibodies were used at a dilution of 1:1000, except for anti-GAPDH and anti-sacsin antibodies (N-terminal, sc-515118, Santa Cruz Biotechnologies (Dallas, TX, USA); and C-terminal, ABN1019, Merck-Millipore (Burlington, MA, USA) which were used at 1:2000 and 1:200 dilutions, respectively. Membranes were then washed three times with TBS-T for 10 min, followed by incubation with HRP-conjugated secondary antibodies (1:10,000) in blocking solution for 2h. After washing off the

secondary antibody three times with TBS-T for 10 min, chemiluminescence detection was performed using the Pierce ECL Plus Western Blotting Substrate kit and the Amersham Imager 680 blot and gel imager (Cytiva, Marlborough, MA, USA). The integrated intensity of each band was calculated using computer-assisted densitometry analysis with ImageJ software, normalized to the loading control GAPDH as appropriate.

3.9. Filter Trap Assays

For filter trap assays, cells were washed once with PBS and collected by scraping in native lysis buffer (173 mM NaCl, 50 mM Tris pH 7.4, 5 mM EDTA) supplemented with protease and phosphatase inhibitor cocktails. Samples were sonicated for 10 s at 5 mA using a UP200S Sonicator (Hielscher, Teltow, Germany). Protein extracts (supernatants) were collected after sample centrifugation at 10,000×*g* for 10 min at 4 °C and quantified by means of the Bradford method, as described above. One hundred µg of native protein extracts were diluted in PBS to produce a final volume of 100 µL and SDS was added to a final concentration of 1% (*w/v*). Samples were loaded on a dot-blotting device and filtered by vacuum through nitrocellulose membranes previously incubated with 1% (*w/v*) SDS solution in PBS. After filtration, membranes were washed twice with 1% (*w/v*) SDS solution in PBS and processed for immunoblotting detection, as described above.

3.10. Fluorescence Microscopy of Live Cells and Immunocytochemistry

For fluorescent microscopy, C6 and C6$^{Sacs-/-}$ cells were seeded at the density of 10^5 cells/cm^2 on 35 mm glass-bottom dishes. Twenty-four hours after seeding, cells were incubated with either sirActin kit (Spirochrome, Stein am Rhein, Germany) and Tubulin tracker deep red (Invitrogen,

Carlsbad, CA, USA) following manufacturer's instructions. To visualize mitochondria, cells were incubated with MitoTracker Red CMXRos (25 nM) for 30 min at 37 ºC in 5% CO_2 atmosphere before processing samples for immunocytochemistry. Cells were then fixed in ice-cold methanol for 20 min and blocked with 1% (*w/v*) BSA in PBST (PBS supplemented with 0.1% Tween-20) for 1 h at RT. Overnight incubation at 4 ºC was performed with the following primary antibodies diluted in blocking solution: mouse monoclonal anti-sacsin (1:50), rabbit polyclonal anti-GFAP (1:200), mouse monoclonal anti-nestin (1:100) and mouse monoclonal anti-vimentin (1:100). Cells were incubated with the corresponding goat anti-mouse or anti-rabbit secondary antibodies conjugated with AlexaFluor 488 (Thermo Fisher Scientifics, Waltham, MA, USA) or AlexaFluor 594 (Thermo Fisher Scientifics, Waltham, MA, USA) (1:800) for 2 h at RT, and counterstained with the nuclear markers Hoechst 33342 or DAPI (Thermo Fisher Scientifics, Waltham, MA, USA). Images were acquired by means of a Leica TCS SPE high-resolution spectral confocal system (Wetzlar, Germany) equipped with a Leica DFC 365 FX camera (Wetzlar, Germany) using a 63X/1.4 oil objective (Wetzlar, Germany) and processed by Leica LAS X Core (Wetzlar, Germany) and ImageJ software (National Institutes of Health, Bethesda, MD, USA). To assess the effects of serum-starvation on nuclear material, cells stained with *Hoechst 33342* were further analysed with NII Plugin of the Image J Software. The Image J Software's NII Plugin was created to extract morphometric information about nuclei for use in the Nuclear morphometric Analysis (NMA) tool. The analysis utilises nuclear area measurements as well as four irregularity parameters known as Aspect, Area/Box, Radius Ratio, and Roundness. These four parameters are used to calculate a Nuclear Irregularity Index (NII), which, when combined with area measurement, categorizes nuclei as normal (N), irregular (I), small and

regular (SR), small and irregular (SI), large and regular (LR) or large and irregular (LI).

DAPI images of at least 100 nuclei were acquired for each experimental condition (10% FBS versus 0% FBS). To assess morphometric data to NMA (area, aspect, area box, radius ratio and roundness), the surrounding nuclei were marked using the Image J NII plugin. After obtaining raw data, a group of nuclei from the control condition was selected, and the nuclei in mitosis or with clear abnormalities were excluded. The data obtained was used to set the parameters for the normal population. The parameters were adjusted to define the 'normal ellipse' and the threshold that better separates the populations (10% FBS versus 0% FBS). The percentage of nuclei in each population was then analysed and compared.

3.11. RNA Extraction and RT-qPCR

Total RNA was extracted from HMC3 and HMC3$^{Sacs-/-}$ using TRIzol® reagent (Life Technologies, Carlsbad, CA, United States), according to the manufacturer's instructions. Total RNA obtained from the cells, was quantified in Nanodrop® ND-100 Spectrophotometer (NanoDrop Technologies, Wilmington, DE, United States). In order to determine mRNA levels (gene expression), equal amounts of total RNA were reverse-transcribed into cDNA using the GRS cDNA Synthesis Master Mix kit (GRiSP, Porto, Portugal), and RT-qPCR was performed using Xpert Fast Sybr Blue (GRiSP) as a master mix with specific predesigned primers. Running conditions were as follows: 50°C for 2 min followed by 95°C for 2 min and finally 40 cycles at 95°C for 5 s and 62°C for 30 s. mRNA RT-qPCR was performed on a QuantStudio 7 Flex Real-Time PCR System (Applied Biosystems, Waltham, MA, United States). A melt-curve analysis was performed to verify amplification specificity immediately after the amplification protocol. Glyceraldehyde 3-phosphate dehydrogenase

(GAPDH) was used as a reference gene for mRNAs. Results were normalized and expressed as $2^{-\Delta\Delta CT}$ (fold-change) and/or $\log_2$-transformed, as appropriate. All samples were quantified in duplicate and compared to respective controls, depending on the performed analysis.

3.12. Irradiation of Cells

C6 and $C6^{Sacs-/-}$ were seeded in 96-well plates at a density of 10^4 cells/well. Twenty-four hours later, cells were incubated with 10 *μ*M DCFH-DA for 30 min in the dark, washed once with PBS and then irradiated with doses of 1, 2, 5, and 10 Gy in a Co-60-based irradiator PRECISA-22 (CTN). F luorescence was measured immediately after the irradiation and every 15 min to a total time of 2 h using a Varioskan™ LUX Multimode Microplate Reader at 522 nm.

3.13. Proteomics

3.13.1. Filter aided sample preparation (FASP digestion)

FASP digestion was carried out as described elsewhere (Wiśniewski et al., 2009), with some minor modifications. Briefly, aliquot of cellular extract, with initial protein input of 20 µg, was diluted to 200 µL with reconstitution buffer (8M Urea, 100mM ammonium bicarbonate -ABC, pH 7.8) and transferred to pre wetted Nanosep™ centrifugal filters, with membrane cut-off of 10kDa (Omega™ - modified polyethersulfone). Buffer exchange was performed adding 200 µL of fresh reconstitution buffer, in five centrifugal cycles (12000 rpm, 5 min), discarding the flow through fraction. Subsequently, 6 µL of 100mM DTT/100mM ABC was added to the samples and incubated for 50 min at 56ºC, 600 rpm. Reduction was followed by alkylation adding 20 µL of 500 mM IAA/100mM ABC (30 min at dark). The reconstitution buffer was replaced with 100 mM ABC in four centrifugal

cycles (12000 rpm, 5 min) maintaining the buffer volume at 100 µL. Proteolysis was carried out in-filter, in a wet-chamber at 37ºC, during 16h, at 600 rpm, with a mixture of trypsin and LysC (Promega) at an enzyme to substrate ratio of 1:50. Peptides were sequentially eluted by 100 mM ABC (12000 rpm, 5 min) adding in the last step 0.5% formic acid. Samples were concentrated by means of a vacuum concentrator (SpeedVac, Savant) followed by clean-up with in-house prepared stage tips (AttractSPE® Disks C18, 200 mL tip). Peptides were sequentially eluted (2 x 10 µL) with a solvent mixture of 5% acetonitrile /0.1%FA/ millyQ water, ready for LC/MS analysis.

3.13.2. nLC-MS/MS analysis

Chromatographic separation was performed on nano Elute™ nano flow ultra high-pressure LC (Bruker, Daltonics) coupled to an ultra-high-resolution quadrupole-time-of-flight mass spectrometer (UHR QqTOF, Impact II™ Bruker, Daltonics) with a CaptiveSpray nano booster™ ion source (Bruker, Daltonics). Two microliters of sample were loaded to the Acclaim™ PepMap™ 100 C18 trap column (Thermo Scientific™). Separation was performed on Bruker fifteen™ column (C18, 15 cm × 75 um, 1.9 um, 120 Å) in a 120 min linear gradient using 0.1% formic acid in MilliQ water (solvent A) and 0.1% formic acid in acetonitrile (solvent B) with constant flow of 300 nl/min in the following regimen: 0 to 115 min., 5 - 35% B; 115 to 118 min., 35 – 95% B; 118-125 min. 95% B. Column was kept at 40ºC. The MS acquisition was performed with the following parameters: capillary voltage was set at 1500 V, the drying gas flow rate was 3.0 L/min at a temperature of 150ºC, nanobooster at 0.2 bar. The acquisition was performed in the positive ionization mode at spectra rate of 1 Hz, in the range of 150 to 2200 m/z. LC-MS/MS data were acquired using data-dependent (DDA) auto MS/MS method, cycle time 3.0 s, active exclusion was triggered after one spectrum, release after 0.5 min. Reconsider precursor if current

intensity/previous intensity is set up to three, and intensity threshold for fragmentation was 2500 counts. The collision energy was tuned between 23–65 eV as a function of the m/z value. The spectra were internally calibrated by post-run infusion of the 1µM sodium formate. Calibration of MS files was performed using Compass Data Analysis 4.4 (Bruker, Daltonics) in high precision calibration mode (HPC) giving error of <1 ppm and standard deviation <0.2 ppm for the mass range between 90 to 1500 m/z.

3.13.3. Protein identification and label free quantification (LFQ)

The raw files from the mass spectrometer were analysed using MaxQuant software (ver. No. 2.2.0.0.), as previously reported, using default parameters (Tyanova et al., 2016). Andromeda search engine was employed for peptide search against the UniProt-SwissProt Rattus Norvegicus database as a reference and contaminants database for common contaminants. Briefly, trypsin was used as protease with maximum two missed cleavages allowed. The maximum false discovery rate for peptide and protein was 0.01. Main search (parent ion) and peptide (daughter) search tolerances were 20 and 4.5 ppm respectively. The oxidation of methionine and acetylation were used for variable modification while for the fixed modification carbamidomethylation of cysteine was used. The LFQ Label-free quantification (LFQ) was performed using classic normalization and a minimum ratio count of 2. A reverse sequence library was generated to control the false discovery rate at less than 1%.

3.13.4. Proteomics differential abundance analysis

LFQ values were used for protein quantification. Only proteins with at least two LFQ values in at least one of the replicate groups ($C6^{Sacs-/-}$ or C6) were kept for further analysis. Additionally, only proteins with more than one unique peptide detected were kept. LFQ values were log2 transformed and

normalized by the median of the subgroup of proteins that were detected in the six samples. Two methods of missing value imputation were applied. When the protein was detected in two replicates, the missing value in that replicate group was defined with the k-nearest neighbors (knn) algorithm, using the average values of the five proteins (k=5) more similar (euclidean distance between LFQ values across samples) to the protein with the missing value. When the protein was detected in less than two samples in the replicate group, the missing values were defined as random values from a normal distribution with mean equal to the minimum LFQ of that sample and standard deviation equal to a global estimate made with all proteins with replicate values. It was previously checked that standard deviation estimates were not significantly affected by protein average abundance or number of detected peptides.

Statistical testing of differential abundance between the two conditions was performed with the Limma R package (Ritchie et al., 2015). Adjusted p-values lower than 0.05 were considered significant (False Discovery Rate (FDR) - 10%). To avoid artifacts induced by the missing value imputation with random numbers, this imputation was repeated 30 times, and only proteins with differential abundances consistently (>50% of the times) considered statistically significant were selected for further analysis. The R code used for the analysis is available at https://github.com/GamaPintoLab/sacsin/.

3.13.5. Functional Enrichment Analysis

We conducted Gene Ontology (GO) analysis (biological process, molecular function, and cellular component) and Kyoto Encyclopedia of Genes and Genomes (KEGG) analysis to identify biological functions and pathways enriched from the different expressed proteins. The functional enrichment analysis was conducted by using the online bioinformatics tool, the Database for Annotation, Visualization and Integrated Discovery

(DAVID, https://david.ncifcrf.gov/). The terms with adjusted p values <0.05 were selected.

3.14. Atomic Force Microscopy

The cells were analysed with a PicoLE Molecular Imaging system from Agilent Technologies (Keysight Technologies, Inc., Santa Rosa, CA, USA). A CP-qp-SCONT-SiO-A Nanoandmore cantilever, with nominal stiffness of 0.01 N/m and a nominal tip radius of 1 um was used in all experiments. The cantilevers are transparent to the laser except at its extremity which reduces issues with calibration. The same tip was used to measure cells of all different types to reduce bias due to different cantilever stiffness'. In total 12 cantilevers were used. To measure the mechanical properties of cells we perform grids of typically 32×32 approach/retract force-displacement curves in a range of about 30 μm. For the determination of the Young modulus of the cell we used the Hertz contact model to fit the contact portion of the approach force curve as explained elsewhere (Carapeto et al., 2020). A total of 211 cells (C6) and 168 cells ($C6^{Sacs-/-}$) were measured.

3.15. Statistical Analysis

Statistical analysis and graphical representation of data were performed using Graph-Pad Prism software Version 8 (GraphPad, San Diego, CA, USA). Sample data are represented as mean ± standard error (SEM) of three independent experiments. For statistical evaluation, one-way or two-way Analysis of Variance (ANOVA) and Tukey's post hoc test were used for multiple comparisons. Student's *t*-test was applied for comparisons in experiments with two groups. Results were considered significant when $p < 0.05$.

4. RESULTS

This chapter contains results published in:

Fernanda Murtinheira, Mafalda Migueis, Ricardo Letra-Vilela, Mickael Diallo, Andrea Quezada, Cláudia A. Valente, Abel Oliva, Carmen Rodriguez, Vanesa Martin, and Federico Herrera. 2022. "Sacsin Deletion Induces Aggregation of Glial Intermediate Filaments". Cells 11, no. 2: 299. https://doi.org/10.3390/cells11020299

Fernanda Murtinheira, Elisa Farsetti, Luana Macedo, Ana Sofia Boasinha, Mário S. Rodrigues, Adelaide Fernandes and Federico Herrera (2024). A human microglial cell model of autosomal recessive spastic ataxia of Charlevoix-Saguenay. Biochimica et Biophysica Acta (BBA) - Molecular Basis of Disease, 1870, 8. https://doi.org/10.1016/j.bbadis.2024.167452

This chapter also contains parts of the following publications:

Fernanda Murtinheira, Ana Sofia Boasinha, João Belo, Luana Macedo, Elisa Farsetti, Tiago T. Robalo, Vukosava M. Torres, Francisco R. Pinto, Adelaide Fernandes, Patricia Nascimento, Mario S. Rodrigues, Federico Herrera (2024). Subcellular, biochemical and biophysical alterations in two glial cell models of ARSACS. bioRxiv 2024.04.15.589510; doi: https://doi.org/10.1101/2024.04.15.589510.

Fernanda Murtinheira, João Belo, Ana Sofia Boasinha, Tiago T. Robalo, Vukosava M. Torres, Francisco R. Pinto, Patricia Nascimento, Mario S. Rodrigues, and Federico Herrera. Mechanical alterations in a glial model of autosomal recessive spastic ataxia of Charlevoix-Saguenay. *Under revision in Movement Disorders*.

Acknowledgement of collaborative work within the thesis

I obtained most of the results presented in the results section, except for content derived from co-authored publications. Below are the contributions made by other authors to this work:

Figure 13D, E: Carina Coelho performed the irradiation experiments and analysed the data.

Figure 16A: Patrícia Nascimento conducted the immunofluorescence experiments on the Golgi apparatus.

Figure 17: Dr. Vukosava Torres carried out the filter-aided sample preparation (FASP digestion), nLC-MS/MS analysis, protein identification, and label-free quantification (LFQ). Dr. Francisco Pinto performed the proteomics differential abundance analysis.

Figure 18: João Belo and Tiago Robalo conducted the AFM analysis.

Figures 22A-E: Luana Macedo collaborated on the immunofluorescence and western blot experiments with clone C2.

Figures 22D,F-I and 24: RT-PCR, phagocytic activity, and morphology evaluation (sphericity, surface area to volume ratio) were performed by Elisa Farsetti and Dr. Adelaide Fernandes.

4.1. DEVELOPMENT AND CHARACTERIZATION OF THE FIRST ASTROGLIAL-LIKE CELL MODEL OF ARSACS

4.1.1. Abstract

Autosomal recessive spastic ataxia of Charlevoix-Saguenay (ARSACS) is a neurodegenerative disorder commonly diagnosed in infants and characterized by progressive cerebellar ataxia, spasticity, motor sensory neuropathy and axonal demyelination. ARSACS is caused by mutations in the *SACS* gene that lead to truncated or defective forms of the 520 kDa multidomain protein, sacsin. Sacsin function is exclusively studied on neuronal cells, where it regulates mitochondrial network organization and facilitates the normal polymerization of neuronal intermediate filaments (i.e., neurofilaments and vimentin). Here, we show that sacsin is also highly expressed in astrocytes, C6 rat glioma cells and N9 mouse microglia. Sacsin knockout in C6 cells ($C6^{Sacs-/-}$) induced the accumulation of the glial intermediate filaments glial fibrillary acidic protein (GFAP), nestin and vimentin in the juxtanuclear area, and a concomitant depletion of mitochondria. $C6^{Sacs-/-}$ cells showed impaired responses to oxidative challenges (Rotenone) and inflammatory stimuli (Interleukin-6). GFAP aggregation is also associated with other neurodegenerative conditions diagnosed in infants, such as Alexander disease or Giant Axonal Neuropathy. Our results, and the similarities between these disorders, reinforce the possible connection between ARSACS and intermediate filament-associated diseases and point to a potential role of glia in ARSACS pathology.

4.1.2. Introduction

The autosomal recessive spastic ataxia of Charlevoix-Saguenay (ARSACS) is a rare, early-onset neurodegenerative disorder, usually diagnosed at gait initiation (12–18 months) (Artero Castro et al., 2019). ARSACS is clinically characterized by cerebellar ataxia, spasticity, axonal demyelination, sensory-motor peripheral neuropathy, amyotrophy, dysarthria, skeletal finger and feet abnormalities, nystagmus, retinal hypermyelination and variable intellectual dysfunction (Vermeer, van de Warrenburg, Kamsteeg, et al., 1993). Its histopathological features include the atrophy of the anterior vermis, associated with the loss of Purkinje cells in the cerebellum (Artero Castro et al., 2019; Vermeer, van de Warrenburg, Kamsteeg, et al., 1993) and deposits of lipofuscin in cerebellar cortical neurons and skin (Stevens et al., 2013). ARSACS is caused by mutations in the *SACS* gene that are located on chromosome 13q12 and encode the cytoplasmic protein sacsin (Vermeer, van de Warrenburg, Kamsteeg, et al., 1993). Sacsin knockout mice show histopathological and neurological features consistent with ARSACS, indicating that the disease is caused by sacsin loss-of-function (Larivière et al., 2015). Sacsin function remains barely understood, but the nature and architecture of its domains suggest that it is a molecular chaperone involved in protein quality control (Anderson et al., 2011; Parfitt et al., 2009), mitochondrial integrity (Bradshaw et al., 2016; Girard, Larivieѐ, et al., 2012) and the assembly/dynamics of neuronal intermediate filaments (Duncan et al., 2017; Gentil et al., 2018).

Intermediate filaments (IFs) are one of the three major filament types of the cytoskeleton and are found in most eukaryotic cells, including neurones and glia in the central nervous system. They play a pivotal role in the mechanical and viscoelastic properties of cells and tissues, but they are also scaffolds associated with signal transduction (Nishimura et al., 2019). IFs

can interact with various cellular components, organelles, and molecules through linker proteins from the plakin gene family, such as plectin (Winter & Wiche, 2013). Unlike microtubules and actin microfilaments, IFs comprise an extremely diverse family of proteins that shows cell- and tissue-specific expression patterns (Omary, 2009). For example, neuronal IF networks are constituted by vimentin and light, medium and heavy neurofilaments, while astroglial IFs are vimentin, nestin and the glial fibrillary acidic protein (GFAP). Mutations in IFs or their interacting proteins underlie more than 80 rare disorders, including Epidermolysis Bulbosa Simplex, progeria, Alexander disease (AxD), Giant Axonal Neuropathy (GAN) or predisposition to Amyotrophic Lateral Sclerosis (Omary, 2009).

Scientific literature on sacsin function and dysfunction was largely focused on neuronal cells, just as it happened historically for more common neurodegenerative disorders, such as Huntington's, Parkinson's, and Alzheimer's diseases. However, glial cells play key roles in neurodegenerative disorders (Liddelow et al., 2017). AxD is an extreme but illustrative example of the important role of glial cells in neurodegeneration. AxD is a fatal leukodystrophy caused by dominant mutations in GFAP, the major intermediate filament of astrocytes (Messing, 2018). Mutant GFAP accumulates in astrocytes in cytoplasmic inclusions known as Rosenthal fibres. As ARSACS, AxD is most commonly diagnosed in the first months of life (0–2 years), and AxD patients often display ataxia, spasticity, seizures and dysarthria (Messing, 2018). GFAP aggregation is also present in GAN, another early-onset neurological disease characterized by an extensive aggregation of different types of Ifs (Armao et al., 2019).

In this sense, there are strong indications of a wider expression pattern for sacsin in both neural and non-neural cells and tissues, which could also be relevant for understanding both sacsin normal function and ARSACS

pathology. The Protein Atlas public database indicates that medium-high sacsin mRNA levels can be found in human primary cells and cell lines from virtually any tissue, although there are significant variations between cell types within the same tissue. This database does not provide specific information on sacsin expression levels in most non-neuronal brain cells, such as astrocytes, oligodendrocytes or microglia, but it shows that Müller glia and macrophages, similar in some respects to astrocytes and microglia, respectively, express sacsin mRNA. Human glioblastoma cell lines with mixed features of astrocytes and neural precursor cells also express sacsin and, according to Harmonizome and BrainRNASeq public transcriptomics datasets, high levels of sacsin mRNA were also found in both mouse and human astrocytes. Mouse sacsin RNA expression is as high in astrocytes as in neurones, displaying the highest levels in younger animals (postnatal day 7) and decreasing with age (Clarke et al., 2018). Human foetal astrocytes express the same RNA expression levels as neurones, also decreasing as astrocytes mature (Y. Zhang et al., 2016). In both mouse and human, neurones and astrocytes express higher levels than oligodendrocytes, microglia and endothelial cells. However, these data focus on mRNA levels, and data on protein expression are scarce.

In this report, we show that the sacsin protein is indeed expressed in astroglia. We developed an astroglial model of ARSACS by deleting sacsin in the C6 rat glioma cell line. Our results indicate that sacsin also regulates glial IF organization, suggesting a potential link between the ARSACS, AxD and GAN pathologies.

4.1.3. Results

4.1.3.1. Astroglia Express Sacsin

Public databases indicated that glial cells contain sacsin mRNA, but data are scarce and there is no empirical evidence that sacsin mRNA is actually translated into protein. The sacsin protein is easily detected by immunoblotting in rat primary astroglia and C6 rat glioblastoma cells at approximately the same levels (Fig.11A). Sacsin levels in glial cells were relatively higher than in other human and rodent cell lines, some of them described to express medium-high levels of sacsin mRNA in The Protein Atlas, such as HEK293 or HeLa cells (Fig.11B,C). Surprisingly, C6 and N9 rat microglial cells had higher sacsin levels than the HT22 mouse cell line, of neuronal origin (Fig.11C). We failed in our attempts to detect sacsin in adult rat neural precursor cells from the dentate gyrus and the subventricular zone (data not shown). The immunocytochemistry of astrocytes and C6 glioma cells showed the expected cytoplasmic distribution of sacsin with some mitochondrial localization (Fig.11D). These data suggest that sacsin expression is not exclusive to neurons, but also expressed in glial cells. We next aimed to develop a glial model of ARSACS, deleting sacsin in C6 cells by means of a CRISPR/Cas9 approach (Fig.11E,F). We isolated 96 individual clones, of which 42% (40/96) survived and proliferated. Eighteen clones were probed for sacsin protein expression, and around 17% (3/18) of the clones did not express detectable levels of sacsin. We randomly selected one of them for further studies (Fig.11G) and verified by DNA sequencing. We observed deletions in the gRNA targeting region, resulting in *SACS* mutant gene.

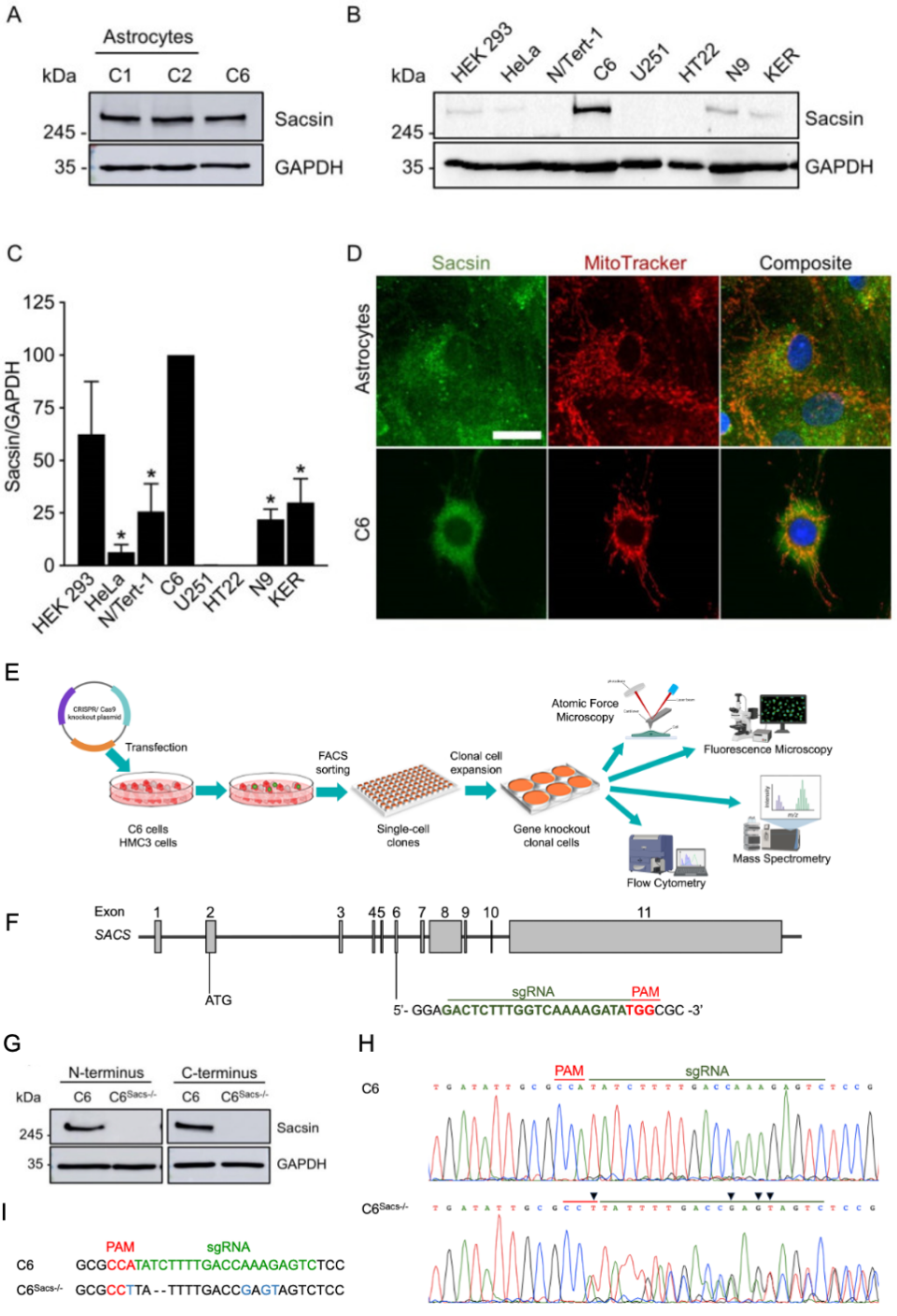
A
Astrocytes
kDa
C1
C2
C6
245
35
Sacsin
GAPDH
B
kDa
HEK 293
HeLa
N/Tert-1
C6
U251
HT22
N9
KER
245
35
Sacsin
GAPDH
C
Sacsin/GAPDH
125
100
75
50
25
0
HEK 293
HeLa
N/Tert-1
C6
U251
HT22
N9
KER
D
Sacsin
MitoTracker
Composite
Astrocytes
C6
E
CRISPR/ Cas9 knockout plasmid
Transfection
C6 cells
HMC3 cells
FACS sorting
Single-cell clones
Clonal cell expansion
Gene knockout clonal cells
Atomic Force Microscopy
Fluorescence Microscopy
Mass Spectrometry
Flow Cytometry
F
Exon
SACS
1
2
3
45
6
7
8
9
10
11
ATG
sgRNA
PAM
5'- GGAGACTCTTTGGTCAAAAGATATGGCGC -3'
G
N-terminus
C-terminus
kDa
C6
C6Sacs-/-
C6
C6Sacs-/-
245
35
Sacsin
GAPDH
H
C6
PAM
sgRNA
C6Sacs-/-
I
PAM
sgRNA
C6 GCGCCATATCTTTTGACCAAAGAGTCTCC
C6Sacs-/- GCGCCTTA--TTTTGACCGAGTAGTCTCC

Figure 11: Glial cells express sacsin. (**A**) Representative Western blot images indicate that primary rat astrocytes have sacsin levels similar to C6 glioblastoma cells, with C1 and C2 indicating independent cultures of primary astrocytes. (**B**) Sacsin was detected in HEK293, HeLa, N/Tert-1 and N9 cell lines and primary human keratinocytes by Western blot, but at lower levels than C6 cells. (**C**) Sacsin was not detected in HT22 mouse hippocampal cell lines or U251 glioblastoma cells in these conditions, but we cannot rule out that they express very low levels of the protein. Data were analysed by means of a one-way ANOVA, followed by a Tukey post hoc test, *, significant vs. C6 reference strain, $p < 0.05$. (**D**) Representative images of immunocytochemistry for endogenous sacsin (green) in primary rat astrocytes and C6 cells. Mitochondria were counterstained with Mitotracker (red) and nuclei with Hoechst (blue). Scale bar, 20 µm. (**E**), Diagram illustrating the workflow for CRISPR/Cas9-mediated generation of $C6^{Sacs-/-}$ cell lines. Cells were transfected with CRISPR/Cas9 plasmids, sorted by FACS and clonally expanded. Resulting clonal populations were then tested for sacsin expression and phenotype. (**F**) Schematic representation of the *SACS* gene structure with exons. Exons and introns are indicated with grey rectangles and black line, respectively. The sequence targeted by sgRNA in the CRISPR-Cas9 system is shown in green. The TGG protospacer adjacent motif (PAM) is indicated in red. (G) Representative Western blot analyses of a $C6^{Sacs-/-}$ clone, using two different sacsin antibodies against its N- and C-termini (refs. sc-515118 and ABN1019, respectively). Sacsin protein could not be detected in the $C6^{Sacs-/-}$ clone by western blot. GAPDH was used as loading control. (H) Partial sequencing chromatograms of PCR products from the genome sequencing of C6 reference strain and $C6^{Sacs-/-}$ cells. Black arrows indicate sites of mutations. (I) Partial sequence alignment of C6 reference strain and selected $C6^{Sacs-/-}$ clone. Green bases indicate targeting sequences for sgRNA; red bases indicate PAM site; blue bases indicate mutation sites; – indicate deleted bases.

4.1.3.2. Sacsin Loss Induces Higher Sensitivity to Oxidative Stress and Starvation Challenges

Mitochondrial alterations and oxidative stress are common hallmarks in neurodegenerative disorders, and ARSACS is no exception (Criscuolo et al., 2015; Girard, Larivière, et al., 2012). $C6^{Sacs-/-}$ cells showed a significantly higher level of basal oxidative stress (Fig.12A). Next, reference C6 cells and the $C6^{Sacs-/-}$ strain were treated with rotenone, a mitochondrial Complex I

inhibitor, to determine whether sacsin loss could undermine their response to oxidative challenges. Incubation with rotenone for 4 h had similarly mild toxicity in wildtype and C6$^{Sacs-/-}$ cells (Fig.12B,C; Supplementary Fig.S1). Neither MTT or LDH cytotoxicity assays gave indications of significant toxicity in these conditions in both cell lines (Fig.12B; Supplementary Fig. S1A). However, a flow-cytometry-based DAPI exclusion assay suggested a non-significant tendency to higher toxicity in C6$^{Sacs-/-}$ cells (Supplementary Fig.S1B), and these cells showed a stronger decrease in cell size (forward scatter, FSC-A, Fig.12D) consistent with a higher degree of damage. C6$^{Sacs-/-}$ cells also show a significantly higher increase in oxidative stress upon rotenone exposure, often accompanied by a slight increase in DAPI staining, which is indicative of membrane damage (Fig.12E–I).

To confirm whether this higher sensitivity was specific of mitochondrial stress or a general sensitivity to any form of stress, we submitted cells to serum deprivation and irradiation (Fig.13). Removal of serum was also more toxic to C6$^{Sacs-/-}$ cells as indicated by changes in the morphology (Fig. 13A), loss of viability (Fig.13B), ROS production (Fig.13C). C6 and C6$^{Sacs-/-}$ cells show similar behaviour for lower doses of radiation (1 and 2 Gy) without a marked increase in oxidative stress levels. However, for higher doses (5 and 10 Gy), there was an increase in oxidative stress levels, with the peak being reached in the first 35 minutes after exposure. Subsequently, a slow reduction occurs in both cell lines until reaching initial levels. However, it is noteworthy that at the highest dose (10Gy) in C6$^{Sacs-/-}$ cells, the levels of oxidative stress were higher than in the reference C6 cells (Fig.13D,E).

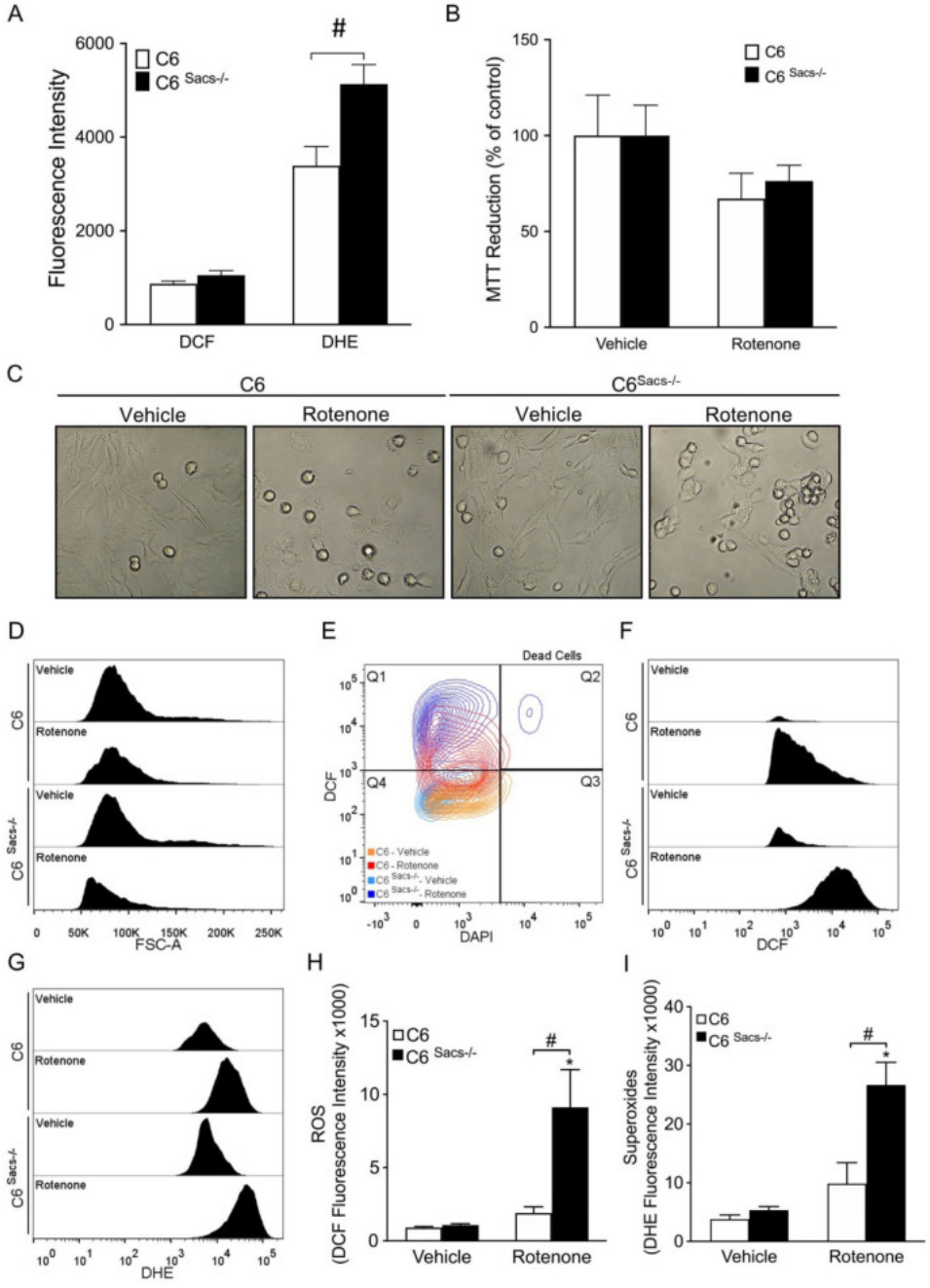
A
Fluorescence Intensity
6000
4000
2000
0
C6
C6 Sacs-/-
#
DCF
DHE
B
MTT Reduction (% of control)
150
100
50
0
C6
C6 Sacs-/-
Vehicle
Rotenone
C
C6
C6Sacs-/-
Vehicle
Rotenone
Vehicle
Rotenone
D
C6
C6 Sacs-/-
Vehicle
Rotenone
Vehicle
Rotenone
0 50K 100K 150K 200K 250K
FSC-A
E
Dead Cells
Q1
Q2
Q4
Q3
DCF
DAPI
C6 - Vehicle
C6 - Rotenone
C6 Sacs-/- - Vehicle
C6 Sacs-/- - Rotenone
F
C6
C6 Sacs-/-
Vehicle
Rotenone
Vehicle
Rotenone
DCF
G
C6
C6 Sacs-/-
Vehicle
Rotenone
Vehicle
Rotenone
DHE
H
ROS
(DCF Fluorescence Intensity x1000)
15
10
5
0
C6
C6 Sacs-/-
#
*
Vehicle
Rotenone
I
Superoxides
(DHE Fluorescence Intensity x1000)
40
30
20
10
0
C6
C6 Sacs-/-
#
*
Vehicle
Rotenone

Figure 12: Sacsin knockout renders cells more sensitive to rotenone-induced stress. (A) Under basal conditions, C6$^{Sacs-/-}$ had levels of reactive oxygen species (ROS) similar to C6 cells, as determined by DCF fluorescence. However, C6$^{Sacs-/-}$ showed higher levels of superoxide radicals, as determined by DHE fluorescence. Data were analyzed by means of two-way ANOVA followed by a Tukey post hoc test, #, significant vs. C6 reference strain, $p < 0.05$. **(B)** Both C6 and C6$^{Sacs-/-}$ displayed a non-significant decrease in viability when challenged with rotenone (5 µM) or its vehicle (DMSO 0.1%) for 4 h. **(C)** Representative brightfield images show similar gross morphological alterations in both cell strains following rotenone treatment, but flow cytometry analysis **(D)** indicated a stronger decrease in size (Forward-Scatter, FSC-A) in C6$^{Sacs-/-}$ cells. **(E)** Representative flow cytometry plot showing DAPI and DCF staining of C6 and C6$^{Sacs-/-}$ cells after incubation with rotenone (red and dark blue, respectively) or its vehicle (orange and light blue). Rotenone increases ROS levels in both C6 cell strains, but with more intensity in C6$^{Sacs-/-}$ (Quadrant 1, Q1). In C6$^{Sacs-/-}$ cells it only induces some residual cell death (DAPI staining, quadrants 2 and 3, Q2/Q3). **(F,G)** Representative histograms from flow cytometry analysis using DCF and DHE in C6 and C6$^{Sacs-/-}$ cells after treatment with rotenone. **(H,I)** Quantification of oxidative stress levels in 3 independent experiments (mean ± SEM). Data were analysed by means of two-way ANOVA, followed by a Tukey post hoc test, *, significant vs. vehicle; #, significant vs. C6 reference strain, $p < 0.05$.

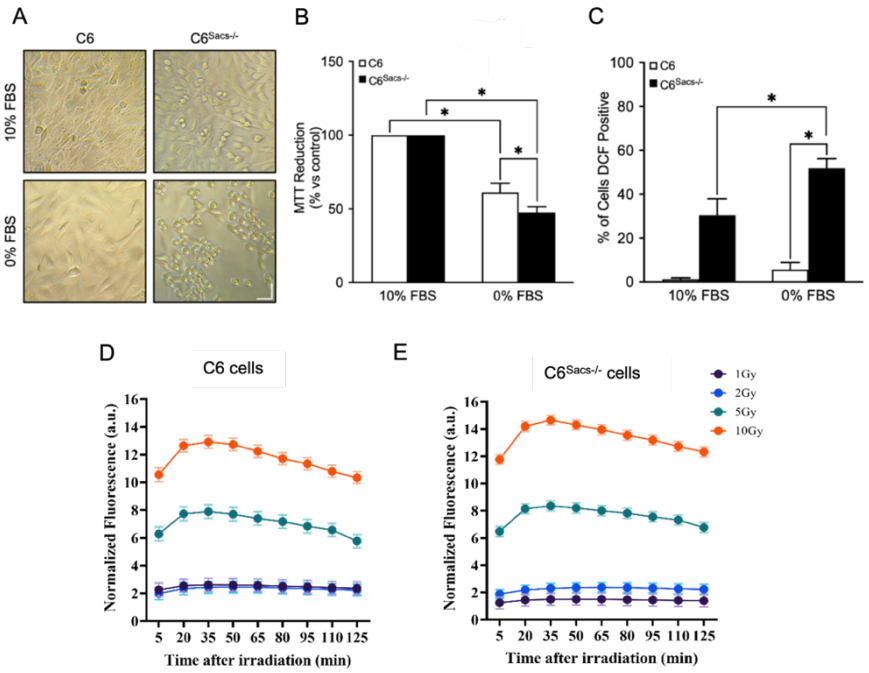

Figure 13: Sacsin-knockout cells have higher sensitivity to serum starvation and radiation. Serum starvation reduces cell viability in C6$^{Sacs-/-}$ cells. C6 and C6$^{Sacs-/-}$ cells were grown with or without 10% FBS for 48h. **(A)** Representative bright-field images of cell morphology and density under the serum starvation stress. In both C6 and C6$^{Sacs-/-}$ cells was observed a decrease in cell density. Serum-starved C6 cells were larger than the controls, growing as a confluent monolayer and C6$^{Sacs-/-}$ cells displayed a rounded morphology. **(B)** Cell viability was analysed using the MTT assay. A significant decrease in the percentage of viable cells was observed in C6 and C6$^{Sacs-/-}$ compared to controls. **(C)** Intracellular ROS levels were monitored by DCFDA staining followed by flow cytometry. Data are represented as the mean ± SEM (standard error in the mean). Statistical significance was determined by One-way analysis of variance (ANOVA), followed by Holm-Šídák's multiple comparisons test. The differences were considered statistically significant when $p < 0.05$. Radiation-induced ROS production was evaluated by the DCFH-DA assay in C6 **(D)** and C6$^{Sacs-/-}$ **(E)** cells irradiated with different radiation doses at C2TN. Data were normalized to the respective measured control (0 Gy).

4.1.3.3. Sacsin Deletion Leads to Juxtanuclear Accumulation of Glial IFs

Sacsin deletion in neuronal cells induces the accumulation of neurofilament light, medium and heavy polypeptides (NFL, NFM and NFH, respectively), peripherin, α-internexin and vimentin in the juxtanuclear region, with the concomitant depletion of mitochondria in the same region (Duncan et al., 2017; Gentil et al., 2018). Immunocytochemistry analysis unmasked a similar profile for vimentin, nestin and GFAP in C6$^{Sacs-/-}$ cells (Fig.14A–C; Supplementary Fig.S2): juxtanuclear accumulation of the three glial intermediate filaments and depletion of mitochondria from this region. Transformation of widefield images by the Nano J Super-Resolution Radial Fluctuations (SRRF) ImageJ plugin (Gustafsson et al., 2016) showed more condensed IF networks in this juxtanuclear region (Fig.14B). However, the impact was different for each IF: approximately 40% of cells showed accumulation of GFAP, 60 % of nestin, and 60 % of Vimentin (Fig.14C).

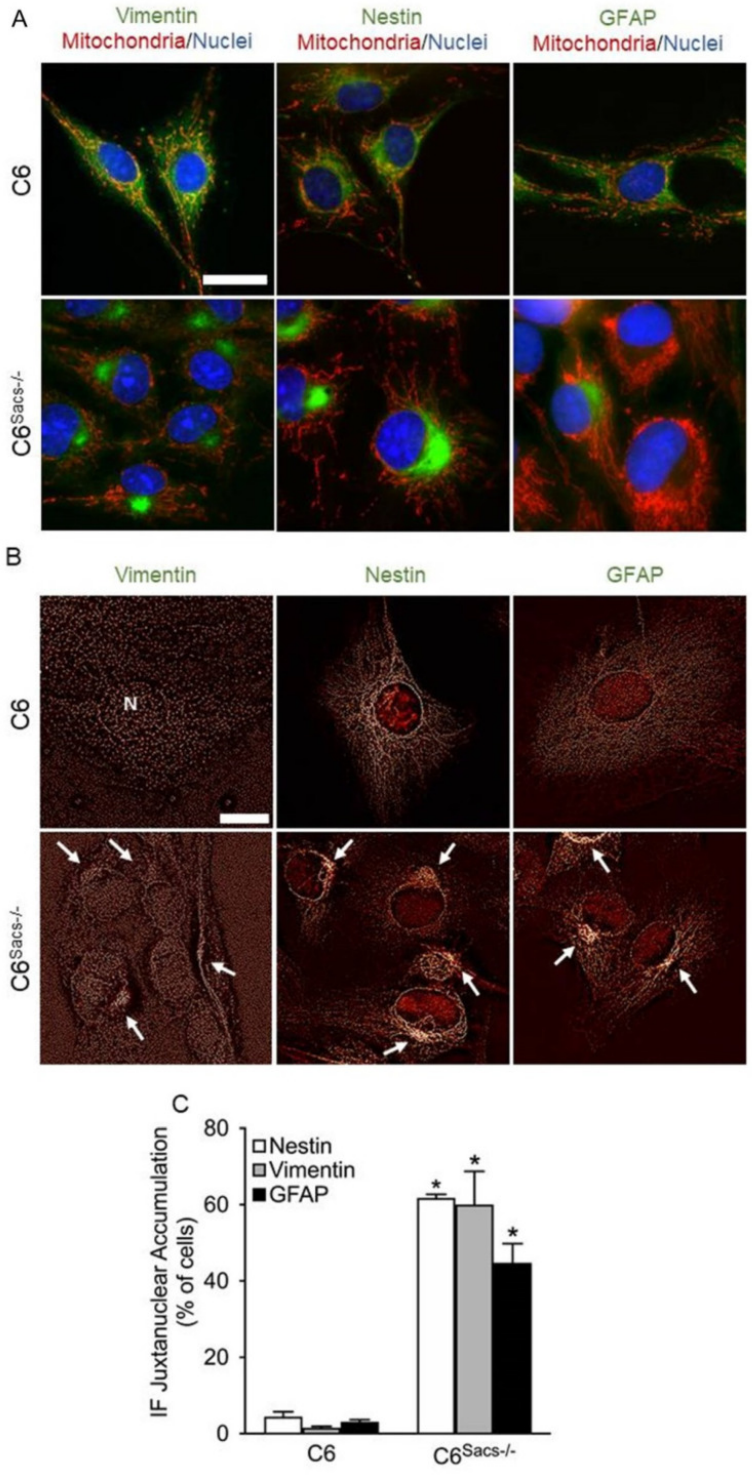
A
Vimentin
Mitochondria/Nuclei
Nestin
Mitochondria/Nuclei
GFAP
Mitochondria/Nuclei
C6
C6Sacs-/-
B
Vimentin
Nestin
GFAP
C6
N
C6Sacs-/-
C
IF Juxtanuclear Accumulation (% of cells)
80
60
40
20
0
Nestin
Vimentin
GFAP
*
*
*
C6
C6Sacs-/-

Figure 14: Sacsin deletion disrupts glial intermediate filament networks. (A) Representative immunocytochemistry images showing the distribution of the glial intermediate filaments vimentin, nestin and GFAP (green); mitochondria (Mitotracker, red); and nuclei (Hoechst, blue) in C6 and C6$^{Sacs-/-}$ cells. Vimentin, nestin and GFAP accumulate in the juxtanuclear area in C6$^{Sacs-/-}$ cells. Scale bar, 20 µm. **(B)** Widefield images of C6 and C6$^{Sacs-/-}$ cells were further analysed by means of the Nano J Super-Resolution Radial Fluctuations (SRRF) algorithm, which provided higher resolution details to obtain a more defined image of the intermediate filament networks. N, nucleus. White arrows, intermediate filament aggregates. Scale bar, 20 µm. **(C)** Quantification of microscopy images from 3 independent experiments (mean ± SEM). *, significant vs. C6 reference strain ($p < 0.05$, Student's t-test). The total numbers of reference C6 cells counted in 3 independent experiments were 549 (GFAP), 464 (Nestin) and 353 (Vimentin). The total numbers of C6$^{Sacs-/-}$ cells counted in 3 independent experiments were 836 (GFAP), 697 (Nestin) and 438 (Vimentin).

The protein levels of glial IFs were generally higher in C6$^{Sacs-/-}$ than in reference C6 cells (Fig.15A), but the increase in nestin levels did not achieve significance (Fig.15B). Filter trap assays supported the aggregation of these IFs (Fig.15C), although the increase in vimentin aggregation did not achieve statistical significance (Fig.15D). Further analysis of organelles and cytoskeletal components indicated that alterations are not restricted to mitochondria or intermediate filaments. The plectin cytolinker that connects intermediate filaments to microtubules, actin filaments and various cellular components, has been identified as a sacsin interactor, and its distribution is altered in Purkinje cells and fibroblasts in ARSACS models (Bondio et al., 2023). In our C6$^{Sacs-/-}$ model, plectin also showed a change in the cellular distribution, being absent from the juxtanuclear region where the IFs accumulate, just like mitochondria (Fig.16A,B). This is consistent with reports showing that plectin co-localizes with mitochondria in striated muscle (Reipert et al., 1999) or directly binds to both vimentin and mitochondria (Winter et al., 2008). The Golgi apparatus also becomes dispersed upon sacsin deletion, distributing around IF aggregates (Fig.16A,B) as in

ARSACS patients´ fibroblasts (Duncan et al., 2017). However, no significant alterations were observed in the basic organization and distribution of actin or microtubule networks (Supplementary Fig.S3). Our results suggest that IF juxtanuclear accumulation pushes plectin, mitochondria and Golgi out of the dense bundles.

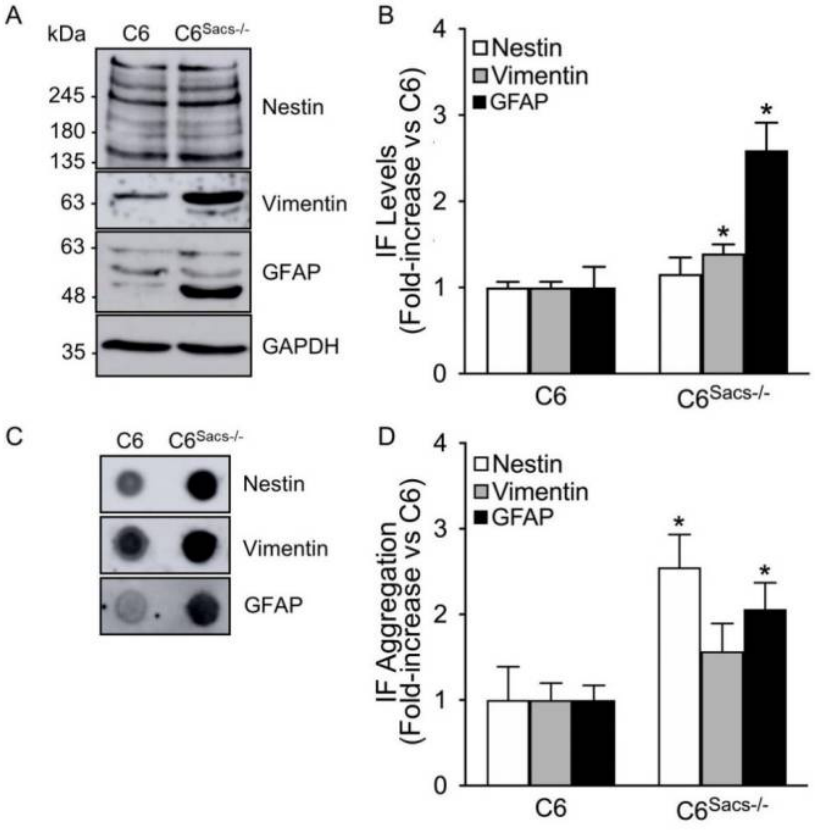

Figure 15: Sacsin deletion increases protein levels and aggregation of glial intermediate filaments. (A) Representative Western blots showing the expression patterns of the glial intermediate filaments. **(B)** Densitometric analysis of Western blots from at least 3 independent experiments normalized versus GAPDH. The levels of GFAP and vimentin proteins are increased in $C6^{Sacs-/-}$ cells. **(C)** Filter trap assays confirmed higher aggregation of intermediate filaments in $C6^{Sacs-/-}$ cells. **(D)** Densitometric analysis of filter traps normalized versus the reference C6 strain. *, significant vs. C6 reference strain ($p < 0.05$, Student's t-test).

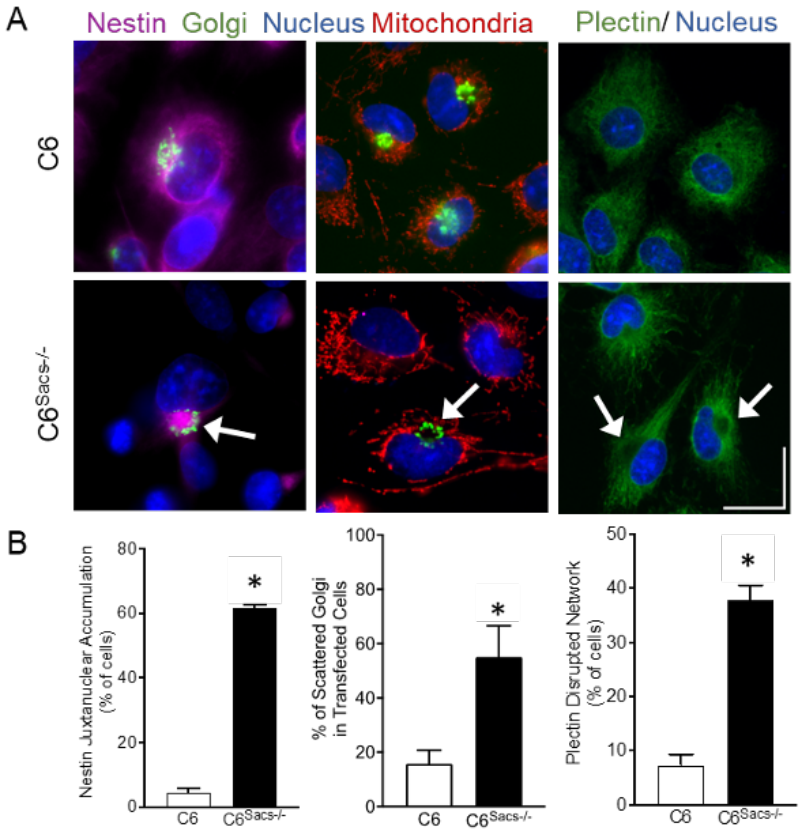

Figure 16: Sacsin deletion causes severe cytoskeletal-related alterations in C6 astroglial-like cells. (A) Representative immunofluorescence images show the Golgi apparatus, mitochondria, nestin and plectin distribution in C6 and C6$^{Sacs-/-}$ cells. Cells were transfected with EYFP-Golgi7 (green, Addgene plasmid # 56590) and immunostained with an antibody against nestin (magenta, Santa Cruz Biotechnologies, Sc-33677, 1:1000) or plectin (green, Santa Cruz Biotechnologies, Ref. Sc-33649, 1:1000). Mitochondria were counterstained with Mitoview Fix 640 (Biotium; Fremont, CA, USA) for 2h before imaging (red) and nuclei with Hoechst (blue). White arrows indicate abnormal distribution sites. Scale, 20 µm. **(B)** Images were analysed using ImageJ/Fiji software (Rasband, W.S., ImageJ, U. S. National Institutes of Health, Bethesda, Maryland, USA, https://imagej.net/ij/). Graphs show the mean ± SEM of at least 3 independent experiments, as indicated. Nestin: n=4, a total of 588 C6 cells and 995 C6$^{Sacs-/-}$ cells were considered. Golgi: n=3, 344 C6 cells and 322 C6$^{Sacs-/-}$ cells were considered. Plectin n=3, 464 C6 cells and 697 cells C6$^{Sacs-/-}$ cells. *, significant vs. C6 reference strain ($p < 0.05$, Student's t-test).

4.1.3.4. Sacsin Deletion Triggers Widespread Proteomic and Molecular Changes in C6 Cells

Such striking structural changes could either produce or be indicative of global molecular alterations in $C6^{Sacs-/-}$ cells, as has been observed in other cell and animal models of ARSACS (Morani et al., 2019, 2021, 2022; L. E. L. Romano et al., 2022). Label-free proteomics were carried out on C6 and $C6^{Sacs-/-}$ native protein extracts to identify possible alterations in our glial cell model of ARSACS. We identified 1552 proteins: 1490 common to both C6 and $C6^{Sacs-/-}$ cells, 103 unique to C6 reference cells and 30 exclusives to $C6^{Sacs-/-}$ cells (Fig.17A). The expression of 140 proteins significantly differed between reference and $C6^{Sacs-/-}$ cells; 104 were downregulated, and 36 were upregulated (Fig.17B). Gene ontology analysis results showed that, according to biological process, differentially expressed proteins were enriched in terms such as cell adhesion and migration, cellular response to mechanical stimulus or negative regulation of cell proliferation (Fig.17C). According to the cellular component, differentially expressed proteins play a role in structural integrity (e.g. cytoskeleton, filopodium, podosomes and stress fibres) and cellular connection and communications (e.g. cell-cell adherent junction and focal adhesion proteins) (Fig.17D). These results are consistent with disorganization of the IF networks and alterations in the mechanical properties of cells and resemble proteome and transcriptome profiles found in other cell and animal models of ARSACS (Morani et al., 2019, 2021, 2022; L. E. L. Romano et al., 2022).

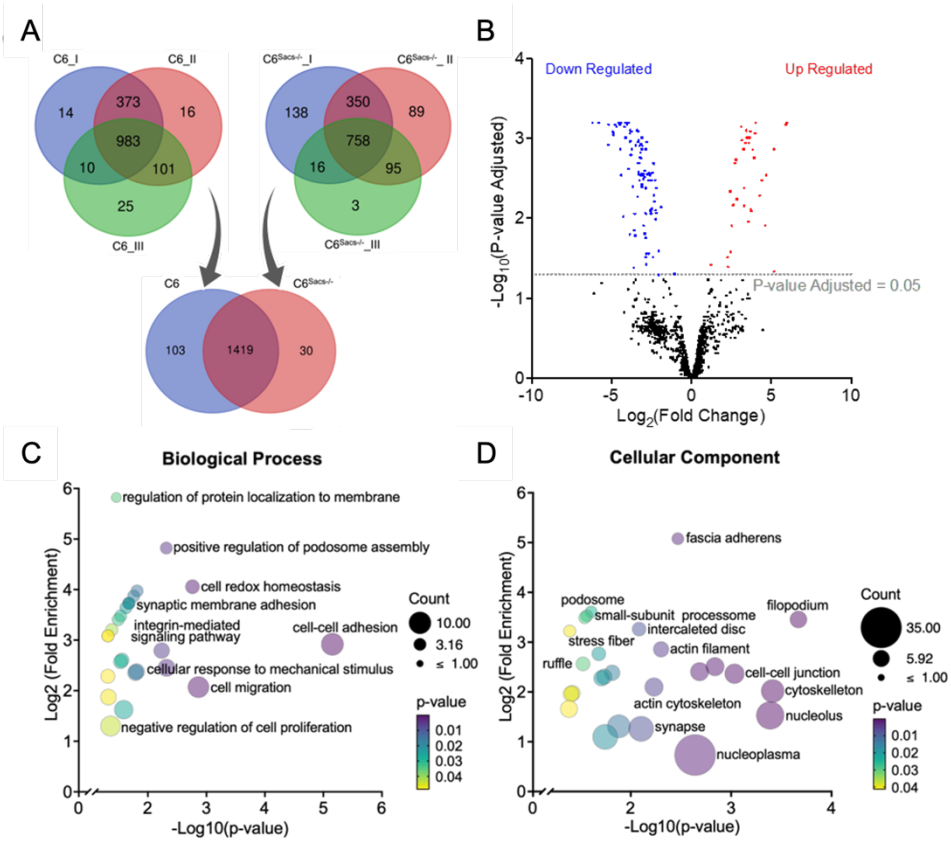

Figure 17: Sacsin deletion produces profound changes in functions associated with cell motility and mechanics. (A) Venn diagram illustrating the number of proteins detected in 3 replicates of C6 and C6$^{Sacs-/-}$ cells. The overlapping areas indicate the numbers of commonly expressed proteins. **(B)** LFQ values were used to quantify proteins with at least two LFQ values in one replicate group and more than one unique peptide. Log2 transformed LFQ values were normalized by the median of proteins detected in all samples. Missing value imputation was applied with the knn algorithm (1 missing replicate) or with the minimum LFQ of each sample (>1 missing replicate). Differential expression was tested with the limma R package (Ritchie et al., 2015). Adjusted p-values<0.05 were considered significant. The R code is available at https://github.com/GamaPintoLab/sacsin/. Black, unchanged proteins; red, upregulated; blue, downregulated; the horizontal dashed line indicates adjusted p-value = 0.05. **(C, D)** Functional enrichment analysis was done with Database for Annotation, Visualization and Integrated Discovery (DAVID, https://david.ncifcrf.gov/). Terms with adjusted p values <0.05 were selected.

4.1.3.5. Sacsin Deletion Produces Profound Changes in Functions Associated with Cell Motility and Mechanics

In fact, IFs are essential for the maintenance of mechanical and viscoelastic properties of cells (Pogoda & Janmey, 2023; Sivaramakrishnan et al., 2008), but these properties have never been tested in ARSACS models. This approach allowed us to produce a topology map, i.e. the height of the different sections of the cell body a given amount (Fig. 18A), as well as an elasticity map, i.e. a measure of the pressure needed to deform the different sections of the cell body (Fig.18B), for each cell. The highest point of cells corresponded to the location of the nucleus, which later served as reference for comparisons: in Fig. 18C, R is the radial distance from the highest point. We thus confirmed a significant decrease in the apparent Young modulus of $C6^{Sacs-/-}$ cells as we moved farther from the nucleus. In a radius R lower than 5 µm around the highest point (Fig.18C, top graph), still, on top of the nuclei, elasticity was similar in both cell strains. In a radius below 10 µm, including the perinuclear region of the cytoplasm, elasticity is already significantly lower in cells losing sacsin. The difference in elasticity reaches its maximum beyond this region in the cytoplasm (Fig.18C, bottom graph). These results further support the structural alterations we described in the cytoplasmic cytoskeleton, leading to lower elasticity and higher stiffness of the cytoplasmic regions. In contrast, the elasticity of the nuclear region, mainly supported by nuclear lamin IFs, seems unaffected by sacsin loss.

The widespread mechanical and cytoskeletal alterations described in C6 cells upon sacsin loss could strongly impact cell proliferation and motility, and these astroglial functions are especially relevant in severe neuroinflammation (Kwon & Koh, 2020). To evaluate this possibility, we carried out Wound healing assays and cell cycle analysis of C6 and $C6^{Sacs-/-}$

cells. Consistently, C6$^{Sacs-/-}$ cells showed a significantly delayed wound closure response after 24 h (Fig.18D), a decrease in the proportion of cells in G0/G1 phase and a higher proportion of cells in G2/M phase (Fig.18E). These results suggest that sacsin loss disrupts C6 proliferation and motility.

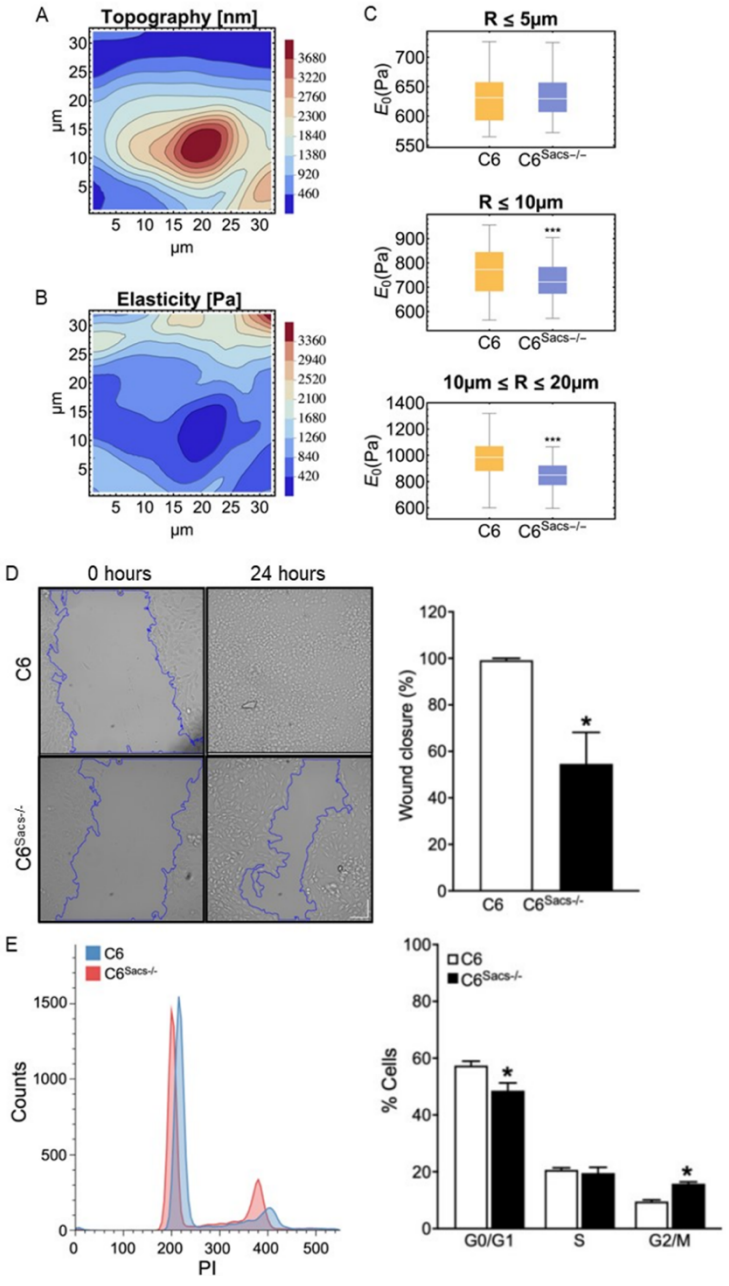

Figure 18: Mechanical alterations caused by sacsin loss and IF disorganization in C6 cells. (A) Topology of an example cell. The colour code of the contour plot indicates height (Z dimension) in nm. The X and Y axis indicate distance in these two horizontal dimensions in µm. **(B)** Contour Plot of the elasticity modulus (in Pascals, Pa) of the example cell in (A). The X and Y axis indicate distance in these two horizontal dimensions in µm. **(C)** Box plots of the elastic modulus (E0, in Pascals) obtained within a radius of 5 µm (top graph), 10 µm (middle graph) and between 10 and 20 µm (bottom graph) from the cell top, respectively. R = distance from the cell top. **(D)** Wound healing assay: Representative brightfield microscopy images were acquired at 0 and 24h after scratch (Scale bar, 75 µm) and quantification of the percentage of wound closure at 24 hours post scratch in 3 independent experiments (mean ± SEM). The gap distance was quantitatively evaluated using the Wound healing size tool plugin of ImageJ*TM* software. *, significant vs. C6 cells ($p < 0.05$, Student's t-test). **(E)** Representative cell cycle profiles of C6 and $C6^{Sacs-/-}$ cells based on the intensity of DNA staining by propidium iodide, and quantitative analysis of the distribution of the cells in each phase of the cell cycle. Data are represented as the mean ± SEM of 4 independent experiments. *, significant vs. C6 reference strain ($p < 0.05$, Student's t-test). Flow cytometry data were analysed by means of Floreada online software (https://floreada.io/).

4.1.3.6. Sacsin Deletion Produces Alterations in the Response to Inflammatory Cytokines

Astroglia participates in neuroinflammation, where cytokine signalling plays a key role (Herrmann et al., 2008), and IFs are currently considered important scaffolds actively involved in signal transduction (Muñoz-Lasso et al., 2020). We hypothesized that sacsin deletion could interfere with specific signalling/ inflammatory pathways, such as the Signal Transducer and Activator of Transcription 3 (STAT3) pathway, which plays key roles in neuroinflammation (X. Wang et al., 2021; J. Zhao et al., 2020). Reference C6 cells respond poorly to LIF, IL-6 (Fig.19A) and Tumor Necrosis Factor-alpha (data not shown). However, they show STAT3 activation after 20 min of incubation with IL-6 in combination with its soluble receptor IL-6R (Fig.19A–E), as determined by key STAT3 post-translational modifications,

such as Y705 and S727 phosphorylation or K49 acetylation. This activation is accompanied by a significant increase in total STAT3 levels, which is not observed in C6$^{Sacs-/-}$ cells (Fig.19B). The lower levels of total STAT3 C6$^{Sacs-/-}$ cells could explain why we also observe lower levels of post-translational modifications in these cells, as the corresponding PTM/total STAT3 ratios are not significantly different from reference C6 cells (Fig.19C–E). These results suggest that the impairment in STAT3 signalling is not by direct regulation of STAT3 modifications but by regulation of STAT3 levels, a hypothesis that is consistent with sacsin's role as a chaperone.

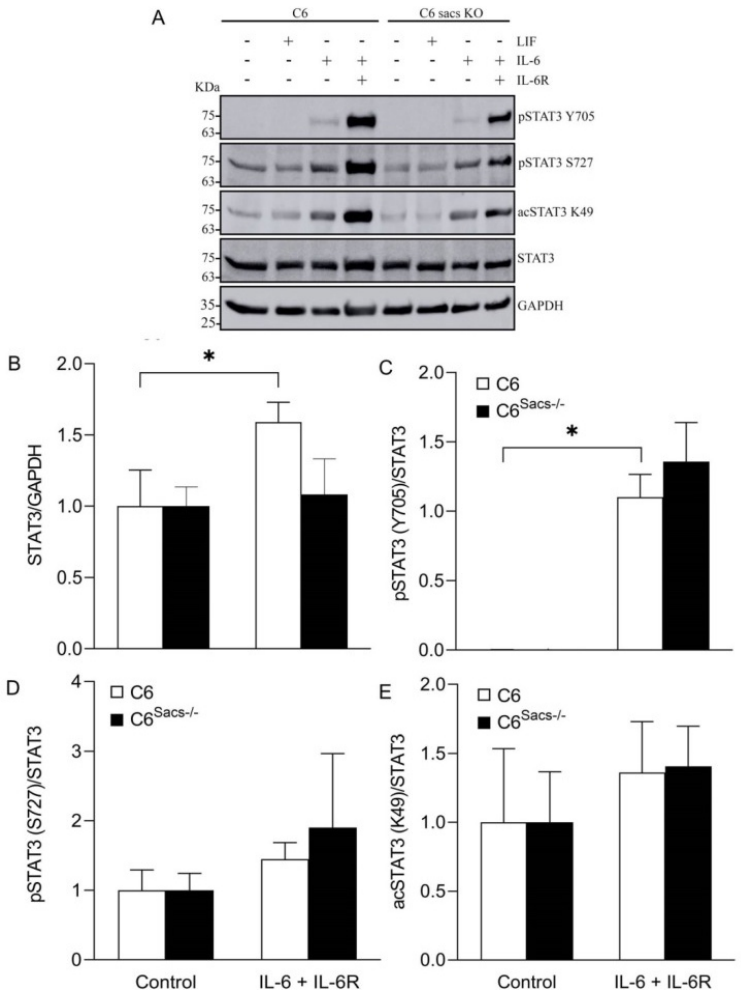

Figure 19: Sacsin deletion impairs response to inflammatory cytokines. Reference C6 and C6$^{Sacs-/-}$ strains were incubated with LIF and IL-6 cytokines (200 and 30 ng/mL, respectively) for 20 min, but a strong response was only observed upon the addition of the soluble IL-6 receptor (IL-6R, 60 ng/mL) in combination with IL-6. Rate-limiting, post-translational modifications of STAT3 were used as surrogates of STAT3 activation, namely Y705 and S727 phosphorylation and K49 acetylation. **(A)** Representative Western blot images. **(B–E)** Densitometry analysis of bands from at least 3 independent experiments normalized to GAPDH or total STAT3. White bars, reference C6 cell strain; black bars, C6$^{Sacs-/-}$ cells. Data were analysed by means of two-way ANOVA, followed by a Tukey post hoc test. * $p < 0.05$, significant vs. IL-6+IL-6R in C6 cell strain.

4.1.3.7. Sacsin Deletion Induce Alterations in the Levels of Key Regulators of Stress-associated Pathways

Proteomics analyses of C6 and C6$^{Sacs-/-}$ protein extracts also suggested possible alterations in the levels of Endoplasmic reticulum oxidase 1 (ERO1), NAD(P)H:quinone oxidoreductase (NQO1), Glutaredoxin 3 (GLRX3) and E3 ubiquitin ligase (Ube3A) which we tried to confirm individually by immunoblotting (Fig.20). We confirmed reduced levels of ERO1 and NQO1 upon sacsin deletion in C6 cells but did not find significant alterations in GLRX3 levels. ERO1, a thiol oxidase, is essential for the oxidative process of protein folding within the ER, and an increase in oxidative protein folding can lead to generation of ROS in the ER (Bhandary et al., 2012). ERO1 is overexpressed in cancer and altered in diabetes and neurodegenerative diseases (Shergalis et al., 2020). The reduction of ERO1 levels observed in C6$^{Sacs-/-}$ cells can also disrupt the redox equilibrium and accumulate misfolded proteins in the ER. Proteomic analysis in other ARSACS models showed involvement of ER calcium-binding proteins associated with protein folding quality control, such as the chaperone calreticulin (CALR) (Morani et al., 2022). Additionally, impaired ER and mitochondrial trafficking to distal dendrites may be the cause of Ca^{2+}

dysregulation in these locations (Bondio et al., 2023). These observations suggest a connection between the ER and ARSACS. NQO1 is a chemoprotective enzyme against the harmful oxidative effects of quinones (Ross & Siegel, 2021). The absence of this enzyme can result in alterations in intracellular redox state and seizures, suggesting an important role of the protein in the CNS. Neurones do not contain significant amounts of this protein, but it is relatively abundant in glial cells (Stringer et al., 2004). NQO1 was also reduced in another ataxia, SCA17, but increased in patients with Alzheimer's disease (L. C. Lee et al., 2014; SantaCruz et al., 2004).

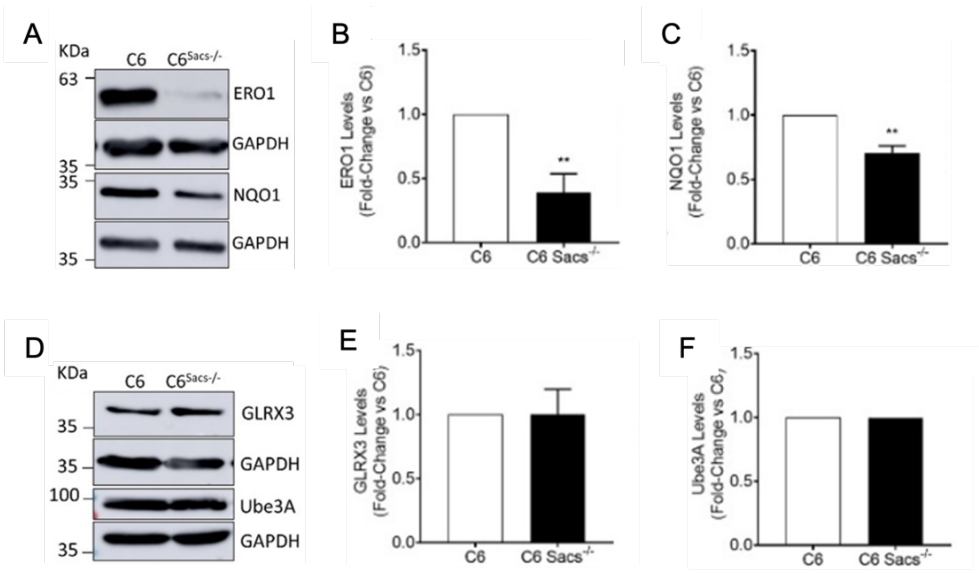

Figure 20: Sacsin deletion in C6 cells leads to alterations in various intracellular pathways. (A, D) Representative Western blots showing ERO1, NQO1, GLRX3 and Ube3A expression levels in C6 and C6$^{Sacs-/-}$ cells. **(B, C, E, F)** Densitometric analysis of Western blots normalized to the loading control, GAPDH. Fold-change representation of ERO1, NQO1, GLRX3 and Ube3A, compared to C6 reference strain. NQO1 and ERO1 were downregulated (p-value = 0.0054 and p-value = 0.0065, respectively, unpaired Student's t-test).

4.1.3.8. Sacsin Deletion Induce Alterations in the Levels of SMAD1, a Transcription Factor Relevant for Development and Neuroinflammation

We have previously shown that C6$^{Sacs-/-}$ cells show alterations in cytokine pathways relevant to development and neuroinflammation, such as STAT3 (Murtinheira et al., 2022). Smad1 is a transcription factor that mediates TGF-beta and Bone Morphogenetic Proteins (BMPs), and that is relevant for development and neuroinflammation. We and others have shown that Smad1 also forms complexes with STAT3, bridged by p300/CBP, and both pathways can have synergistic effects in the expression of glial-specific genes, such as GFAP (Herrera et al., 2010). We observed that the levels of Smad1 were significantly decreased in C6$^{Sacs-/-}$ cells (Fig. 21).

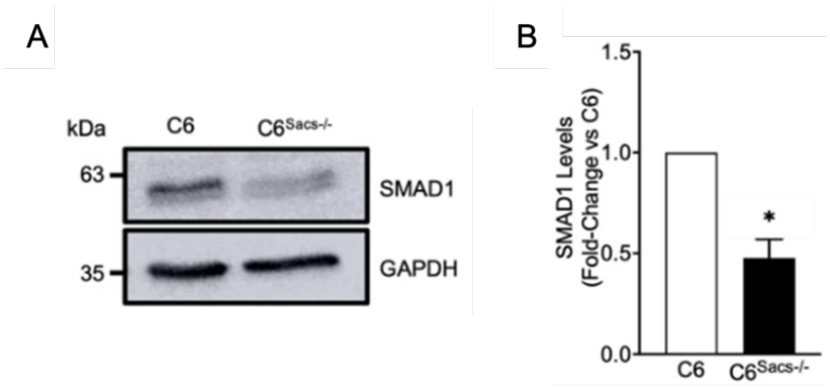

Figure 21: Sacsin deletion inhibits the expression of key developmental transcription factor Smad1 in astroglial cell model of ARSACS. (A) Representative Western blots showing SMAD1 expression levels in C6 and C6$^{Sacs-/-}$ cells. **(B)** Densitometric analysis of Western blots normalized to the loading control, GAPDH. Fold-change representation of SMAD1, compared to C6 reference strain. Data are represented as the mean ± SEM. *, significant vs. C6 reference strain ($p < 0.05$, Student's t-test).

4.1.4. Discussion

Sacsin mRNA is present in most tissues, although its expression levels show some cell specificity (source: The Protein Atlas). In the central nervous system, it was described to have higher levels in Purkinje cells, pyramidal neurones, thalamic and pontine nuclei and reticular formation (Larivière et al., 2015). However, public transcriptomics data indicated that sacsin is also expressed in glial cells, including astrocytes, Müller glia, oligodendrocyte precursor cells, mature oligodendrocytes and microglia (Clarke et al., 2018; Zhang et al., 2016). Astrocytes express sacsin RNA levels as high as neurones, especially in younger individuals (Clarke et al., 2018). Our results confirm that the sacsin protein is present at high levels in astrocytes, and possibly in microglia, since we could detect sacsin in N9 microglial cells.

To the best of our knowledge, scientific studies of sacsin function focused almost exclusively on neurones, and a possible role of glial cells in ARSACS pathogenesis is completely unknown. We developed a new cellular model to investigate the role of sacsin in glial cells based on C6 rat glioma cells (Fig.11). The fact that they are rodent cells will enable comparative studies in mice models of ARSACS and primary astroglial cells from rats. The loss of sacsin in C6 cells produces the accumulation of intermediate filaments - vimentin, nestin and GFAP - in the juxtanuclear area, where there is a concomitant depletion of mitochondria (Fig.14 and 15). These results are consistent with previous reports where sacsin knockout from human HEK-293T (embryonic kidney) and SH-SY5Y (neuroblastoma) cells induced alterations in vimentin and/or neurofilament networks (Duncan et al., 2017; Gentil et al., 2018). Sacsin is also expressed in keratinocytes and fibroblasts, and ARSACS patients showed skin alterations and lipofuscin deposits (Stevens et al., 2013). These data suggest that sacsin could have a far-reaching role in the organization and

dynamics of different intermediate filaments beyond neurons, and ARSACS could belong to the growing family of IF-pathies, as AxD or GAN (Didonna & Opal, 2019; Messing, 2018; Omary, 2009).

Although ARSACS, AxD and GAN are different genetic diseases with their own clinical profiles (Kuhn & Cascella, 2022; Messing, 2018; Tazir et al., 2009; Vermeer, van de Warrenburg, & Kamsteeg, 1993), the similarities between some of their symptoms (e.g., paediatric diagnosis, ataxia, dysarthria, nystagmus) and histopathological features (e.g., white matter loss, IF disruption and, at least in ARSACS and GAN mitochondrial dysmotility) are remarkable (Didonna & Opal, 2019; Israeli et al., 2016; Larivière et al., 2015; Lowery et al., 2016). The three pathologies have mixed features of neurodegenerative and neurodevelopmental disorders. Vimentin, nestin and GFAP are also typically found in neural precursor cells (Alvarez-Buylla et al., 2001; Dawley et al., 2012), and C6 cells show properties of both astroglia and neural precursor cells (S. J. Zhang et al., 2011; Zheng et al., 2007). Although we were unable to detect sacsin in adult neural precursor cells from the rat dentate gyrus and the subventricular zone (Data not shown), sacsin could regulate the organization of IFs in precursor cells during development, with potential implications for the disease onset. Our results should encourage further studies in these directions.

Oxidative stress and neuroinflammation are central to neurodegenerative diseases, and astrocytes are major players in these processes. IFs are involved in signal transduction as scaffolds for signalling proteins and mitochondrial motility (Muñoz-Lasso et al., 2020; Nekrasova et al., 2011), and disruption of GFAP alone in AxD models disrupts various signalling pathways (Jones et al., 2018). Our results indicate that sacsin deletion impairs the REDOX status of C6 cells and their response of cells to oxidative challenges and cytokines (Fig. 12 and 19). The impairment of

STAT3 signalling in $C6^{Sacs-/-}$ cells seems to be mediated by the regulation of STAT3 levels rather than its post-translational modifications (Fig.19). Bearing in mind the role of sacsin as a chaperone (Anderson et al., 2011; Parfitt et al., 2009), it is possible that it contributes directly or indirectly to STAT3 folding or stability. The consequences of disrupting the response of glia to inflammatory cues are difficult to predict, but could be relevant for disease onset and progression, especially if this disruption affects both astroglia and microglia.

In summary, to the best of our knowledge, our study is the first to show that astrocytes express sacsin at the protein level and that their depletion in glial-like cells causes pathological hallmarks of ARSACS similar to those observed in neuronal cells. Sacsin knockout cells showed a dysregulation in their REDOX balance and altered responses to inflammatory cues. These data support a potential role of astroglia, microglia or even neural precursor cells in ARSACS, which should be further analysed. Future studies should test our findings in *post-mortem* brain tissues from ARSACS patients and existing mouse models of the disease and analyse how the functions of primary astroglia are disrupted by sacsin loss. Considering the developmental nature of ARSACS, these studies should probably focus on embryonic or perinatal stages.

4.1.5. Supplementary material

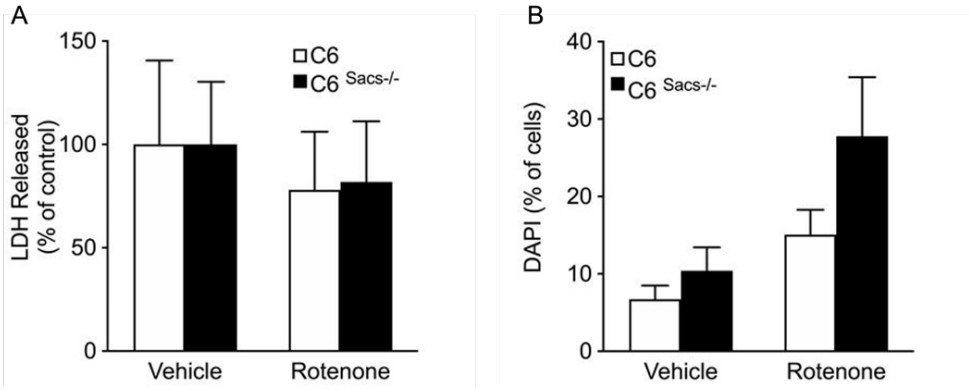

Figure S 1: Toxicity of short treatment of rotenone in C6 strains. (A) Released LDH was determined after incubation of C6 strains with rotenone 5 µM for 4 h and normalized versus total LDH and control values. No significant changes in LDH released were registered. **(B)** Incubation with rotenone for 4 h increases slightly the percentage of DAPI-positive cells in both C6 cell strains, the differences not achieving statistical significance. Graphs show the average of 3 independent experiments (mean ± SEM), data were analysed by means of two-way ANOVA, followed by a Tukey post-hoc test. Significance threshold was $p < 0.05$.

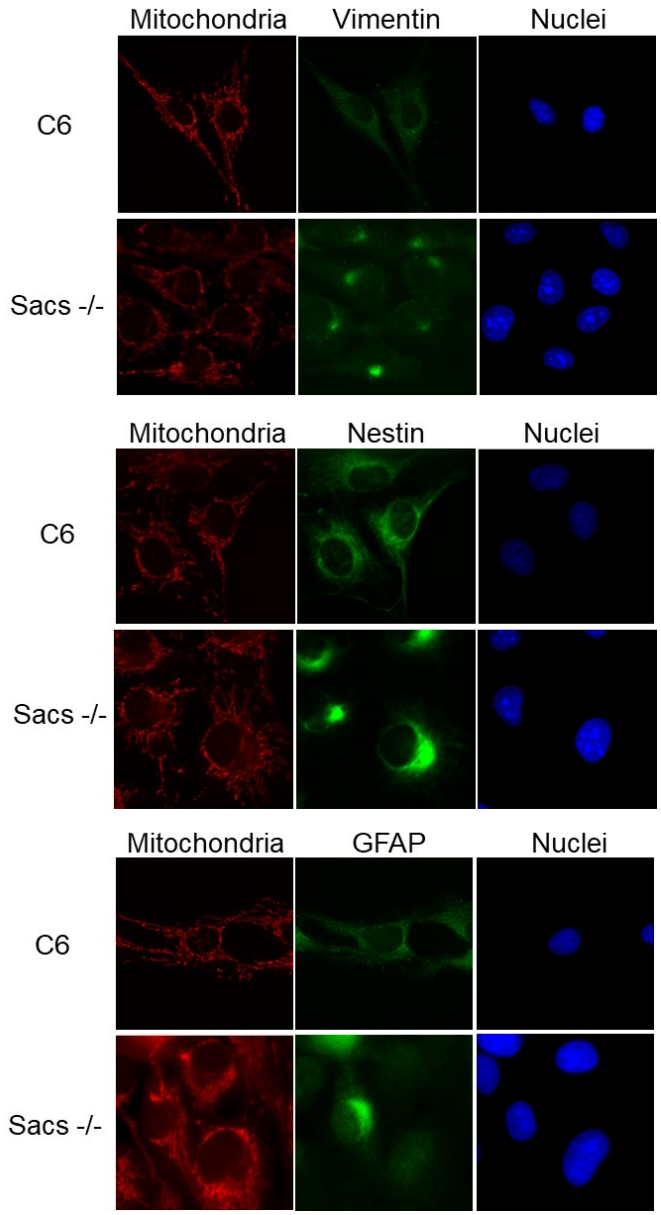

Figure S 2: Separation of channels corresponding to Figure 14A. Representative immunocytochemistry images showing the distribution of the glial intermediate filaments vimentin, nestin and GFAP (green), mitochondria (Mitotracker, red) and nuclei (Hoechst, blue) in C6 and $C6^{Sacs-/-}$ cells. Vimentin, nestin and GFAP accumulate in the juxtanuclear area in $C6^{Sacs-/-}$ cells.

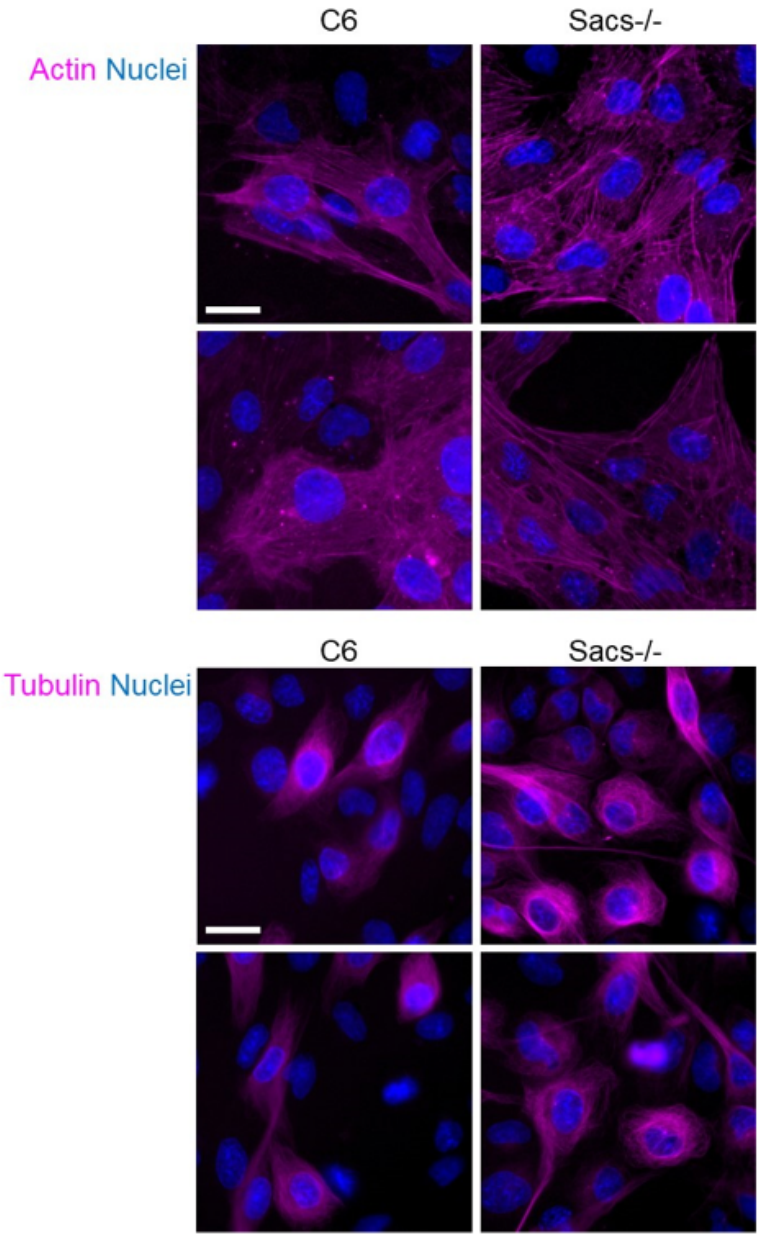

Figure S 3: Sacsin knockout does not produce gross changes in actin and microtubule networks. Representative immunocytochemistry images showing the distribution of actin microfilaments or microtubules (magenta) and nuclei (Hoechst, blue) in C6 and C6$^{Sacs-/-}$ cells. Live cells were stained with sirActin kit (Spirochrome) and Tubulin tracker deep red (Invitrogen) following manufacturer´s instructions. Scale bar, 20 µM.

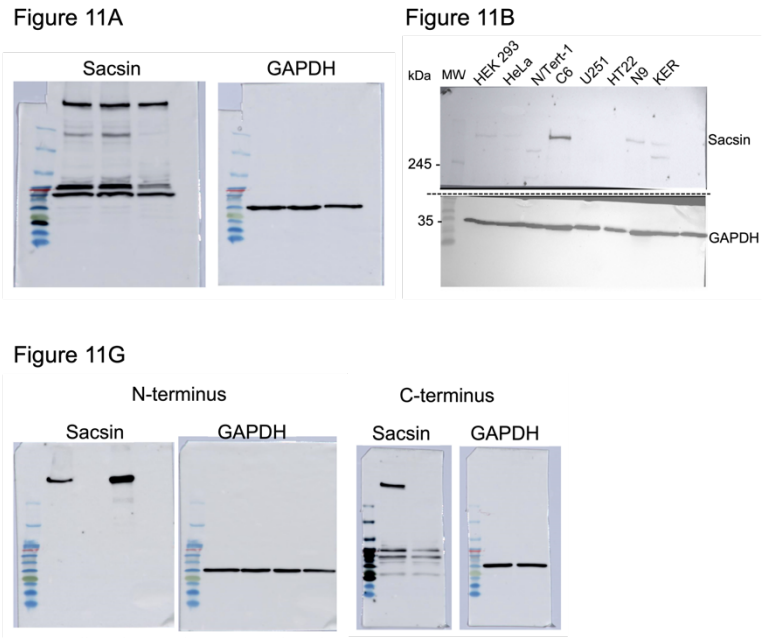

Figure S 4: Full membranes and molecular weight markers for western blots in Figure 11.

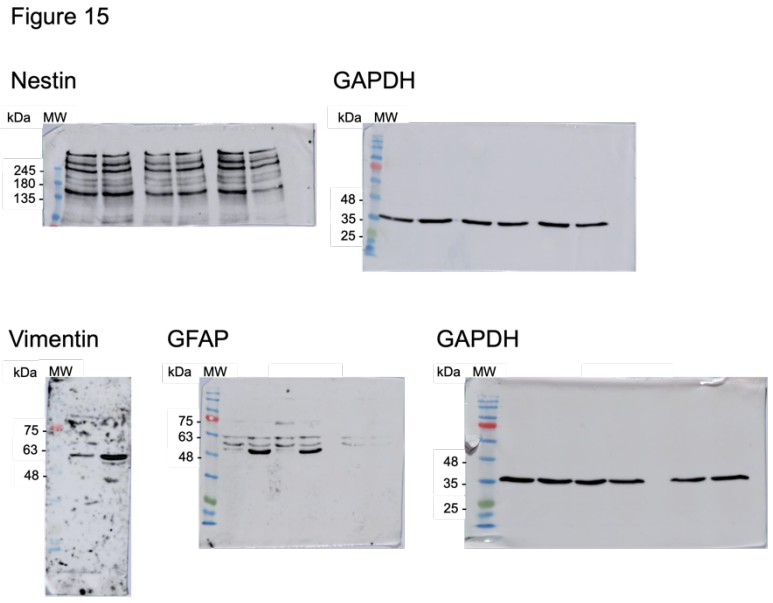

Figure S 5: Full membranes and molecular weight markers for western blots in Figure 15.

Figure 19

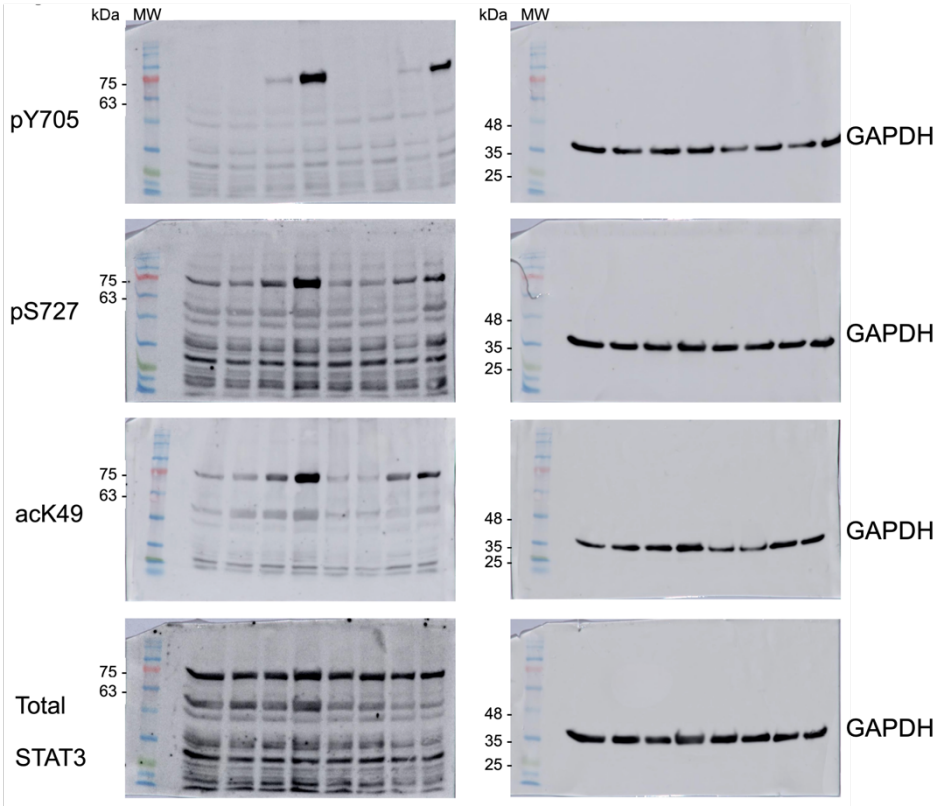

Figure S 6: Full membranes and molecular weight markers for western blots in Figure 19.

4.2. DEVELOPMENT AND CHARACTERIZATION OF THE FIRST HUMAN MICROGLIAL CELL MODEL OF ARSACS

4.2.1. Abstract

Autosomal recessive spastic ataxia of Charlevoix-Saguenay (ARSACS) is a rare disorder caused by loss-of-function mutations in the sacsin chaperone. Sacsin was initially described as a neuronal protein but is also found in astroglia and microglia. We developed and characterized a new microglial cell model of ARSACS based on human HMC3 cells. Sacs−/− HMC3 cells show aberrant distribution of vimentin and mitochondrial networks, and other alterations with potential consequences on neuroinflammation. Our results support a possible role for microglial cells in ARSACS and provide a new tool to understand glial-specific mechanisms involved in this pathology.

4.2.2. Introduction

Autosomal recessive spastic ataxia of Charlevoix-Saguenay (ARSACS) is caused by loss-of-function of the sacsin co-chaperone (Larivière et al., 2015). The actual biological functions of sacsin are barely understood. Structural analysis of the sacsin amino acid sequence predicted a ubiquitin-like domain, a J-domain and at least one nucleotide-binding domain, all of them indicative of functions in the ubiquitin-proteasome system (Parfitt et al., 2009). Sacsin actually binds to the proteasome and the ubiquitin ligases PARK2 and UBE3A, as well as neurodegeneration-related proteins synuclein and superoxide dismutase 1, among other proteins associated to proteostasis (retrieved from the Biogrid database), and prevents aggregation of ataxin-1, a protein associated with Spinocerebellar Ataxia 1 (Parfitt et al., 2009). Sacsin also interacts with a few cytoskeletal (e.g. vimentin) and structural (e.g. actinin, JIP3), and plays a key role in the homeostasis of

intermediate filaments (IFs) and membrane organelle networks (Duncan et al., 2017; Francis et al., 2022; Gentil et al., 2018; Murtinheira et al., 2022; Pogoda & Janmey, 2023). The most obvious and striking consequence of sacsin deletion is the abnormal accumulation of IFs in thicker bundles or juxtanuclear aggregates. IFs are the most diverse and flexible (yet least dynamic) element of the cytoskeleton, providing structural support and maintaining cell and tissue shape, especially under mechanical tensions (Pogoda & Janmey, 2023). The mechanical properties of cells are important for a wide range of cellular functions, such as cell migration, division, and differentiation. Very importantly, IFs are scaffolds involved in signal transduction and distribution of membrane organelles, such as mitochondria, lysosomes and the Golgi apparatus. It is therefore not surprising that ARSACS models systematically show abnormal distribution and function of these organelles (Duncan et al., 2017; Francis et al., 2022; Murtinheira et al., 2022, 2024).

According to public databases (The Protein Atlas, Harmonizome and BrainRNASeq), sacsin is far from being a neuron-specific protein, showing a relatively ubiquitous expression pattern in both neural and non-neural tissues. We and others have confirmed that astroglial and microglial cells express medium-high levels of sacsin mRNA and protein (Murtinheira et al., 2022; Y. Zhang et al., 2016). Knockout of sacsin in astroglial-like C6 rat glioblastoma cells led to dysregulation of the three main astroglial IFs (Nestin, Glial Fibrillary Acidic Protein and Vimentin); alterations in mitochondrial and Golgi morphology and distribution; loss of elasticity; higher sensitivity to stress; decrease in the expression of key stress-, development- and neuroinflammation-related proteins, such as the oxidase ERO1 and the transcription factors STAT3 or SMAD1; and alterations in the response to cytokines related to both neural development and neuroinflammation (Murtinheira et al., 2022, 2024). Additionally, increased

astroglial and microglial markers of neuroinflammation have been found in ARSACS (Bondio et al., 2023). However, the potential role for glial cell dysfunction in ARSACS is completely unknown due, at least in part, to the lack of glial models of the disease.

Here, we aimed at developing a new human microglial model of ARSACS based on HMC3 cells (ATCC Ref. CRL-3304). HMC3 cells are currently the reference human microglial cell line, originally immortalized via the SV40 antigen from primary human microglia (Dello Russo et al., 2018). They express the main microglial cell markers, and their behaviour is consistent with microglial cells, including the secretion of inflammatory cytokines in response to bacterial lipopolysaccharide (LPS) or amyloid beta peptides.

4.2.3. Results

4.2.3.1. Sacsin Deletion in HMC3 Cells Disrupts Vimentin and Mitochondrial Networks

HMC3 cells were knocked out for sacsin as previously described, using a CRISPR/Cas9 tool commercially available (Santa Cruz Biotechnology) and a FACSAria III cell sorter (BD Biosciences) (Murtinheira et al., 2022). Resulting clones were tested for loss of sacsin expression by immunoblotting with a specific antibody (Fig.22A, Fig.23A) and one of the $HMC3^{Sacs-/-}$ clones (C2) was selected for further characterization by immunoblotting and immunocytochemistry, as previously described (Murtinheira et al., 2022, 2024). Microglial cells express vimentin as their main IF, but do not express GFAP or Nestin, as C6 cells and astrocytes. While vimentin levels do not change upon sacsin deletion (Fig.22A), their filaments collapse into the juxtanuclear region in >80% of cells (Fig.22B,C). Mitochondrial networks are pushed out of this region and their morphology is substantially different from wild-type HMC3 cells, where mitochondria are

more abundant but smaller in average and distribute homogeneously through the cytoplasm (Fig.22B).

4.2.3.2. Sacsin Deletion in HMC3 Human Microglial Cells Impairs Mitochondrial Dynamics

The morphology and distribution of mitochondrial networks are the result of a fine balance between fission and fusion events, and these alterations deserve further attention. Quantitative RT-PCR was carried out as previously described (Garcia et al., 2022) to analyse possible alterations in the mRNA levels of fission 1 protein (DRP1) and mitofusin-2 (MFN-2), two markers of mitochondrial fission and fusion, respectively. HMC3$^{Sacs-/-}$ cells showed increased levels of both DRP1 and MFN-2 (Fig.22D), consistent with alterations in the distribution and morphology of mitochondrial networks. Perturbations in mitochondrial morphologies in ARSACS are frequently consistent with hyperfusion or decreased fission, both of which resemble Drp1 knockdown or deficiency (Bradshaw et al., 2016; Girard, Larivière, et al., 2012). Sacsin interacts with Drp1, and sacsin loss produces an increase in the density of Drp1-positive foci, but a decrease in their co-localization with mitochondria, their diameter and intensity (Bradshaw et al., 2016). However, other reports show no change or a non-significant increase in certain conditions (Louit et al., 2023). In sacsin-knockout SH-SY5Y cells, MFN-2 was not found altered at a protein level, and it decreased in response to stress (Morani et al., 2019). To the best of our knowledge, this is the first time an alteration in MFN-2 expression has been observed in the context of ARSACS. The differences between our results and the literature may be due to cell type-specific adaptation to the lack of sacsin.

4.2.3.3. Sacsin Deletion Induce Alterations in the Levels of Key Regulators of Stress-associated Pathways in HMC3 Cells

These morphological phenotypes were extremely similar to the C6 astroglial-like model of ARSACS, where we had recently confirmed downregulation of the development- and neuroinflammation-related transcription factors STAT3 and SMAD1, and the ER-stress related protein ERO1; and upregulation of autophagy-related protein LC3 (Murtinheira et al., 2022, 2024). In HMC3$^{Sacs-/-}$ cells, STAT3, SMAD1 and ERO1 levels are significantly decreased, the latter virtually disappearing (Fig.22E). In contrast, LC3 protein showed no significant alterations. This differs from both our results in C6 cells and the decrease in LC3 levels observed in SHSY5Y human neuroblastoma cells knocked out for sacsin (Morani et al., 2021). These results suggest that alterations in autophagy could be cell type-dependent. However, to be completely comparable, further analyses should be carried out to understand how the autophagic flux is altered in C6 and HMC3 cells (Morani et al., 2021). We also analysed the expression levels of NAD(*P*)H:quinone oxidoreductase (NQO1) and Glutaredoxin 3 (GLRX3), two stress-related proteins for which we had more variable, non-significant alterations in the C6 model (Murtinheira et al., 2024). NQO1 and GLRX3 did not display significant alterations in HMC3$^{Sacs-/-}$ cells, although GLRX3 showed a tendency to decrease (Fig.22E).

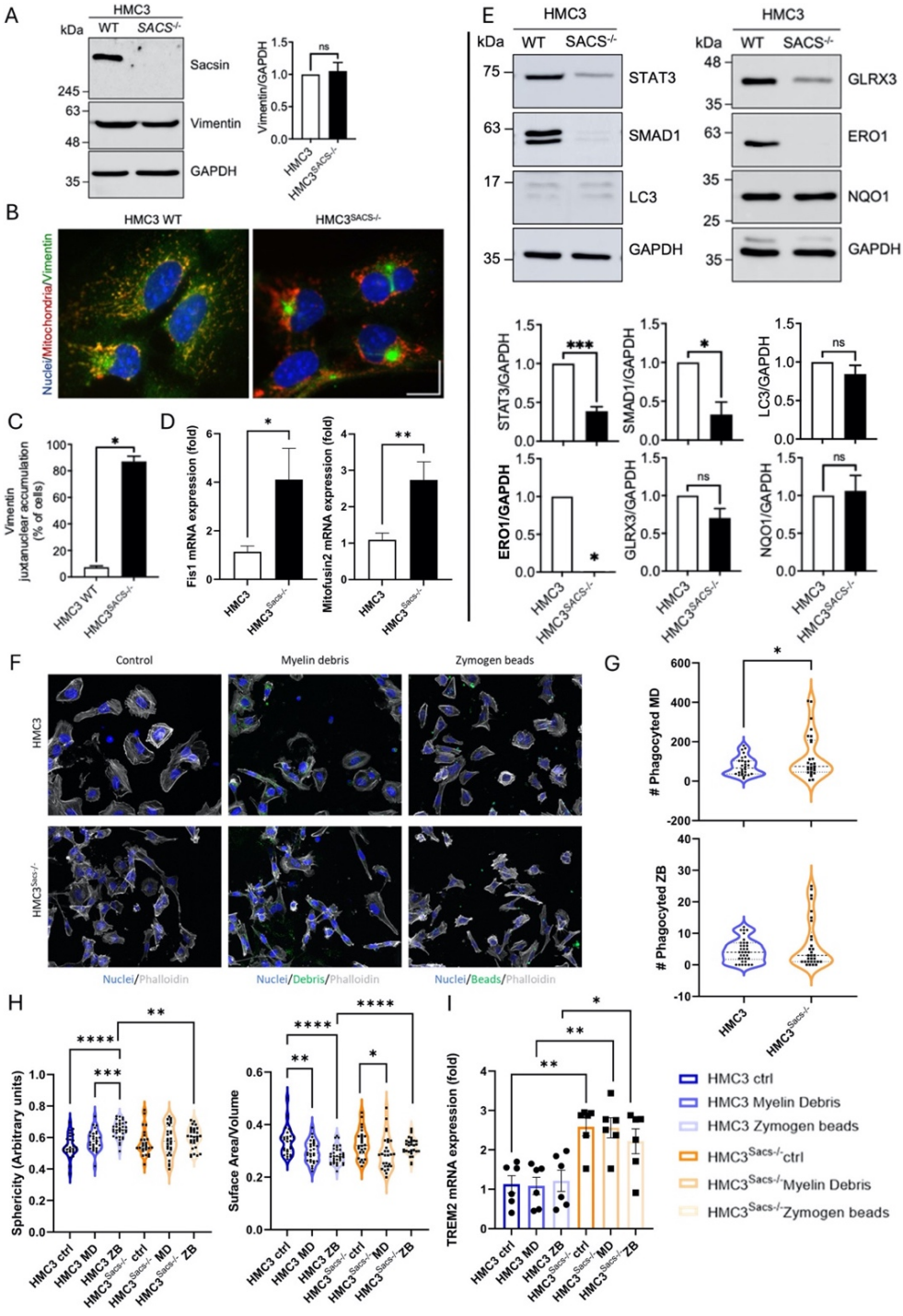
A
HMC3
kDa
WT
SACS-/-
Sacsin
Vimentin
GAPDH
245
63
48
35
Vimentin/GAPDH
ns
HMC3
HMC3SACS-/-
B
HMC3 WT
HMC3SACS-/-
Nuclei/Mitochondria/Vimentin
C
Vimentin juxtanuclear accumulation (% of cells)
*
HMC3 WT
HMC3SACS-/-
D
Fis1 mRNA expression (fold)
*
Mitofusin2 mRNA expression (fold)
**
HMC3
HMC3Sacs-/-
E
HMC3
kDa
WT
SACS-/-
75
STAT3
63
SMAD1
17
LC3
35
GAPDH
48
35
GLRX3
63
ERO1
35
NQO1
25
35
GAPDH
STAT3/GAPDH
***
SMAD1/GAPDH
*
LC3/GAPDH
ns
ERO1/GAPDH
*
GLRX3/GAPDH
ns
NQO1/GAPDH
ns
HMC3
HMC3SACS-/-
F
Control
Myelin debris
Zymogen beads
HMC3
HMC3Sacs-/-
Nuclei/Phalloidin
Nuclei/Debris/Phalloidin
Nuclei/Beads/Phalloidin
G
Phagocyted MD
*
Phagocyted ZB
HMC3
HMC3Sacs-/-
H
Sphericity (Arbitrary units)
Suface Area/Volume
HMC3 ctrl
HMC3 MD
HMC3 ZB
HMC3Sacs-/- ctrl
HMC3Sacs-/- MD
HMC3Sacs-/- ZB
I
TREM2 mRNA expression (fold)
HMC3 ctrl
HMC3 Myelin Debris
HMC3 Zymogen beads
HMC3Sacs-/-ctrl
HMC3Sacs-/-Myelin Debris
HMC3Sacs-/-Zymogen beads

Figure 22: Sacsin deletion disrupts vimentin networks, stress and neuroinflammation pathways, and phagocytic functions in HMC3 human microglial cells. (A) Representative Western blots of total cell lysates from HMC3 human microglial cells and an HMC3$^{Sacs-/-}$ clone showing the expression patterns of sacsin and vimentin. Vimentin bands from 3 independent experiments (n=3) were quantified by densitometry, and results were normalized versus GAPDH. **(B)** Representative immunocytochemistry images showing the distribution of vimentin (green); mitochondria (Mitoview, red) and nuclei (Hoechst, blue) in HMC3 and HMC3$^{Sacs-/-}$ cells. Scale bar 20 µm. **(C)** Microscopy images from 3 independent experiments were quantified (777 HMC3 reference cells and 831 HMC3$^{Sacs-/-}$ cells). **(D)** mRNA was extracted from HMC3 and HMC3$^{Sacs-/-}$ cells and the levels of DRP1 (Fis1) and MTN-2 were measured by quantitative RT-PCR, as previously described (Garcia et al., 2022). n=6 *, significant vs. HMC3 reference strain, $p < 0.05$ (Welch's t-test). **(E)** Representative Western blots showing the expression patterns of SMAD1, STAT3, LC3, GLRX3, ERO1 and NQO1. Densitometric analysis of Western blots from at least 3 independent experiments normalized versus GAPDH. Results represented as mean ± SEM. *, significant vs. HMC3 reference strain, $p < 0.05$ (Welch's t-test). **(F)** Representative images of wild-type HMC3 and HMC3$^{Sacs-/-}$ cells showing their ability to phagocyte myelin debris (green) or zymogen beads (green). **(G)** Quantification of myelin debris or zymogen beads phagocyted by HMC3 and HMC3$^{Sacs-/-}$ cells from 3 independent experiments (40 cells/experimental group). *, significant vs. wild-type HMC3 cells ($p < 0.05$, Welch's t-test). **(H)** Quantification of cell membrane sphericity and surface area to volume ratio of HMC3 wild-type and HMC3$^{Sacs-/-}$ cells from 3 independent experiments (40 cells/experimental group), using AIVIA software. **(I)** The mRNA levels of TREM2 were quantified by quantitative RT-PCR, n=6. (in G and I, *$p < 0.05$, **$p < 0.01$, ***$p < 0.001$, ****$p < 0.0001$, One-way ANOVA). (For interpretation of the references to colour in this figure legend, the reader is referred to the web version of this article.)

Analysis of two additional independent HMC3$^{Sacs-/-}$ clones indicated that these molecular features are largely clone-independent (Fig.23). The two additional clones also displayed alterations in vimentin distribution not associated with its expression levels (Fig.23A-D); and an overall decrease in STAT3, GLRX3 and ERO1 levels, that in some cases did not achieve statistical significance (Fig.23E-F). The expression levels of NQO1 were the most variable between clones, resembling our previous results in C6 cells: one of the clones

confirmed the original phenotype (i.e. no change) while the other showed increased expression levels (Fig.23E-F).

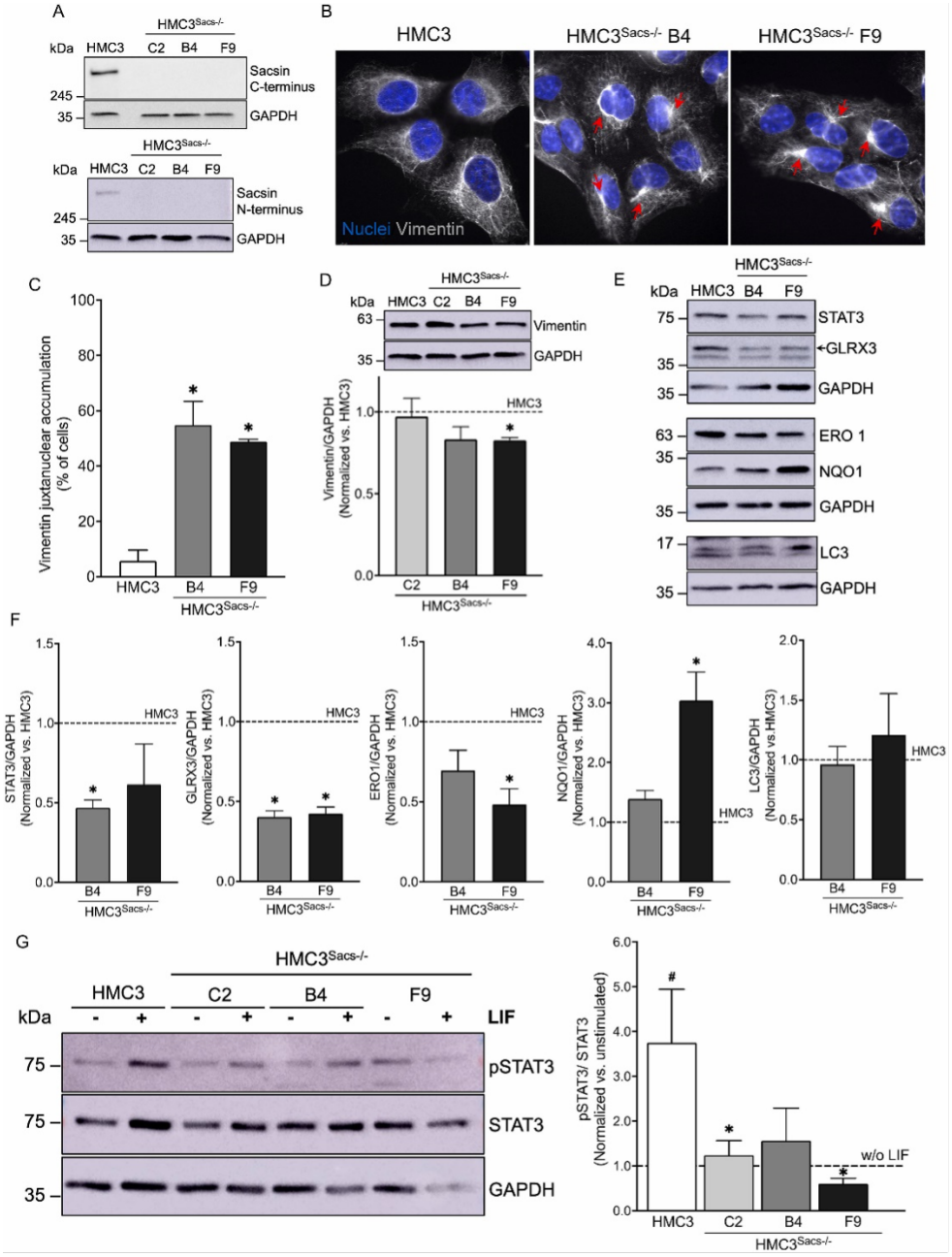

Figure 23:Independent HMC3$^{Sacs-/-}$ clones display similar molecular phenotypes. (A) Representative Western blots of total cell lysates from HMC3 human microglial cells and HMC3$^{Sacs-/-}$ clones C2 (the main clone described in Fig.22), B4 and F9 showing that no detectable levels of sacsin, as determined by two different sacsin antibodies against its C- and N-termini (refs. ABN1019 and sc-515118, respectively). **(B-C)** The distribution of the intermediate filament vimentin (gray) was analysed in HMC3$^{Sacs-/-}$ clones B4 and F9 by immunofluorescence microscopy and quantified. Scale bar 20 μm. Red arrows, vimentin aggregates. Data are shown as the percentage of cells displaying abnormal vimentin networks. The number of cells analysed were n=285 (HMC3), n=403 (B4), n=338 (F9). Results were analysed using One-way ANOVA followed by a Tukey post hoc test. *, significant vs. HMC3 reference strain, $p < 0.05$. **(D)** Representative images of vimentin immunoblotting bands from total cell lysates from HMC3 cells and HMC3$^{Sacs-/-}$ clones C2, B4 and F9; and densiometric analysis of Western blots from 3 independent experiments normalized versus GAPDH. Results presented as mean ± SEM. *, significant vs. HMC3 reference strain ($p < 0.05$, Student's t-test). **(E)** Representative Western blots of total cell lysates from HMC3 cells and HMC3$^{Sacs-/-}$ clones B4 and F9 showing ERO1, NQO1, GLRX3, LC3 and STAT3 expression levels. **(F)** Densitometric analysis of Western blots from 3 independent experiments for these 5 proteins, always normalized versus GAPDH levels. Results presented as mean ± SEM. *, significant vs. HMC3 reference strain ($p < 0.05$, Student's t-test). **(G)** Representative Western blot images of total protein extracts from HMC3 cells and HMC3$^{Sacs-/-}$ clones C2, B4 and F9 stimulated with LIF (200 ng/mL) for 20 minutes in the absence of serum. Cells were incubated in serum-free medium for 2 h before adding LIF. STAT3 phosphorylation at residue Y705 (pSTAT3) was used as a surrogate of STAT3 activation. The ratio pSTAT3/STAT3 was normalized versus the ratio of unstimulated cells from the same clone. Data is shown as mean ± SEM of 3 independent experiments. Results were analysed using One-way ANOVA and Tukey post hoc test. #, significant vs. unstimulated HMC3 reference strain, $p < 0.05$; *, significant vs. LIF stimulated HMC3 reference strain.

We could not find a direct relationship between ERO1 and microglial function in the literature. On the other hand, STAT3 and SMAD1 pathways are connected to microglia at different levels. STAT3 is an essential transcription factor during development, since mice knockout for STAT3 or other members of the pathway (e.g. gp130) are embryonic lethal [Reviewed in (Diallo & Herrera, 2022)]. During neuroinflammation, STAT3 mediates

Interleukin-6 and -10 signalling, two key regulators of immune response (Diallo & Herrera, 2022; Z. Fan et al., 2022; H. Liu et al., 2021). Our results in C6 cells indicate that STAT3 response to the IL-6 family of cytokines is altered in sacsin-knockout cells (Murtinheira et al., 2022). Consistently, HMC3$^{Sacs-/-}$ cells showed a deficient response to another cytokine from the IL-6 family, Leukemia Inhibitory Factor (LIF) (Fig.23G). The transcriptional activity of SMAD1 is triggered by TGF-beta and Bone Morphogenetic Proteins (BMPs), which are also relevant for both embryonic development and neuroinflammation (Hegarty et al., 2013). STAT3 and SMAD1 pathways are tightly interconnected, producing synergistic effects in the expression of glial-specific genes (Diallo & Herrera, 2022). Most interestingly, both STAT3 and SMAD1 regulate microglial morphology, phagocytic activity and homeostasis (Z. Fan et al., 2022; H. Liu et al., 2021; Zöller et al., 2018).

4.2.3.4. Sacsin Deletion Disrupts Phagocytic Functions in HMC3 Human Microglial Cells

Bearing this information in mind, we next assessed the function of HMC3$^{Sacs-/-}$ cells by addressing their phagocytosis ability (Fig.22F-H). HMC3 and HMC3$^{Sacs-/-}$ cells were incubated with 1 mg/ml of myelin debris previously stained with BASHY probe as described (Pinto et al., 2021) for 1 h to mimic microglia neuroprotective ability to remove debris; or with 0.0025 % (*v*/v) 1 mm zymogen-coated fluorescent latex beads (Sigma Chemical) for 75 min to mimic microglia reactivity against infections (innate immune response). HMC3$^{Sacs-/-}$ cells maintain their phagocytic ability, but with a higher variability than wild-type HMC3 cells. Indeed, HMC3$^{Sacs-/-}$ cells phagocyted a significantly higher amount of myelin debris and a slightly higher number of zymogen beads than the HMC3 ones (Fig.22F,G), suggesting a potentially increased ability for clearance and pathogen reactivity. Reactive microglia usually shift their morphology into a more

spherical volume, so we next evaluated cell sphericity and surface area to volume ratio (Fig.22H). While HMC3 cells react to both myelin debris and zymogen beads altering their shape into a more spheroid morphology and showing a lower surface area to volume ratio (in accordance with a more reactive morphology), HMC3$^{Sacs-/-}$ cells fail to change their morphology upon stimulation, suggesting that an altered cytoskeleton response may be present. Consistently, the TREM2 receptor involved in phagocytic activity of microglia (Cignarella et al., 2020) showed higher expression in HMC3$^{Sacs-/-}$ regardless of the type of phagocytosis analysed (Fig.22I). These results are aligned with a previous report showing that Sacs-/- mice show an upregulation of microglial density and higher gene expression of the phagocytic marker CD68 (Bondio et al., 2023).

Changes in HMC3 cells morphology are usually associated with increased reactivity and release of cytokines (Dello Russo et al., 2018; Fernandes et al., 2014). HMC3$^{Sacs-/-}$ cells express lower levels of TNF-alpha and increased levels of IL-1beta, while IL-6 expression was not significantly altered (Fig.24). Increased IL- 1beta expression has been associated with increased clearance of Abeta plaques by microglia (Rivera-Escalera et al., 2019), which is consistent with the observed increase in phagocytosis in HMC3$^{Sacs-/-}$ cells.

4.2.4. Discussion

Our results indicate that alterations in the IF and mitochondrial networks induced by sacsin loss in microglia could have biologically relevant consequences in the context of ARSACS. Although HMC3 cells are an immortalized cell line, and therefore could behave differently than primary microglia, they are a reference cell line in the field of neuroimmunology, being extensively used for analysis of microglial profiles and functions (Dello Russo et al., 2018; Fernandes et al., 2014). Microglial cells play a key role

during neuroinflammation, in coordination with astroglia, and both cell types show reactivity in ARSACS. The function of both astroglial and microglial cells is regulated by their particular intermediate filament networks and specific transcription factors that mediate their response to cytokines during development and neuroinflammation. Further analysis on glial dysfunction before and after the disease onset should be carried out, and our new microglial model could enable advances in this direction.

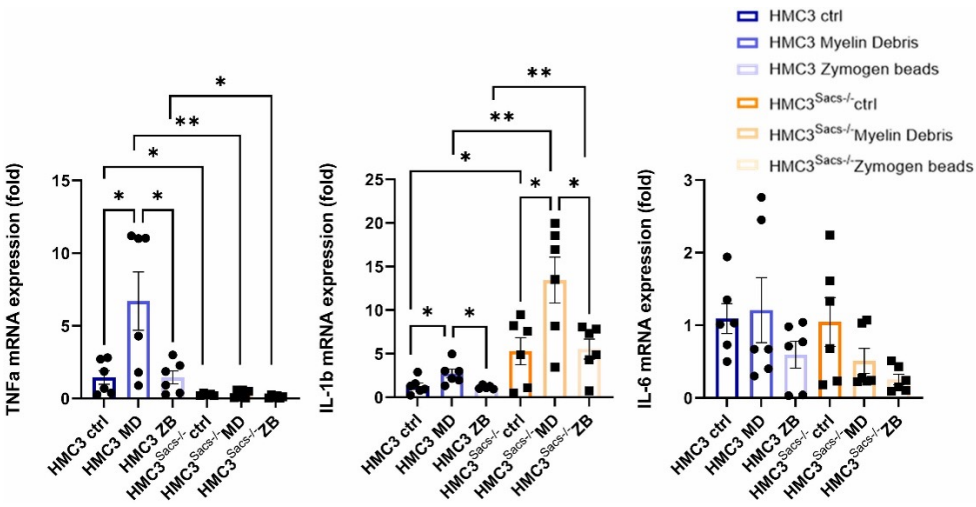

Figure 24: Sacsin deletion induces alterations in the expression of inflammatory cytokines in HMC3 microglial cells. RT-PCR analysis of mRNA levels for TNF-alpha, IL-1beta and IL-6 in HMC3 and HMC3$^{Sacs-/-}$ cells in the presence or absence of myelin debris and zymogen beads, two conditions that test different types of phagocytosis. Results show the mean ± SEM of 6 independent experiments, *p < 0.05, **p < 0.01, One-way ANOVA.

5. CONCLUSIONS AND FUTURE PERSPECTIVES

The role of glial cells, particularly astrocytes, in neurodegenerative diseases has recently been explored, with a large body of evidence supporting the importance of neuron-glia interactions and the involvement of astrocytes and microglia in the progression of several neurodegenerative diseases, including Alzheimer's, Parkinson's, and Huntington's (Kaminsky et al., 2016; Liddelow et al., 2017; Miller et al., 2004). The potential involvement of astrocytes and microglia in ARSACS has yet to be explored, creating a significant gap in the field. This study aimed to investigate the effects of sacsin deletion on astrocytes and microglia. Utilising CRISPR/Cas9 genome editing with C6 rat glioblastoma cells and HMC3 human microglial cells, we have developed new glial cell models of ARSACS (Fig.11; Fig.22). These models may prove valuable in clarifying the roles of astrocytes and microglia in this early-onset neurodegenerative disorder. Our major findings are discussed below:

5.1. Astroglia and microglia express sacsin at a protein level.

We were the first to demonstrate that sacsin protein is expressed at high levels in glial cells, including rat primary astrocytes, C6 rat glioblastoma cells, N9 rat microglial cells, and HMC3 human microglial cells (Fig.11A,B; Fig.22A). Its localization in these cells is mainly cytoplasmatic with minor mitochondrial localization, as described in other cell types (Girard, Larivière, et al., 2012). When we started this investigation, it was very unclear whether sacsin was expressed in non-neuronal cells in the central nervous system. We found information in public databases that sacsin mRNA was present in various glial cell types, but no published reference to support it (The Protein Atlas, Harmonizome and BrainRNASeq). Furthermore, personal communications from various ARSACS experts suggested that astroglia and

microglia expressed little or no sacsin, at least in comparison with neuronal cells. We decided to move on and develop the first astroglial cell model of ARSACS when we confirmed that primary cultures of rat astrocytes actually expressed sacsin at very high levels (Fig.11A). The second decisive clue came from the reviewers of our first manuscript: they found two published articles where sacsin mRNA expression was found as high as in neurones in both mouse and human foetal astrocytes, decreasing its expression as the central nervous system matured and developed (Clarke et al., 2018; Y. Zhang et al., 2016). These data were hard to find, as these articles were not focused on sacsin but on astroglia, and the expression of sacsin by non-neuronal central nervous system cells remains a matter of discussion. As an example, the most recent single-cell transcriptomics data on mice brain and cerebellum during development presented at the International Congress for Ataxia Research 2024 (November 2024) continued to show lower levels of expression of sacsin in astroglia and microglia than in Purkinje neurones and endothelial cells (as a curiosity, the articles mentioned above indicated that endothelial cells expressed lower levels than astroglia). However, these inconsistencies regarding sacsin expression should not be taken as a sign that glial cells are irrelevant to ARSACS pathology.

On one hand, expression levels are not necessarily related to biological relevance. Low levels of sacsin could play key roles in astroglia, and high levels of sacsin in Purkinje cells can be just a consequence of the intricate tree-like structure of these cells, which probably needs higher structural support than resting-state astrocytes (Beekhof et al., 2021; Fernández Santoro et al., 2024; Pekny & Pekna, 2014). On the other hand, these inconsistencies could also be explained by different developmental stages or astroglial functional changes occurring during stress or insults (Dusart & Flamant, 2012; Y. Y. Fan & Huo, 2021; Kato & De Schutter, 2023; Vivi & Di Benedetto, 2024). During neuroinflammation, astrocytes can react, grow in

size, proliferate and migrate towards damaged tissue. These changes require energy from mitochondria and coordination of intermediate filament networks, both regulated by sacsin (Brambilla, 2019; Gentil et al., 2018; Girard, Larivière, et al., 2012; Kato & De Schutter, 2023; Y. Zhao et al., 2024). The pathways that regulate these phenomena, such as the JAK/STAT and TGFbeta/Smad pathways, are also involved in astroglial differentiation during normal embryonic development (Diallo & Herrera, 2022; Hegarty et al., 2013). ARSACS mice recently showed signs of neuroinflammation correlated with the onset of the disease (Bondio et al., 2023). It could be interesting to check if: 1) astroglial reactivity is accompanied by higher expression levels of sacsin in both normal and ARSACS astrocytes, and 2) sacsin loss of function produces alterations in the neuroinflammatory profile of ARSACS astrocytes. The defects we observe in the response of $C6^{Sacs-/-}$ cells to the IL-6 family of cytokines could indicate that this could be the case. But sacsin is expressed at higher levels in foetal astrocytes, and astrocytes are also relevant for neuronal development and maturation (Araujo et al., 2019; Reemst et al., 2016; Tan et al., 2021; Vivi & Di Benedetto, 2024). Therefore, it could be interesting to study if there are alterations at the level of embryonic development when astrocytes are defective for sacsin function. So far, there have not been developed conditional mouse models where sacsin knockout is restricted to non-neuronal cells. Personal communication to experts in the field indicates that they are reluctant to check earlier during development, because these mice do not show overt phenotypes until 5-8 months after birth. Additionally, studying embryos require killing the mothers and it would be more expensive in funding and time. However, we consider that it would be very interesting to test these hypotheses in mouse models of ARSACS.

5.2. Development of the first two glial cell models of ARSACS

After verifying that glial cells express sacsin, we decided to generate astroglial and microglial cell models of ARSACS since the absence of glial models of ARSACS creates a critical gap in understanding the disease's pathophysiology. We chose to utilise C6 rat glioma cells due to their astroglial-like characteristics, facilitating comparative studies with mouse models of ARSACS and primary astroglial cells from rats and their significant expression of sacsin (S. J. Zhang et al., 2011). HMC3 cells were selected because they are the current reference human microglial cell line, having been immortalised from primary human microglia. They express the primary microglial cell markers and behave similarly to microglia, including releasing inflammatory cytokines (Dello Russo et al., 2018). Our ARSACS glial models provide advantages by allowing for the investigation of sacsin-related processes specific to astroglia and microglia and their potential interactions with neurones, contributing to a broader view of ARSACS pathophysiology. We are currently in collaboration with Dr. Paul Chapple (Faculty of Medicine and Dentistry, Queen Mary University of London) to carry out transcriptomics analysis on our glial cell models and compare them with other neuronal and non-neuronal models of ARSACS, including brains from mouse models and patients, in order to find neuron- and glia-specific signatures of the disease as well as universal alterations. Additionally, we plan to develop the first endothelial cell models of ARSACS, in both human and mouse cell lines, and test the potential alterations of the blood-brain-barrier in this disease, as it happens with other ataxias (Carvey et al., 2009; Duarte Lobo et al., 2020; Shimizu, 2024; M. D. Sweeney et al., 2018; Wu et al., 2021).

Functional studies to assess mitochondrial activity, cytoskeletal structure, and stress responses confirmed the model's relevance to ARSACS research. Despite their benefits, limitations remain, including the need for

further validation employing primary astrocytes and microglia from ARSACs mice models, patient-derived glial cells, and 3D culture systems that better mimic *in vivo* conditions. We are currently collaborating with Dr. Benoit Gentil (McGill University, Montreal, Canada) to send us primary cultures of these cells for comparisons. However, so far, we have been unsuccessful because ARSACS astrocytes always arrived weak and non-proliferative. We believe they are extremely sensitive to the stress of transoceanic transportation, which would be consistent with the elevated stress sensitivity of our cell models (Fig.12, Fig.13). Another disadvantage of our cell models is that both C6 and HMC3 cell lines have low transfection efficiency, which, combined with the size of sacsin, makes it challenging to perform rescue phenotype experiments. We are considering viral infection to improve genetic transformation, but this is a method that still needs to be implemented in our laboratory. Future research should investigate co-culture models with neurones and use this system for therapeutic testing of astrocyte- or microglial-targeted therapies.

5.3. Sacsin loss induces aggregation of glial intermediate filaments

Current evidence indicates that one of the main hallmarks of sacsin deficiency is the pathological reorganization of the intermediate filament (IF) cytoskeleton (Dabbaghizadeh et al., 2022; Duncan et al., 2017; Francis et al., 2022; Gentil et al., 2018). In the absence of sacsin, neurofilaments (NFs, in various neurone types) and vimentin (in ARSACS patient fibroblasts, Sacs-/- HEK293T and SH-SY5Y cells) both accumulate and form abnormally thick bundles (Dabbaghizadeh et al., 2022; Duncan et al., 2017; Gentil et al., 2018). ARSACS brains and neurones from Sacs-/- mice also exhibit distinct accumulations of non-phosphorylated NFH (Larivière et al., 2015). Based on this evidence, we aimed to investigate whether the absence of sacsin affected cytoskeletal organisation in C6 and HMC3 cells. Our data indicated

substantial alterations and remodelling of the cytoskeletal network in sacsin-depleted cells, characterised by the accumulation of glial intermediate filaments vimentin, nestin, and GFAP in the juxtanuclear area (Fig.14, Fig.22, Fig.23). Our results are therefore consistent with previous reports in other ARSACS models and cell types. However, most Sacs-/- cells show thicker IFs instead of juxtanuclear accumulation. Further studies should be carried out to understand whether this phenotype is cell type-specific or has other technical or biological causes.

It is also noticeable that there are no published studies on the mechanical properties of Sacs-/- cells. IFs are the least dynamic but most flexible of the cytoskeletal fibres, and the main responsible for the mechanical and viscoelastic properties of cells and tissues (Block et al., 2015; Etienne-Manneville, 2018; Pradeau-Phélut & Etienne-Manneville, 2024). These properties are extremely relevant for resistance to stretching and other types of mechanical stress, as well as for normal cell and organ function: Consider for example the biological importance of the permeability of epithelia, the integrity of the blood brain barrier or the strong mechanical forces acting during embryonic development and cell migration within crowded tissues. If any of these phenomena are defective, they could easily explain ARSACS clinical features. And yet, we were the first to test and publish an extremely detailed description of the mechanical properties of cells losing ARSACS by Atomic Force Microscopy, in collaboration with an expert in the field, Dr. Mário S. Rodrigues (Faculty of Sciences, University of Lisbon, Portugal). Our results indicate that the cytoplasmic region is the most affected, while the nuclear region seems to preserve their mechanical resistance and viscoelasticity (Fig.18A-C). This is consistent with the strong alterations we observed in the cytoplasmic IFs but not in the nuclear IFs, such as Lamin A-C. A recent personal communication with Dr. Paul Chapple indicated that they had previously carried out Atomic Force Microscopy studies on

SHSY5Y$^{Sacs-/-}$ cells, but never published the data because they did not know how to interpret them. They had opposite tendencies in mechanical resistance and viscoelasticity, the mechanical resistance results being more or less consistent with our own results. After careful consideration, we concluded that their results are not directly comparable to our results, as they did not differentiate between different areas of the cell and their approach to measure resistance to deformation and viscoelastic properties was substantially different regarding both the equipment and the mathematical calculations.

Sacsin may influence the IFs organisation directly (as the chaperone that folds them) or indirectly (via a mediator). Investigations are ongoing to determine the exact molecular connection between IFs and sacsin, but they are largely hindered due to the very big size of the sacsin gene and protein. A potential reason for the observed phenotype is microtubule depolymerisation or alterations. Although we did not observe clear modifications in the microtubule or actin networks, a recent report indicates profound functional alterations in microtubular trafficking (L. E. L. Romano et al., 2022). Preliminary results from Dr. Walid Houry (University of Toronto, Canada) indicate that sacsin could be a ring, where the N-terminus connects with the C-terminus, but they achieved very low resolution and crystallography, or cryo-electron microscopy should be carried out to confirm his findings. Sacsin´s interactome is also not very well-defined, with no more than 100 interactors identified, but so far it does not show strong direct interactions with intermediate filaments, with the possible exception of vimentin. We tried to immunoprecipitate sacsin and check for its interactors, but we could not confirm co-immunoprecipitation of nestin, vimentin or GFAP in our models. According to the BioGrid public database, sacsin actually interacts with ubiquitin ligases and proteasome subunits related to protein homeostasis (UBE3A, PARK2, PSMA3), cytoskeletal proteins (actinin,

myosin, vimentin, plakophilin, …) as well as with other proteins related to neurodegenerative disorders (SOD1, PARK2). However, even at this level results are not always consistent, as the IntAct public database does not reflect some of these interactors, such as vimentin.

Post-translational modifications (PTMs) regulate IFs dynamics and organisation. The characteristics of IFs assembly and organization are closely linked to their phosphorylation status (Kraxner & Köster, 2023; Sanghvi-Shah & Weber, 2017). Sacsin interacts with several protein kinases and phosphatases, according to BioGrid, some of them linked to vimentin phosphorylation status, such as Polo-like kinase 1 (PLK1) and protein phosphatase type 1 (PPP1) (J. Li et al., 2016; Yamaguchi et al., 2005). Sacsin loss might impair this critical pathway, resulting in IFs aggregation and mislocalisation. In the future, we should analyse the phosphorylation status of the glial IFs in Sacs-/- cells, and the levels of their regulators.

5.4. Sacsin loss disrupts mitochondrial networks in glial cells

Mitochondrial defects have been identified in several ARSACS models (Bradshaw et al., 2016; Girard, Larivière, et al., 2012). In our glial models, mitochondria are absent from the juxtanuclear area, where the intermediate filaments are accumulated, and their morphology is substantially different from wild-type cells, where mitochondria are smaller in average and distribute homogeneously through the cytoplasm (Fig.14A, Fig.16A, Fig.22B). Prior studies demonstrated hyperfused mitochondrial morphology in fibroblasts from ARSACS patients, MEFs, and Sacs-/- SH-SY5Y cells (Bradshaw et al., 2016; Girard, Larivière, et al., 2012). This phenotype was proposed to occur due to defective recruitment of fission machinery (DRP1) to mitochondria in the absence of sacsin (Bradshaw et al., 2016). Data from $HMC3^{Sacs-/-}$ cells indicate increased mRNA levels of DRP1 and MFN-2, which are markers of mitochondrial fission and fusion, respectively (Fig.22D). We

are currently studying whether these two genes are also altered in C6$^{Sacs-/-}$ cells. Research from other laboratories indicates a reduction in the number of mitochondria, specifically in the dendrites of Sacs-/- primary Purkinje cells (Girard, Larivière, et al., 2012). These observations suggest an impairment in mitochondrial transport to distal neuronal processes, where the demand for mitochondria is highest. Mitochondrial transport primarily occurs on microtubules and actin filaments. However, increasing evidence suggests that mitochondria can directly associate with neurofilaments and vimentin (Gentil et al., 2012; Nekrasova et al., 2011; Schwarz & Leube, 2016; H. L. Tang et al., 2008; Wagner et al., 2003). Although no direct alterations in the mitochondrial respiratory chain have been described in ARSACS models, omics approaches suggest severe alterations in mitochondrial functions, and not only their morphology (Bondio et al., 2023; Galatolo et al., 2024; L. E. L. Romano et al., 2022). These alterations could explain the higher basal levels of reactive oxygen species in C6$^{Sacs-/-}$ cells and their higher sensitivity to various forms of stress.

5.5. Sacsin loss induces higher sensitivity to stress in C6 cells

The elevated basal oxidative stress found in C6$^{Sacs-/-}$ cells highlights the critical function of sacsin in maintaining cellular homeostasis (Fig.12A). Sacsin likely predisposes cells to sustained ROS accumulation, disrupting redox balance and amplifying oxidative stress (Dabbaghizadeh et al., 2022; Martinelli et al., 2020). The inherent vulnerability observed in C6$^{Sacs-/-}$ cells matches the findings in ARSACS fibroblasts and neurones, where sacsin deficiency disrupts mitochondrial dynamics and elevates ROS levels (Bradshaw et al., 2016; Girard, Larivière, et al., 2012).

Upon exposure to rotenone, a mitochondrial Complex I inhibitor, sacsin-deficient cells exhibited a significantly higher oxidative stress response than wild-type controls. Although MTT and LDH assays indicated mild toxicity in

both cell types (Fig.12B, Fig.S1A), flow cytometry revealed increased DAPI staining and a marked reduction in cell size in C6$^{Sacs-/-}$ cells (Fig.12D,E), consistent with elevated cellular damage. We also observed that C6$^{Sacs-/-}$ cells exhibited a more prominent increase in DAPI staining upon rotenone exposure, indicating membrane damage (Fig.12E-I). These findings suggest that the loss of sacsin compromises the ability of C6 astroglial-like cells to manage oxidative stress effectively, probably exacerbating mitochondrial dysfunction, as well as loss of membrane integrity and cell viability, aligning with previous studies in neuronal models (Duncan et al., 2017; Girard, Larivieѐre, et al., 2012; Kozlov et al., 2011; Larivière et al., 2015; X. Li & Gehring, 2015; Márquez et al., 2023).

Given that C6 cells are astroglial-like cells and take into account the critical role of astrocytes in maintaining homeostasis in the cerebellum, including the regulation of neurotransmitter levels and ion balance, the increased oxidative stress observed in C6$^{Sacs-/-}$ cells may impair these functions, leading to dysregulation of cerebellar signalling and contributing to the neurodegenerative processes associated with ARSACS ((Y. Y. Fan & Huo, 2021; Haim & Rowitch, 2017; Tan et al., 2021; Verkhratsky et al., 2023)

The observed oxidative stress may also result from cytoskeletal disruptions, a hallmark of sacsin deficiency. Sacsin loss induces neurofilament aggregation in neurones, impairing cytoskeletal integrity and mitochondrial trafficking (Girard, Larivieѐre, et al., 2012; Morani et al., 2021, 2022; L. E. L. Romano et al., 2022). Similar intermediate filament aggregation in astroglial cells could exacerbate oxidative stress by hindering mitochondrial function and compromising structural stability. In astrocytes, oxidative stress disrupts critical functions essential for cerebellar health (Y. Chen et al., 2020; X. Wang & Michaelis, 2010). Impaired glutamate uptake by astroglia may lead to excitotoxicity, while reduced potassium buffering

and antioxidant support could compromise neuronal survival, particularly in vulnerable Purkinje cells (Bylicky et al., 2018; Y. Chen et al., 2020; B. Liu et al., 2017). These alterations may contribute to the progressive neurodegeneration associated with ARSACS.

5.6. Sacsin loss induces alterations related to glial function in neuroinflammation

We have observed alterations in the response of $C6^{Sacs-/-}$ and $HMC3^{Sacs-/-}$ cells to cytokines from the IL-6 family (IL-6 and LIF), as measured by the canonical JAK/STAT3 response to these cytokines (Fig.19, Fig.S6 and Fig.23E-G). The IL-6 family of cytokines and the JAK/STAT3 pathway play crucial roles in normal CNS development, neuroinflammation, and various neurological disorders and injuries (Erta et al., 2012). IL-6 is a pleiotropic cytokine that participates in neurogenesis and gliogenesis, influencing both neurones and glial cells. IL-6 expression and secretion increases rapidly in response to CNS infection, injury, or various neurological diseases. The IL-6 family of cytokines plays a critical role in transitioning from innate to acquired immunity in the CNS, which is crucial for properly dealing with injured or infected CNS tissue; and modulates the expression of many genes involved in inflammation, apoptosis, and oxidative stress, including the inflammatory cytokine TNFalpha (Erta et al., 2012). In this sense, we also observe a significant reduction in the expression of TNFalpha and an increase in the expression of IL-1b in $HMC3^{Sacs-/-}$ cells (Fig.24). Activation of the JAK2/STAT3 signalling pathway contributes to normal brain development, early brain injury, cerebral vasculopathy, and neurological deficits in conditions such as subarachnoid haemorrhage (SAH) (Z. V. Zheng et al., 2022). STAT3 activation in microglia modulates microglial polarization and exacerbates microglial activation and neuroinflammation after ischemic stroke (Z. V. Zheng et al., 2022; Zhu et al., 2021). STAT3

signalling may directly regulate the NLRP3 inflammasome, a key component of the innate immune response (Zhu et al., 2021). ARSACS brains show signs of neuroinflammation, and the alterations in the response of our astroglial-like and microglial cell models to IL-6 cytokines mediated by STAT3 can therefore be relevant to this disease.

We have also observed alterations in phagocytic function and morphology in our microglial cell model of ARSACS (Fig.22). Microglial phagocytosis plays a crucial role in neuroinflammation, contributing to both neuroprotective and potentially harmful processes in the central nervous system (Galloway et al., 2019). As the primary immune cells of the brain, microglia are essential for maintaining CNS homeostasis and responding to various pathological conditions. Under normal conditions, microglia clear the CNS of cellular debris and apoptotic cells, prune synaptic terminals, regulate brain development and carry out immune surveillance (Fu et al., 2014). In response to CNS injury, infection, or neurodegenerative diseases, microglia become activated and change from a ramified "resting" state to an amoeboid "active" state, move towards the site of injury and show enhanced phagocytic capacity. Microglial phagocytosis is relevant to other neurodegenerative disorders, such as Alzheimer´s disease, Parkinson´s disease and multiple sclerosis (Fu et al., 2014; Janda et al., 2018; Koenigsknecht & Landreth, 2004). While it serves essential functions in maintaining CNS health and responding to pathological conditions, its dysregulation can contribute to disease progression. The alterations we observe in HMC3$^{Sacs-/-}$ microglial cells could therefore be relevant to ARSACS.

In summary, the IL-6/STAT3 axis and phagocytosis are potentially relevant to both CNS development and neuroinflammation. Considering that 1) ARSACS is an early onset neurological disease, diagnosed early after

birth and 2) ARSACS brains show neuroinflammation, a role for glial sacsin in development and neuroinflammation cannot be ruled out in this disease.

6. REFERENCES

Ababneh, N. A., Ali, D., Al-Kurdi, B., Sallam, M., Alzibdeh, A. M., Salah, B., Ryalat, A. T., Azab, B., Sharrack, B., & Awidi, A. (2020). Identification of APTX Disease-Causing Mutation in Two Unrelated Jordanian Families With Cerebellar Ataxia and Sensitivity to DNA Damaging Agents. *Plos One*, *15*(8), e0236808. https://doi.org/10.1371/journal.pone.0236808

Abdelazim, A. M., & Abomughaid, M. M. (2024). Oxidative stress: an overview of past research and future insights. *All Life*, *17*(1), 2316092. https://doi.org/10.1080/26895293.2024.2316092

Adams, C. J., Kopp, M. C., Larburu, N., Nowak, P. R., & Ali, M. M. U. (2019). Structure and molecular mechanism of ER stress signaling by the unfolded protein response signal activator IRE1. *Frontiers in Molecular Biosciences*, *6*(MAR), 439177. https://doi.org/10.3389/FMOLB.2019.00011/BIBTEX

Ady, V., Toscano-Márquez, B., Nath, M., Chang, P. K., Hui, J., Cook, A., Charron, F., Larivière, R., Brais, B., McKinney, R. A., & Watt, A. J. (2018). Altered synaptic and firing properties of cerebellar Purkinje cells in a mouse model of ARSACS. *Journal of Physiology*. https://doi.org/10.1113/JP275902

Almanza, A., Carlesso, A., Chintha, C., Creedican, S., Doultsinos, D., Leuzzi, B., Luís, A., McCarthy, N., Montibeller, L., More, S., Papaioannou, A., Püschel, F., Sassano, M. L., Skoko, J., Agostinis, P., de Belleroche, J., Eriksson, L. A., Fulda, S., Gorman, A. M., … Samali, A. (2018). Endoplasmic reticulum stress signalling – from basic mechanisms to clinical applications. *The Febs Journal*, *286*(2), 241. https://doi.org/10.1111/FEBS.14608

Almazán, G., Vela, J. M., Molina-Holgado, E., & Guaza, C. (2001). Re-evaluation of nestin as a marker of oligodendrocyte lineage cells. *Microscopy Research and Technique*, *52*(6), 753–765. https://doi.org/10.1002/JEMT.1060

Alvarez-Buylla, A., García-Verdugo, J. M., & Tramontin, A. D. (2001). A unified hypothesis on the lineage of neural stem cells. *Nature Reviews. Neuroscience*, *2*(4), 287–293. https://doi.org/10.1038/35067582

Aly, K. A., Moutaoufik, M. T., Zilocchi, M., Phanse, S., & Babu, M. (2022). Insights into SACS pathological attributes in autosomal recessive spastic ataxia of Charlevoix-Saguenay (ARSACS)☆. *Current Opinion in Chemical Biology*, *71*, 102211. https://doi.org/10.1016/J.CBPA.2022.102211

Amore, G., Spoto, G., Ieni, A., Vetri, L., Quatrosi, G., Di Rosa, G., & Nicotera, A. G. (2021). A Focus on the Cerebellum: From Embryogenesis to an Age-Related Clinical Perspective. *Frontiers in Systems Neuroscience*, *15*. https://doi.org/10.3389/fnsys.2021.646052

Anantharaman, V., Makarova, K. S., Burroughs, A. M., Koonin, E. V., & Aravind, L. (2013). Comprehensive analysis of the HEPN superfamily: identification of novel roles in intra-genomic conflicts, defense, pathogenesis and RNA processing. *Biology Direct 2013 8:1*, *8*(1), 1–28. https://doi.org/10.1186/1745-6150-8-15

Anderson, J. F., Siller, E., & Barral, J. M. (2010). The Sacsin Repeating Region (SRR): A Novel Hsp90-Related Supra-Domain Associated with Neurodegeneration. *Journal of Molecular Biology*, *400*(4), 665–674. https://doi.org/https://doi.org/10.1016/j.jmb.2010.05.023

Anderson, J. F., Siller, E., & Barral, J. M. (2011). The Neurodegenerative-Disease-Related Protein Sacsin Is a Molecular Chaperone. *Journal of Molecular Biology*, *411*(4), 870–880. https://doi.org/https://doi.org/10.1016/j.jmb.2011.06.016

Anheim, M., Tranchant, C., & Koenig, M. (2012). The Autosomal Recessive Cerebellar Ataxias. *New England Journal of Medicine*, *366*(7), 636–646. https://doi.org/10.1056/NEJMRA1006610

Apolloni, S., Milani, M., & D'ambrosi, N. (2022). Neuroinflammation in Friedreich's Ataxia. *International Journal of Molecular Sciences*, *23*(11), 6297. https://doi.org/10.3390/IJMS23116297

Apsley, E. J., & Becker, E. B. E. (2022). Purkinje Cell Patterning—Insights from Single-Cell Sequencing. *Cells 2022, Vol. 11, Page 2918*, *11*(18), 2918. https://doi.org/10.3390/CELLS11182918

Araujo, A. P. B., Carpi-Santos, R., & Gomes, F. C. A. (2019). The Role of Astrocytes in the Development of the Cerebellum. *Cerebellum*, *18*(6), 1017–1035. https://doi.org/10.1007/S12311-019-01046-0/FIGURES/4

Armao, D., Bouldin, T. W., Bailey, R. M., Hooper, J. E., Bharucha, D. X., & Gray, S. J. (2019). Advancing the pathologic phenotype of giant axonal neuropathy: Early involvement of the ocular lens. *Orphanet Journal of Rare Diseases*, *14*(1), 1–5. https://doi.org/10.1186/S13023-018-0957-5/FIGURES/2

Artero Castro, A., Machuca, C., Rodriguez Jimenez, F. J., Jendelova, P., & Erceg, S. (2019). Short Review: Investigating ARSACS: models for understanding cerebellar degeneration. *Neuropathology and Applied Neurobiology*, *45*(6), 531–537. https://doi.org/10.1111/NAN.12540

Baets, J., Deconinck, T., Smets, K., Goossens, D., Van Den Bergh, P., Dahan, K., Schmedding, E., Santens, P., Rasic, V. M., Van Damme, P., Robberecht, W., De Meirleir, L., Michielsens, B., Del-Favero, J., Jordanova, A., & De Jonghe, P. (2010). Mutations in SACS cause atypical and late-onset forms of ARSACS. *Neurology*, *75*(13), 1181–1188. https://doi.org/10.1212/WNL.0B013E3181F4D86C

Baev, A. Y., Vinokurov, A. Y., Novikova, I. N., Dremin, V. V., Potapova, E. V., & Abramov, A. Y. (2022). Interaction of Mitochondrial Calcium and ROS in Neurodegeneration. *Cells*, *11*(4), 706. https://doi.org/10.3390/CELLS11040706

Bagaria, J., Bagyinszky, E., & An, S. S. A. (2022). Genetics of Autosomal Recessive Spastic Ataxia of Charlevoix-Saguenay (ARSACS) and Role of Sacsin in Neurodegeneration. *International Journal of Molecular Sciences*, *23*(1). https://doi.org/10.3390/IJMS23010552

Battaglini, M., Carmignani, A., Martinelli, C., Colica, J., Marino, A., Doccini, S., Mollo, V., Santoro, F., Bartolucci, M., Petretto, A., Santorelli, F. M., & Ciofani, G. (2022). In vitro study of polydopamine nanoparticles as protective antioxidant agents in fibroblasts derived from ARSACS patients. *Biomaterials Science*, *10*(14), 3770–3792. https://doi.org/10.1039/D2BM00729K

Baumann, O., Borra, R. J., Bower, J. M., Cullen, K. E., Habas, C., Ivry, R. B., Leggio, M., Mattingley, J. B., Molinari, M., Moulton, E. A., Paulin, M. G., Pavlova, M. A., Schmahmann, J. D., & Sokolov, A. A. (2015). Consensus paper: the role of the cerebellum in perceptual processes. *Cerebellum (London, England)*, *14*(2), 197–220. https://doi.org/10.1007/s12311-014-0627-7

Bchetnia, M., Bouchard, L., Mathieu, J., Campeau, P., Morin, C., Brisson, D., Laberge, A.-M., Vézina, H., Gaudet, D., & Laprise, C. (2021). Genetic burden linked to founder effects in Saguenay-Lac-Saint-Jean illustrates the importance of genetic screening test availability. *J Med Genet*, *0*, 1–13. https://doi.org/10.1136/jmedgenet-2021-107809

Beaudin, M., Klein, C. J., Rouleau, G. A., & Dupré, N. (2017). Systematic review of autosomal recessive ataxias and proposal for a classification. *Cerebellum and Ataxias*, *4*(1). https://doi.org/10.1186/S40673-017-0061-Y

Beaudin, M., Manto, M., Schmahmann, J. D., Pandolfo, M., & Dupre, N. (2022). Recessive cerebellar and afferent ataxias — clinical challenges and future directions. *Nature Reviews Neurology 2022 18:5*, *18*(5), 257–272. https://doi.org/10.1038/s41582-022-00634-9

Beaudin, M., Matilla-Dueñas, A., Soong, B.-W., Pedroso, J. L., Barsottini, O. G., Mitoma, H., Tsuji, S., Schmahmann, J. D., Manto, M., Rouleau, G. A., Klein, C., & Dupre, N. (2019). The Classification of Autosomal Recessive Cerebellar Ataxias: a Consensus Statement from the Society for Research on the Cerebellum and Ataxias Task Force. *The Cerebellum*, *18*(6), 1098–1125. https://doi.org/10.1007/s12311-019-01052-2

Beaudin, M., Matilla-Dueñas, A., Soong, B.-W., Pedroso, J. L., Barsottini, O., Mitoma, H., Tsuji, S., Schmahmann, J., Manto, M., Rouleau, G., & Dupre, N. (2020). The Classification of Autosomal Recessive Cerebellar Ataxias: A Consensus Statement from the Society for Research on the Cerebellum and Ataxias Task Force (5359). *Neurology*, *94*(15_supplement). https://doi.org/10.1212/WNL.94.15_SUPPLEMENT.5359

Beekhof, G. C., Osório, C., White, J. J., Van Zoomeren, S., Van der Stok, H., Xiong, B., Nettersheim, I. H. M. S., Mak, W. A., Runge, M., Fiocchi, F. R., Boele, H. J., Hoebeek, F. E., & Schonewille, M. (2021). Differential spatiotemporal development of Purkinje cell populations and cerebellum-dependent sensorimotor behaviors. *ELife*, *10*. https://doi.org/10.7554/ELIFE.63668

Bernal, A., & Arranz, L. (2018). Nestin-expressing progenitor cells: function, identity and therapeutic implications. *Cellular and Molecular Life Sciences: CMLS*, *75*(12), 2177. https://doi.org/10.1007/S00018-018-2794-Z

Bertolotti, A., Zhang, Y., Hendershot, L. M., Harding, H. P., & Ron, D. (2000). Dynamic interaction of BiP and ER stress transducers in the unfolded-protein response. *Nature Cell Biology*, *2*(6), 326–332. https://doi.org/10.1038/35014014

Bhandary, B., Marahatta, A., Kim, H. R., & Chae, H. J. (2012). An Involvement of Oxidative Stress in Endoplasmic Reticulum Stress and Its Associated Diseases. *International Journal of Molecular Sciences 2013, Vol. 14, Pages 434-456*, *14*(1), 434–456. https://doi.org/10.3390/IJMS14010434

Bhattarai, K. R., Riaz, T. A., Kim, H. R., & Chae, H. J. (2021). The aftermath of the interplay between the endoplasmic reticulum stress response and redox signaling. *Experimental & Molecular Medicine 2021 53:2*, *53*(2), 151–167. https://doi.org/10.1038/s12276-021-00560-8

Block, J., Schroeder, V., Pawelzyk, P., Willenbacher, N., & Köster, S. (2015). Physical properties of cytoplasmic intermediate filaments. *Biochimica et Biophysica Acta (BBA) - Molecular Cell Research*, *1853* (11, Part B), 3053–3064. https://doi.org/https://doi.org/10.1016/j.bbamcr.2015.05.009

Bloomingdale, P., Karelina, T., Ramakrishnan, V., Bakshi, S., Véronneau-Veilleux, F., Moye, M., Sekiguchi, K., Meno-Tetang, G., Mohan, A., Maithreye, R., Thomas, V. A., Gibbons, F., Cabal, A., Bouteiller, J. M., & Geerts, H. (2022). Hallmarks of neurodegenerative disease: A systems pharmacology perspective. *CPT: Pharmacometrics & Systems Pharmacology*, *11*(11), 1399. https://doi.org/10.1002/PSP4.12852

Bondio, A. Del, Longo, F., De Ritis, D., Spirito, E., Podini, P., Brais, B., Bachi, A., Quattrini, A., & Maltecca, F. (2023). Restoring calcium homeostasis in Purkinje cells arrests neurodegeneration and neuroinflammation in the ARSACS mouse model. *JCI Insight*, *8*(12). https://doi.org/10.1172/JCI.INSIGHT.163576

Borgenheimer, E., Zhang, Y., & Cvetanovic, M. (2022). Single-nuclei RNA sequencing uncovers non-cell autonomous changes in cerebellar astrocytes and oligodendrocytes that may contribute to Spinocerebellar Ataxia Type 1 (SCA1) pathogenesis. *BioRxiv*, 2021.10.28.466301. https://doi.org/10.1101/2021.10.28.466301

Bouchard JP, Barbeau A, Bouchard R, B. R. (1978). Autosomal recessive spastic ataxia of Charlevoix-Saguenay. *Can J Neurol*, *5*, 61–69.

Bouchard, J.-P., Richter, A., Mathieu, J., Brunet, D., Hudson, T. J., Morgan, K., & Melançon, S. B. (1998). Autosomal recessive spastic ataxia of Charlevoix–Saguenay. *Neuromuscular Disorders*, *8*(7), 474–479. https://doi.org/https://doi.org/10.1016/S0960-8966(98)00055-8

Bouhlal, Y., Amouri, R., El Euch-Fayeche, G., & Hentati, F. (2011). Autosomal recessive spastic ataxia of Charlevoix-Saguenay: an overview. *Parkinsonism & Related Disorders*, *17*(6), 418–422. https://doi.org/10.1016/J.PARKRELDIS.2011.03.005

Bradshaw, T. Y., Romano, L. E. L., Duncan, E. J., Nethisinghe, S., Abeti, R., Michael, G. J., Giunti, P., Vermeer, S., & Chapple, J. P. (2016). A reduction in Drp1-mediated fission compromises mitochondrial health in autosomal recessive spastic ataxia of Charlevoix Saguenay. *Human Molecular Genetics*. https://doi.org/10.1093/hmg/ddw173

Brambilla, R. (2019). The contribution of astrocytes to the neuroinflammatory response in multiple sclerosis and experimental autoimmune encephalomyelitis. *Acta Neuropathologica*, *137*(5), 757. https://doi.org/10.1007/S00401-019-01980-7

Brandt, R., & Götz, J. (2023). Special issue on “Cytoskeletal proteins in health and neurodegenerative disease: Concepts and methods.” *Brain Research Bulletin*, *198*, 50–52. https://doi.org/10.1016/J.BRAINRESBULL.2023.04.007

Buffo, A., & Rossi, F. (2013). Origin, lineage and function of cerebellar glia. *Progress in Neurobiology*, *109*, 42–63. https://doi.org/10.1016/J.PNEUROBIO.2013.08.001

Bylicky, M. A., Mueller, G. P., & Day, R. M. (2018). Mechanisms of Endogenous Neuroprotective Effects of Astrocytes in Brain Injury. *Oxidative Medicine and Cellular Longevity*, *2018*, 6501031. https://doi.org/10.1155/2018/6501031

Carapeto, A. P., Vitorino, M. V., Santos, J. D., Ramalho, S. S., Robalo, T., Rodrigues, M. S., & Farinha, C. M. (2020). Mechanical Properties of Human Bronchial Epithelial Cells Expressing Wt- and Mutant CFTR. *International Journal of Molecular Sciences 2020, Vol. 21, Page 2916*, *21*(8), 2916. https://doi.org/10.3390/IJMS21082916

Carvey, P. M., Hendey, B., & Monahan, A. J. (2009). The Blood Brain Barrier in Neurodegenerative Disease: A Rhetorical Perspective. *Journal of Neurochemistry*, *111*(2), 291. https://doi.org/10.1111/J.1471-4159.2009.06319.X

Cerrato, V. (2020). Cerebellar Astrocytes: Much More Than Passive Bystanders In Ataxia Pathophysiology. *Journal of Clinical Medicine 2020, Vol. 9, Page 757*, *9*(3), 757. https://doi.org/10.3390/JCM9030757

Chen, X., Shi, C., He, M., Xiong, S., & Xia, X. (2023). Endoplasmic reticulum stress: molecular mechanism and therapeutic targets. *Signal Transduction and Targeted Therapy 2023 8:1*, *8*(1), 1–40. https://doi.org/10.1038/s41392-023-01570-w

Chen, Y., Lu, X., Jin, Y., Li, D., Ye, X., Tao, C., Zhou, M., Jiang, H., & Yu, H. (2022). A Novel SACS Variant Identified in a Chinese Patient: Case Report and Review of the Literature. *Frontiers in Neurology*, *13*. https://doi.org/10.3389/FNEUR.2022.845318

Chen, Y., Qin, C., Huang, J., Tang, X., Liu, C., Huang, K., Xu, J., Guo, G., Tong, A., & Zhou, L. (2020). The role of astrocytes in oxidative stress of central nervous system: A mixed blessing. *Cell Proliferation*, *53*(3), e12781. https://doi.org/10.1111/CPR.12781

Chiurchiù, V., Orlacchio, A., & Maccarrone, M. (2016). Is Modulation of Oxidative Stress an Answer? The State of the Art of Redox Therapeutic Actions in Neurodegenerative Diseases. *Oxidative Medicine and Cellular Longevity*, *2016*. https://doi.org/10.1155/2016/7909380

Cignarella, F., Filipello, F., Bollman, B., Cantoni, C., Locca, A., Mikesell, R., Manis, M., Ibrahim, A., Deng, L., Benitez, B. A., Cruchaga, C., Licastro, D., Mihindukulasuriya, K., Harari, O., Buckland, M., Holtzman, D. M., Rosenthal, A., Schwabe, T., Tassi, I., & Piccio, L. (2020). TREM2 activation on microglia promotes myelin debris clearance and remyelination in a model of multiple sclerosis. *Acta Neuropathologica*, *140*(4), 513–534. https://doi.org/10.1007/S00401-020-02193-Z/FIGURES/9

Clarke, L. E., Liddelow, S. A., Chakraborty, C., Münch, A. E., Heiman, M., & Barres, B. A. (2018). Normal aging induces A1-like astrocyte reactivity. *Proceedings of the National Academy of Sciences of the United States of America*, *115*(8), E1896–E1905. https://doi.org/10.1073/PNAS.1800165115/SUPPL_FILE/PNAS.1800165115.SD04.XLSX

Colonna, M., & Butovsky, O. (2017). Microglia Function in the Central Nervous System During Health and Neurodegeneration. *Annual Review of Immunology*, *35*(1), 441–468. https://doi.org/10.1146/annurev-immunol-051116-052358

Consalez, G. G., Goldowitz, D., Casoni, F., & Hawkes, R. (2021). Origins, Development, and Compartmentation of the Granule Cells of the Cerebellum. *Frontiers in Neural Circuits*, *14*, 611841. https://doi.org/10.3389/FNCIR.2020.611841/BIBTEX

Criscuolo, C., Procaccini, C., Meschini, M. C., Cianflone, A., Carbone, R., Doccini, S., Devos, D., Nesti, C., Vuillaume, I., Pellegrino, M., Filla, A., De Michele, G., Matarese, G., & Santorelli, F. M. (2015). Powerhouse failure and oxidative damage in autosomal recessive spastic ataxia of Charlevoix-Saguenay. *Journal of Neurology*, *262*(12), 2755–2763. https://doi.org/10.1007/S00415-015-7911-4

Cui, M., Yoshimori, T., & Nakamura, S. (2022). Autophagy system as a potential therapeutic target for neurodegenerative diseases. *Neurochemistry International*, *155*, 105308. https://doi.org/10.1016/J.NEUINT.2022.105308

Cyske, Z., Gaffke, L., Pierzynowska, K., & Węgrzyn, G. (2023). Tubulin Cytoskeleton in Neurodegenerative Diseases–not Only Primary Tubulinopathies. *Cellular and Molecular Neurobiology*, *43*(5), 1867–1884. https://doi.org/10.1007/S10571-022-01304-6/FIGURES/3

Dabbaghizadeh, A., Paré, A., Cheng-Boivin, Z., Dagher, R., Minotti, S., Dicaire, M. J., Brais, B., Young, J. C., Durham, H. D., & Gentil, B. J. (2022). The J Domain of Sacsin Disrupts Intermediate Filament Assembly. *International Journal of Molecular Sciences*, *23*(24), 15742. https://doi.org/10.3390/IJMS232415742/S1

D'angelo, E. (2013). Cerebellar Granule Cell. *Handbook of the Cerebellum and Cerebellar Disorders*, 765–791. https://doi.org/10.1007/978-94-007-1333-8_31

D'Angelo, E., Solinas, S., Mapelli, J., Gandolfi, D., Mapelli, L., & Prestori, F. (2013). The cerebellar Golgi cell and spatiotemporal organization of granular layer activity. *Frontiers in Neural Circuits*, *7*(APR 2013). https://doi.org/10.3389/FNCIR.2013.00093

Dash, U. C., Bhol, N. K., Swain, S. K., Samal, R. R., Nayak, P. K., Raina, V., Panda, S. K., Kerry, R. G., Duttaroy, A. K., & Jena, A. B. (2024). Oxidative stress and inflammation in the pathogenesis of neurological disorders: Mechanisms and implications. *Acta Pharmaceutica Sinica B*. https://doi.org/10.1016/J.APSB.2024.10.004

Dawley, E. M., O.Samson, S., Woodard, K. T., & Matthias, K. A. (2012). Spinal cord regeneration in a tail autotomizing urodele. *Journal of Morphology*, *273*(2), 211–225. https://doi.org/10.1002/JMOR.11019

De Braekeleer, M., Giasson, F., Mathieu, J., Roy, M., Bouchard, J. P., & Morgan, K. (1993). Genetic epidemiology of autosomal recessive spastic ataxia of Charlevoix-Saguenay in northeastern Quebec. *Genetic Epidemiology*, *10*(1), 17–25. https://doi.org/10.1002/gepi.1370100103

De Munter, S., Verheijden, S., Vanderstuyft, E., Malheiro, A. R., Brites, P., Gall, D., Schiffmann, S. N., & Baes, M. (2016). Early-onset Purkinje cell dysfunction underlies cerebellar ataxia in peroxisomal multifunctional protein-2 deficiency. *Neurobiology of Disease*, *94*, 157–168. https://doi.org/10.1016/J.NBD.2016.06.012

De Ritis, D., Ferrè, L., De Winter, J., Tremblay-Desbiens, C., Blais, M., Bassi, M. T., Dupré, N., Baets, J., Filippi, M., & Maltecca, F. (2024). Reduction of sacsin levels in peripheral blood mononuclear cells as a diagnostic tool for spastic ataxia of Charlevoix–Saguenay. *Brain Communications*, *6*(4), fcae243. https://doi.org/10.1093/BRAINCOMMS/FCAE243

De Zeeuw, C. I., & Hoogland, T. M. (2015). Reappraisal of Bergmann glial cells as modulators of cerebellar circuit function. *Frontiers in Cellular Neuroscience*, *9*(JULY). https://doi.org/10.3389/FNCEL.2015.00246

Dello Russo, C., Cappoli, N., Coletta, I., Mezzogori, D., Paciello, F., Pozzoli, G., Navarra, P., & Battaglia, A. (2018). The human microglial HMC3 cell line: where do we stand? A systematic literature review. *Journal of Neuroinflammation*, *15*(1), 259. https://doi.org/10.1186/s12974-018-1288-0

Di Meo, S., Reed, T. T., Venditti, P., & Victor, V. M. (2016). Role of ROS and RNS Sources in Physiological and Pathological Conditions. *Oxidative Medicine and Cellular Longevity*, *2016*(1), 1245049. https://doi.org/10.1155/2016/1245049

Diallo, M., & Herrera, F. (2022). The role of understudied post-translational modifications for the behavior and function of Signal Transducer and Activator of Transcription 3. *FEBS Journal*, *289*(20), 6235–6255. https://doi.org/10.1111/FEBS.16116

Didonna, A., & Opal, P. (2019). The role of neurofilament aggregation in neurodegeneration: lessons from rare inherited neurological disorders. *Molecular Neurodegeneration 2019 14:1*, *14*(1), 1–10. https://doi.org/10.1186/S13024-019-0318-4

Dombroski, B. A., Nayak, R. R., Ewens, K. G., Ankener, W., Cheung, V. G., & Spielman, R. S. (2010). Gene Expression and Genetic Variation in Response to Endoplasmic Reticulum Stress in Human Cells. *American Journal of Human Genetics*, *86*(5), 719. https://doi.org/10.1016/J.AJHG.2010.03.017

Duarte Lobo, D., Nobre, R. J., Oliveira Miranda, C., Pereira, D., Castelhano, J., Sereno, J., Koeppen, A., Castelo-Branco, M., & Pereira De Almeida, L. (2020). The blood-brain barrier is disrupted in Machado-Joseph disease/spinocerebellar ataxia type 3: evidence from transgenic mice and human post-mortem samples. *Acta Neuropathologica Communications*, *8*(1). https://doi.org/10.1186/S40478-020-00955-0

Duncan, E. J., Cheetham, M. E., Chapple, J. P., & van der Spuy, J. (2015). *The Role of HSP70 and Its Co-chaperones in Protein Misfolding, Aggregation and Disease BT - The Networking of Chaperones by Co-chaperones: Control of Cellular Protein Homeostasis* (G. L. Blatch & A. L. Edkins, Eds.; pp. 243–273). Springer International Publishing. https://doi.org/10.1007/978-3-319-11731-7_12

Duncan, E. J., Larivière, R., Bradshaw, T. Y., Longo, F., Sgarioto, N., Hayes, M. J., Romano, L. E. L., Nethisinghe, S., Giunti, P., Bruntraeger, M. B., Durham, H. D., Brais, B., Maltecca, F., Gentil, B.

J., & Chapple, J. P. (2017). Altered organization of the intermediate filament cytoskeleton and relocalization of proteostasis modulators in cells lacking the ataxia protein sacsin. *Human Molecular Genetics*, *26*(16), 3130–3143. https://doi.org/10.1093/hmg/ddx197

Dupont, N., Claude-Taupin, A., Codogno, P., Dupont, N., Claude-Taupin, A., & Codogno, P. (2024). A historical perspective of macroautophagy regulation by biochemical and biomechanical stimuli. *FEBS Letters*, *598*(1), 17–31. https://doi.org/10.1002/1873-3468.14744

Dupré, N., Bouchard, J.-P., Brais, B., & Rouleau, G. A. (2006). Hereditary Ataxia, Spastic Paraparesis and Neuropathy in the French-Canadian Population. *Canadian Journal of Neurological Sciences / Journal Canadien Des Sciences Neurologiques*, *33*(2), 149–157. https://doi.org/DOI: 10.1017/S031716710000490X

Duquette, A., Brais, B., Bouchard, J. P., & Mathieu, J. (2013). Clinical presentation and early evolution of spastic ataxia of Charlevoix-Saguenay. *Movement Disorders*, *28*(14), 2011–2014. https://doi.org/10.1002/MDS.25604

Dusart, I., & Flamant, F. (2012). Profound morphological and functional changes of rodent Purkinje cells between the first and the second postnatal weeks: A metamorphosis? *Frontiers in Neuroanatomy*, *6*(MARCH), 1–26. https://doi.org/10.3389/FNANA.2012.00011/BIBTEX

Edamakanti, C. R., Mohan, V., & Opal, P. (2023). Reactive Bergmann glia play a central role in spinocerebellar ataxia inflammation via the JNK pathway. *Journal of Neuroinflammation*, *20*(1), 1–13. https://doi.org/10.1186/S12974-023-02801-1/FIGURES/7

El Euch-Fayache, G., Lalani, I., Amouri, R., Turki, I., Ouahchi, K., Hung, W. Y., Belal, S., Siddique, T., & Hentati, F. (2003). Phenotypic features and genetic findings in sacsin-related autosomal recessive ataxia in Tunisia. *Archives of Neurology*, *60*(7), 982–988. https://doi.org/10.1001/ARCHNEUR.60.7.982

Ellgaard, L., Molinari, M., & Helenius, A. (1999). Setting the Standards: Quality Control in the Secretory Pathway. *Science*, *286*(5446), 1882–1888. https://doi.org/10.1126/SCIENCE.286.5446.1882

Engert, J. C., Bérubé, P., Mercier, J., Doré, C., Lepage, P., Ge, B., Bouchard, J.-P., Mathieu, J., Melançon, S. B., Schalling, M., Lander, E. S., Morgan, K., Hudson, T. J., & Richter, A. (2000). ARSACS, a spastic ataxia common in northeastern Québec, is caused by mutations in a new gene encoding an 11.5-kb ORF. *Nature Genetics*, *24*(2), 120–125. https://doi.org/10.1038/72769

Erta, M., Quintana, A., & Hidalgo, J. (2012). Interleukin-6, a Major Cytokine in the Central Nervous System. *International Journal of Biological Sciences*, *8*(9), 1254. https://doi.org/10.7150/IJBS.4679

Etienne-Manneville, S. (2018). Cytoplasmic Intermediate Filaments in Cell Biology. *Annual Review of Cell and Developmental Biology*, *34*(1), 1–28. https://doi.org/10.1146/annurev-cellbio-100617-062534

Fan, Y. Y., & Huo, J. (2021). A1/A2 astrocytes in central nervous system injuries and diseases: Angels or devils? *Neurochemistry International*, *148*, 105080. https://doi.org/10.1016/J.NEUINT.2021.105080

Fan, Z., Zhang, W., Cao, Q., Zou, L., Fan, X., Qi, C., Yan, Y., Song, B., & Wu, B. (2022). JAK2/STAT3 pathway regulates microglia polarization involved in hippocampal inflammatory damage due to acute paraquat exposure. *Ecotoxicology and Environmental Safety*, *234*, 113372. https://doi.org/10.1016/J.ECOENV.2022.113372

Fassio, A., Falace, A., Esposito, A., Aprile, D., Guerrini, R., & Benfenati, F. (2020). Emerging Role of the Autophagy/Lysosomal Degradative Pathway in Neurodevelopmental Disorders With Epilepsy.

Frontiers in Cellular Neuroscience, *14*, 518783. https://doi.org/10.3389/FNCEL.2020.00039/BIBTEX

Fernandes, A., Miller-Fleming, L., & Pais, T. F. (2014). Microglia and inflammation: conspiracy, controversy or control? *Cellular and Molecular Life Sciences : CMLS*, *71*(20), 3969–3985. https://doi.org/10.1007/S00018-014-1670-8/METRICS

Fernández Santoro, E. M., Karim, A., Warnaar, P., De Zeeuw, C. I., Badura, A., & Negrello, M. (2024). Purkinje cell models: past, present and future. *Frontiers in Computational Neuroscience*, *18*, 1426653. https://doi.org/10.3389/FNCOM.2024.1426653/BIBTEX

Ferro, A., Sheeler, C., Rosa, J. G., & Cvetanovic, M. (2019). Role of Microglia in Ataxias. *Journal of Molecular Biology*, *431*(9), 1792–1804. https://doi.org/10.1016/J.JMB.2019.01.016

Fewell, S. W., Travers, K. J., Weissman, J. S., & Brodsky, J. L. (2001). The action of molecular chaperones in the early secretory pathway. *Annual Review of Genetics*, *35*(Volume 35, 2001), 149–191. https://doi.org/10.1146/ANNUREV.GENET.35.102401.090313/CITE/REFWORKS

Finkbeiner, S. (2020). The Autophagy Lysosomal Pathway and Neurodegeneration. *Cold Spring Harbor Perspectives in Biology*, *12*(3). https://doi.org/10.1101/CSHPERSPECT.A033993

Fiorenza, M. T., La Rosa, P., Canterini, S., & Erickson, R. P. (2022). The Cerebellum in Niemann-Pick C1 Disease: Mouse Versus Man. *The Cerebellum 2021 22:1*, *22*(1), 102–119. https://doi.org/10.1007/S12311-021-01347-3

Fogel, B. L. (2012). Childhood Cerebellar Ataxia. *Journal of Child Neurology*, *27*(9), 1138. https://doi.org/10.1177/0883073812448231

Francis, V., Alshafie, W., Kumar, R., Girard, M., Brais, B., & McPherson, P. S. (2022). The ARSACS disease protein sacsin controls lysosomal positioning and reformation by regulating microtubule dynamics. *The Journal of Biological Chemistry*, *298*(9). https://doi.org/10.1016/J.JBC.2022.102320

Fu, R., Shen, Q., Xu, P., Luo, J. J., & Tang, Y. (2014). Phagocytosis of Microglia in the Central Nervous System Diseases. *Molecular Neurobiology*, *49*(3), 1422. https://doi.org/10.1007/S12035-013-8620-6

Galatolo, D., Rocchiccioli, S., Di Giorgi, N., Dal Canto, F., Signore, G., Morani, F., Ceccherini, E., Doccini, S., & Santorelli, F. M. (2024). Proteomics and lipidomic analysis reveal dysregulated pathways associated with loss of sacsin. *Frontiers in Neuroscience*, *18*, 1375299. https://doi.org/10.3389/FNINS.2024.1375299/BIBTEX

Galloway, D. A., Phillips, A. E. M., Owen, D. R. J., & Moore, C. S. (2019). Phagocytosis in the brain: Homeostasis and disease. *Frontiers in Immunology*, *10*(MAR), 448505. https://doi.org/10.3389/FIMMU.2019.00790/BIBTEX

Garcia, G., Fernandes, A., Stein, F., & Brites, D. (2022). Protective Signature of IFNγ-Stimulated Microglia Relies on miR-124-3p Regulation From the Secretome Released by Mutant APP Swedish Neuronal Cells. *Frontiers in Pharmacology*, *13*, 833066. https://doi.org/10.3389/FPHAR.2022.833066/BIBTEX

Garcia-Martin, E., Pablo, L. E., Gazulla, J., Vela, A., Larrosa, J. M. anuel, Polo, V., Marques, M. L., & Alfaro, J. (2013). Retinal Segmentation as Noninvasive Technique to Demonstrate Hyperplasia in Ataxia of Charlevoix-Saguenay. *Investigative Ophthalmology & Visual Science*, *54*(10), 7137–7142. https://doi.org/10.1167/IOVS.13-12726

GeneCards – The human gene database, SACS gene, GCID: GC13M023288. (n.d.). Retrieved October 4, 2022, from https://www.genecards.org/cgi-bin/carddisp.pl?gene=SACS

Gentil, B. J., Lai, G.-T., Menade, M., Larivière, R., Minotti, S., Gehring, K., Chapple, J.-P., Brais, B., & Durham, H. D. (2018). Sacsin, mutated in the ataxia ARSACS, regulates intermediate filament assembly and dynamics. *The FASEB Journal*, *33*(2), 2982–2994. https://doi.org/10.1096/fj.201801556R

Gentil, B. J., Minotti, S., Beange, M., Baloh, R. H., Julien, J., & Durham, H. D. (2012). Normal role of the low-molecular-weight neurofilament protein in mitochondrial dynamics and disruption in Charcot-Marie-Tooth disease. *FASEB Journal : Official Publication of the Federation of American Societies for Experimental Biology*, *26*(3), 1194–1203. https://doi.org/10.1096/FJ.11-196345

Ginhoux, F., Lim, S., Hoeffel, G., Low, D., & Huber, T. (2013). Origin and differentiation of microglia. *Frontiers in Cellular Neuroscience*, *7*(MAR). https://doi.org/10.3389/FNCEL.2013.00045

Girard, M., Larivière, R., Parfitt, D. A., Deane, E. C., Gaudet, R., Nossova, N., Blondeau, F., Prenosil, G., Vermeulen, E. G. M., Duchen, M. R., Richter, A., Shoubridge, E. A., Gehring, K., McKinney, R. A., Brais, B., Chapple, J. P., & McPherson, P. S. (2012). Mitochondrial dysfunction and Purkinje cell loss in autosomal recessive spastic ataxia of Charlevoix-Saguenay (ARSACS). *Proceedings of the National Academy of Sciences of the United States of America*, *109*(5), 1661–1666. https://doi.org/10.1073/pnas.1113166109

Giri, P. M., Banerjee, A., Ghosal, A., & Layek, B. (2024). Neuroinflammation in Neurodegenerative Disorders: Current Knowledge and Therapeutic Implications. *International Journal of Molecular Sciences 2024, Vol. 25, Page 3995*, *25*(7), 3995. https://doi.org/10.3390/IJMS25073995

Greer, P. L., Hanayama, R., Bloodgood, B. L., Mardinly, A. R., Lipton, D. M., Flavell, S. W., Kim, T. K., Griffith, E. C., Waldon, Z., Maehr, R., Ploegh, H. L., Chowdhury, S., Worley, P. F., Steen, J., & Greenberg, M. E. (2010). The Angelman Syndrome-associated ubiquitin ligase Ube3A regulates synapse development by ubiquitinating Arc. *Cell*, *140*(5), 704. https://doi.org/10.1016/J.CELL.2010.01.026

Grynberg, M., Erlandsen, H., & Godzik, A. (2003). HEPN: a common domain in bacterial drug resistance and human neurodegenerative proteins. *Trends in Biochemical Sciences*, *28*(5), 224–226. https://doi.org/10.1016/S0968-0004(03)00060-4

Gustafsson, N., Culley, S., Ashdown, G., Owen, D. M., Pereira, P. M., & Henriques, R. (2016). Fast live-cell conventional fluorophore nanoscopy with ImageJ through super-resolution radial fluctuations. *Nature Communications 2016 7:1*, *7*(1), 1–9. https://doi.org/10.1038/ncomms12471

Haim, L. Ben, & Rowitch, D. H. (2017). Functional diversity of astrocytes in neural circuit regulation. *Nature Reviews Neuroscience*, *18*(1), 31–41. https://doi.org/10.1038/nrn.2016.159

Han, J., Back, S. H., Hur, J., Lin, Y. H., Gildersleeve, R., Shan, J., Yuan, C. L., Krokowski, D., Wang, S., Hatzoglou, M., Kilberg, M. S., Sartor, M. A., & Kaufman, R. J. (2013). ER-stress-induced transcriptional regulation increases protein synthesis leading to cell death. *Nature Cell Biology*, *15*(5), 481. https://doi.org/10.1038/NCB2738

Harding, H. P., Zhang, Y., & Ron, D. (1999). Protein translation and folding are coupled by an endoplasmic-reticulum-resident kinase. *Nature 1999 397:6716*, *397*(6716), 271–274. https://doi.org/10.1038/16729

Hashimoto, R., Hori, K., Owa, T., Miyashita, S., Dewa, K., Masuyama, N., Sakai, K., Hayase, Y., Seto, Y., Inoue, Y. U., Inoue, T., Ichinohe, N., Kawaguchi, Y., Akiyama, H., Koizumi, S., & Hoshino, M. (2016). Origins of oligodendrocytes in the cerebellum, whose development is controlled by the

transcription factor, Sox9. *Mechanisms of Development*, *140*, 25–40. https://doi.org/https://doi.org/10.1016/j.mod.2016.02.004

Hegarty, S. V., O'Keeffe, G. W., & Sullivan, A. M. (2013). BMP-Smad 1/5/8 signalling in the development of the nervous system. *Progress in Neurobiology*, *109*, 28–41. https://doi.org/10.1016/J.PNEUROBIO.2013.07.002

Herrera, F., Chen, Q., & Schubert, D. (2010). Synergistic effect of retinoic acid and cytokines on the regulation of glial fibrillary acidic protein expression. *The Journal of Biological Chemistry*, *285*(50), 38915–38922. https://doi.org/10.1074/JBC.M110.170274

Herrmann, J. E., Imura, T., Song, B., Qi, J., Ao, Y., Nguyen, T. K., Korsak, R. A., Takeda, K., Akira, S., & Sofroniew, M. V. (2008). STAT3 is a Critical Regulator of Astrogliosis and Scar Formation after Spinal Cord Injury. *The Journal of Neuroscience*, *28*(28), 7231. https://doi.org/10.1523/JNEUROSCI.1709-08.2008

Heyer, E. (1995). Genetic consequences of differential demographic behaviour in the Saguenay region, Québec. *American Journal of Physical Anthropology*, *98*(1), 1–11. https://doi.org/10.1002/AJPA.1330980102

Hohmann, T., & Dehghani, F. (2019). The Cytoskeleton—A Complex Interacting Meshwork. *Cells*, *8*(4), 362. https://doi.org/10.3390/CELLS8040362

Hoshino, M. (2016). Specification of Cerebellar Neurons. In D. L. Gruol, N. Koibuchi, M. Manto, M. Molinari, J. D. Schmahmann, & Y. Shen (Eds.), *Essentials of Cerebellum and Cerebellar Disorders: A Primer For Graduate Students* (pp. 143–147). Springer International Publishing. https://doi.org/10.1007/978-3-319-24551-5_15

Huang, M., & Verbeek, D. S. (2018). *Why do so many genetic insults lead to Purkinje Cell degeneration and spinocerebellar ataxia? A R T I C L E I N F O*. https://doi.org/10.1016/j.neulet.2018.02.004

Huang, R., Chen, H., Liang, J., Li, Y., Yang, J., Luo, C., Tang, Y., Ding, Y., Liu, X., Yuan, Q., Yu, H., Ye, Y., Xu, W., & Xie, X. (2021). Dual Role of Reactive Oxygen Species and their Application in Cancer Therapy. *Journal of Cancer*, *12*(18), 5543. https://doi.org/10.7150/JCA.54699

Hughes, D., & Mallucci, G. R. (2019). The unfolded protein response in neurodegenerative disorders – therapeutic modulation of the PERK pathway. *The FEBS Journal*, *286*(2), 342–355. https://doi.org/10.1111/FEBS.14422

Hyuk Sung Kwon, S.-H. K. (2020). *Neuroinflammation in neurodegenerative disorders: the roles of microglia and astrocytes*. https://d-nb.info/1224589092/34

Iskusnykh, I. Y., Zakharova, A. A., Kryl'skii, E. D., & Popova, T. N. (2024). Aging, Neurodegenerative Disorders, and Cerebellum. *International Journal of Molecular Sciences 2024, Vol. 25, Page 1018*, *25*(2), 1018. https://doi.org/10.3390/IJMS25021018

Israeli, E., Dryanovski, D. I., Schumacker, P. T., Chandel, N. S., Singer, J. D., Julien, J. P., Goldman, R. D., & Opal, P. (2016). Intermediate filament aggregates cause mitochondrial dysmotility and increase energy demands in giant axonal neuropathy. *Human Molecular Genetics*, *25*(11), 2143–2157. https://doi.org/10.1093/hmg/ddw081

Jain, M., Singh, M. K., Shyam, H., Mishra, A., Kumar, S., Kumar, A., & Kushwaha, J. (2022). Role of JAK/STAT in the Neuroinflammation and its Association with Neurological Disorders. *Annals of Neurosciences*, *28*(3–4), 191. https://doi.org/10.1177/09727531211070532

Jana, N. R. (2012). UnDerstanding the pathogenesis of angelman syndrome through animal models. *Neural Plasticity*, *2012*. https://doi.org/10.1155/2012/710943

Janda, E., Boi, L., & Carta, A. R. (2018). Microglial phagocytosis and its regulation: A therapeutic target in parkinson's disease? *Frontiers in Molecular Neuroscience*, *11*, 350570. https://doi.org/10.3389/FNMOL.2018.00144/BIBTEX

Jones, J. R., Kong, L., Hanna, M. G., Hoffman, B., Krencik, R., Bradley, R., Hagemann, T., Choi, J., Doers, M., Dubovis, M., Sherafat, M. A., Bhattacharyya, A., Kendziorski, C., Audhya, A., Messing, A., & Zhang, S. C. (2018). Mutations in GFAP Disrupt the Distribution and Function of Organelles in Human Astrocytes. *Cell Reports*, *25*(4), 947-958.e4. https://doi.org/10.1016/J.CELREP.2018.09.083

Kaminsky, N., Bihari, O., Kanner, S., Barzilai, A., Kaminsty, N., Bihari, O., Kanner, S., & Barzilai, A. (2016). Connecting Malfunctioning Glial Cells and Brain Degenerative Disorders. *Genomics, Proteomics & Bioinformatics*, *14*(3), 155–165. https://doi.org/10.1016/j.gpb.2016.04.003

Kamionka, M., & Feigon, J. (2004). Structure of the XPC binding domain of hHR23A reveals hydrophobic patches for protein interaction. *Protein Science : A Publication of the Protein Society*, *13*(9), 2370. https://doi.org/10.1110/PS.04824304

Kandel, R., Jung, J., & Neal, S. (2024). Proteotoxic stress and the ubiquitin proteasome system. *Seminars in Cell & Developmental Biology*, *156*, 107–120. https://doi.org/10.1016/J.SEMCDB.2023.08.002

Kato, M., & De Schutter, E. (2023). Models of Purkinje cell dendritic tree selection during early cerebellar development. *PLOS Computational Biology*, *19*(7), e1011320. https://doi.org/10.1371/JOURNAL.PCBI.1011320

Kemp, K. C., Cook, A. J., Redondo, J., Kurian, K. M., Scolding, N. J., & Wilkins, A. (2016). Purkinje cell injury, structural plasticity and fusion in patients with friedreich's ataxia. *Acta Neuropathologica Communications*, *4*(1), 1–15. https://doi.org/10.1186/S40478-016-0326-3/FIGURES/6

Kettel, P., & Elif Karagöz, G. (2024). Endoplasmic reticulum: Monitoring and maintaining protein and membrane homeostasis in the endoplasmic reticulum by the unfolded protein response. *International Journal of Biochemistry and Cell Biology*, *172*. https://doi.org/10.1016/j.biocel.2024.106598

Khan, W., Corben, L. A., Bilal, H., Vivash, L., Delatycki, M. B., Egan, G. F., & Harding, I. H. (2022). Neuroinflammation in the Cerebellum and Brainstem in Friedreich Ataxia: An [18F]-FEMPA PET Study. *Movement Disorders*, *37*(1), 218–224. https://doi.org/10.1002/MDS.28825

Khemani, P. (2022, September). *Adult-Onset Cerebellar Ataxias - Practical Neurology*. https://practicalneurology.com/articles/2022-sept/adult-onset-cerebellar-ataxias/pdf

Klockgether, T., & Paulson, H. (2011). Milestones in ataxia. *Movement Disorders*, *26*(6), 1134–1141. https://doi.org/10.1002/MDS.23559

Koenigsknecht, J., & Landreth, G. (2004). Microglial Phagocytosis of Fibrillar β-Amyloid through a β1 Integrin-Dependent Mechanism. *Journal of Neuroscience*, *24*(44), 9838–9846. https://doi.org/10.1523/JNEUROSCI.2557-04.2004

Koszła, O., & Sołek, P. (2024). Misfolding and aggregation in neurodegenerative diseases: protein quality control machinery as potential therapeutic clearance pathways. *Cell Communication and Signaling 2024 22:1*, *22*(1), 1–23. https://doi.org/10.1186/S12964-024-01791-8

Kozlov, G., Denisov, A. Y., Girard, M., Dicaire, M. J., Hamlin, J., McPherson, P. S., Brais, B., & Gehring, K. (2011). Structural basis of defects in the sacsin HEPN domain responsible for autosomal recessive spastic ataxia of Charlevoix-Saguenay (ARSACS). *The Journal of Biological Chemistry*, *286*(23), 20407–20412. https://doi.org/10.1074/JBC.M111.232884

Kraxner, J., & Köster, S. (2023). Influence of phosphorylation on intermediate filaments. *Biological Chemistry*, *404*(8–9), 821–827. https://doi.org/10.1515/HSZ-2023-0140/MACHINEREADABLECITATION/RIS

Krygier, M., Kwarciany, M., Wasilewska, K., Pienkowski, V. M., Krawczyńska, N., Zielonka, D., Kosińska, J., Stawiński, P., Rudzińska-Bar, M., Boczarska-Jedynak, M., Karaszewski, B., Limon, J., Sławek, J., Płoski, R., & Rydzanicz, M. (2019). A Study in a Polish Ataxia Cohort Indicates Genetic Heterogeneity and Points to <i>MTCL1</I> as a Novel Candidate Gene. *Clinical Genetics*, *95*(3), 415–419. https://doi.org/10.1111/cge.13489

Kuhn, J., & Cascella, M. (2022). *Alexander Disease*.

Kwon, H. S., & Koh, S.-H. (2020). Neuroinflammation in neurodegenerative disorders: the roles of microglia and astrocytes. *Translational Neurodegeneration*, *9*(1), 42. https://doi.org/10.1186/s40035-020-00221-2

Lara-Aparicio, S. Y., Laureani-Fierro, A. J., Morgado-Valle, C., Beltrán-Parrazal, L., Rojas-Durán, F., García, L. I., Toledo-Cárdenas, R., Hernández, M. E., Manzo, J., & Pérez, C. A. (2022). Latest research on the anatomy and physiology of the cerebellum. *Neurology Perspectives*, *2*(1), 34–46. https://doi.org/10.1016/J.NEUROP.2021.12.002

Larivière, R., Gaudet, R., Gentil, B. J., Girard, M., Conte, T. C., Minotti, S., Leclerc-Desaulniers, K., Gehring, K., McKinney, R. A., Shoubridge, E. A., McPherson, P. S., Durham, H. D., & Brais, B. (2015). Sacs knockout mice present pathophysiological defects underlying autosomal recessive spastic ataxia of Charlevoix-Saguenay. *Human Molecular Genetics*, *24*(3), 727–739. https://doi.org/10.1093/hmg/ddu491

Lee, J., Ryu, S. W., Ender, N. A., & Paull, T. T. (2020). *Poly-Adp-Ribosylation Drives Loss of Protein Homeostasis in ATM and Mre11 Deficiency*. https://doi.org/10.1101/2020.10.27.357210

Lee, L. C., Weng, Y. T., Wu, Y. R., Soong, B. W., Tseng, Y. C., Chen, C. M., & Lee-Chen, G. J. (2014). Downregulation of proteins involved in the endoplasmic reticulum stress response and Nrf2-ARE signaling in lymphoblastoid cells of spinocerebellar ataxia type 17. *Journal of Neural Transmission*, *121*(6), 601–610. https://doi.org/10.1007/S00702-013-1157-Z/METRICS

Lennicke, C., & Cochemé, H. M. (2021). Redox metabolism: ROS as specific molecular regulators of cell signaling and function. *Molecular Cell*, *81*(18), 3691–3707. https://doi.org/10.1016/J.MOLCEL.2021.08.018

Letra-Vilela, R., Quiteres, R., Murtinheira, F., Crevenna, A., Hensel, Z., Herrera, F., & Nevels, M. (2020). New tools for the visualization of glial fibrillary acidic protein in living cells. *Experimental Results*, *1*, e4. https://doi.org/DOI: 10.1017/exp.2020.1

Lew, S. Y., Phang, M. W. L., Chong, P. S., Roy, J., Poon, C. H., Yu, W. S., Lim, L. W., & Wong, K. H. (2022). Discovery of Therapeutics Targeting Oxidative Stress in Autosomal Recessive Cerebellar Ataxia: A Systematic Review. *Pharmaceuticals*, *15*(6). https://doi.org/10.3390/PH15060764

Li, J., Wang, R., & Tang, D. D. (2016). Vimentin dephosphorylation at ser-56 is regulated by type 1 protein phosphatase in smooth muscle. *Respiratory Research*, *17*(1), 91. https://doi.org/10.1186/S12931-016-0415-7

Li, L., Acioglu, C., Heary, R. F., & Elkabes, S. (2021). Role of astroglial toll-like receptors (TLRs) in central nervous system infections, injury and neurodegenerative diseases. *Brain, Behavior, and Immunity*, *91*, 740–755. https://doi.org/10.1016/J.BBI.2020.10.007

Li, X., & Gehring, K. (2015). Structural studies of parkin and sacsin: Mitochondrial dynamics in neurodegenerative diseases. *Movement Disorders*, *30*(12), 1610–1619. https://doi.org/10.1002/mds.26357

Li, X., Jiang, O., Chen, M., & Wang, S. (2024). Mitochondrial homeostasis: shaping health and disease. *Current Medicine 2024 3:1*, *3*(1), 1–17. https://doi.org/10.1007/S44194-024-00032-X

Li, X., Ménade, M., Kozlov, G., Hu, Z., Dai, Z., McPherson, P. S., Brais, B., & Gehring, K. (2015). High-Throughput Screening for Ligands of the HEPN Domain of Sacsin. *PLOS ONE*, *10*(9), e0137298.

Li, Y., Huang, S., Wang, J., Dai, J., Cai, J., Yan, S., Huang, Z., He, S., Wang, P., Liu, J., & Liu, Y. (2022). Phosphorylation at Ser724 of the ER stress sensor IRE1α governs its activation state and limits ER stress-induced hepatosteatosis. *The Journal of Biological Chemistry*, *298*(6). https://doi.org/10.1016/J.JBC.2022.101997

Li, Y., Li, S., & Wu, H. (2022). Ubiquitination-Proteasome System (UPS) and Autophagy Two Main Protein Degradation Machineries in Response to Cell Stress. *Cells*, *11*(5), 851. https://doi.org/10.3390/CELLS11050851

Liddelow, S. A., & Barres, B. A. (2017). Reactive Astrocytes: Production, Function, and Therapeutic Potential. *Immunity*, *46*(6), 957–967. https://doi.org/10.1016/J.IMMUNI.2017.06.006

Liddelow, S. A., Guttenplan, K. A., Clarke, L. E., Bennett, F. C., Bohlen, C. J., Schirmer, L., Bennett, M. L., Münch, A. E., Chung, W. S., Peterson, T. C., Wilton, D. K., Frouin, A., Napier, B. A., Panicker, N., Kumar, M., Buckwalter, M. S., Rowitch, D. H., Dawson, V. L., Dawson, T. M., … Barres, B. A. (2017). Neurotoxic reactive astrocytes are induced by activated microglia. *Nature 2017 541:7638*, *541*(7638), 481–487. https://doi.org/10.1038/nature21029

Liu, B., Teschemacher, A. G., & Kasparov, S. (2017). Astroglia as a cellular target for neuroprotection and treatment of neuro-psychiatric disorders. *Glia*, *65*(8), 1205–1226. https://doi.org/10.1002/GLIA.23136

Liu, H., Zhou, Y. C., & Song, W. (2021). Involvement of IL-10R/STAT3 pathway in amyloid β clearance by microlgia in Alzheimer's disease. *International Immunopharmacology*, *101*, 108263. https://doi.org/10.1016/J.INTIMP.2021.108263

Longo, F., De Ritis, D., Miluzio, A., Fraticelli, D., Baets, J., Scarlato, M., Santorelli, F. M., Biffo, S., & Maltecca, F. (2021). Assessment of Sacsin Turnover in Patients With ARSACS: Implications for Molecular Diagnosis and Pathogenesis. *Neurology*, *97*(23), E2315–E2327. https://doi.org/10.1212/WNL.0000000000012962

Louit, A., Beaudet, M. J., Blais, M., Gros-Louis, F., Dupré, N., & Berthod, F. (2023). In Vitro Characterization of Motor Neurons and Purkinje Cells Differentiated from Induced Pluripotent Stem Cells Generated from Patients with Autosomal Recessive Spastic Ataxia of Charlevoix-Saguenay. *Stem Cells International*, *2023*, 1496597. https://doi.org/10.1155/2023/1496597

Lowery, J., Jain, N., Kuczmarski, E. R., Mahammad, S., Goldman, A., Gelfand, V. I., Opal, P., & Goldman, R. D. (2016). Abnormal intermediate filament organization alters mitochondrial motility in giant axonal neuropathy fibroblasts. *Molecular Biology of the Cell*, *27*(4), 608–616. https://doi.org/10.1091/MBC.E15-09-0627/MC-E15-09-0627-S06.MOV

Lowery, J., Kuczmarski, E. R., Herrmann, H., & Goldma, R. D. (2015). Intermediate Filaments Play a Pivotal Role in Regulating Cell Architecture and Function. *The Journal of Biological Chemistry*, *290*(28), 17145. https://doi.org/10.1074/JBC.R115.640359

Magnus, G., Xing, J., Zhang, Y., & Han, V. Z. (2023). Diversity of cellular physiology and morphology of Purkinje cells in the adult zebrafish cerebellum. *The Journal of Comparative Neurology*, *531*(3), 461–485. https://doi.org/10.1002/CNE.25435

Manto, M., & Marmolino, D. (2009). Cerebellar disorders-at the crossroad of molecular pathways and diagnosis. *Cerebellum*, *8*(4), 417–422. https://doi.org/10.1007/S12311-009-0142-4/FIGURES/2

Marí, M., Morales, A., Colell, A., García-Ruiz, C., & Fernández-Checa, J. C. (2009). Mitochondrial Glutathione, a Key Survival Antioxidant. *Antioxidants & Redox Signaling*, *11*(11), 2685. https://doi.org/10.1089/ARS.2009.2695

Márquez, B. T., Leung, T. C. S., Hui, J., Charron, F., McKinney, R. A., & Watt, A. J. (2023). A mitochondrial-targeted antioxidant (MitoQ) improves motor coordination and reduces Purkinje cell death in a mouse model of ARSACS. *Neurobiology of Disease*, *183*. https://doi.org/10.1016/J.NBD.2023.106157

Martinelli, C., Battaglini, M., Pucci, C., Gioi, S., Caracci, C., Macaluso, G., Doccini, S., Santorelli, F. M., & Ciofani, G. (2020). Development of Nanostructured Lipid Carriers for the Delivery of Idebenone in Autosomal Recessive Spastic Ataxia of Charlevoix-Saguenay. *Cite This: ACS Omega*, *5*, 12451–12466. https://doi.org/10.1021/acsomega.0c01282

Marzban, H., Del Bigio, M. R., Alizadeh, J., Ghavami, S., Zachariah, R. M., & Rastegar, M. (2015). Cellular commitment in the developing cerebellum. *Frontiers in Cellular Neuroscience*, *8*(JAN), 1–26. https://doi.org/10.3389/FNCEL.2014.00450/BIBTEX

Masoli, S., Ottaviani, A., Casali, S., & D'Angelo, E. (2020). Cerebellar Golgi cell models predict dendritic processing and mechanisms of synaptic plasticity. *PLoS Computational Biology*, *16*(12). https://doi.org/10.1371/JOURNAL.PCBI.1007937

Ménade, M., Kozlov, G., Trempe, J.-F., Pande, H., Shenker, S., Wickremasinghe, S., Li, X., Hojjat, H., Dicaire, M.-J., Brais, B., McPherson, P. S., Wong, M. J. H., Young, J. C., & Gehring, K. (2018). Structures of ubiquitin-like (Ubl) and Hsp90-like domains of sacsin provide insight into pathological mutations. *Journal of Biological Chemistry*, *293*(33), 12832–12842. https://doi.org/10.1074/jbc.RA118.003939

Messing, A. (2018). Alexander disease. *Handbook of Clinical Neurology*, *148*, 693–700. https://doi.org/10.1016/B978-0-444-64076-5.00044-2

Miller, D. W., Cookson, M. R., & Dickson, D. W. (2004). Glial cell inclusions and the pathogenesis of neurodegenerative diseases. *Neuron Glia Biology*, *1*(1), 13–21. https://doi.org/10.1017/s1740925x04000043

Mohamed, W., Kumar, J., Alghamdi, B. S., Soliman, A. H., & Toshihide, Y. (2023). Neurodegeneration and inflammation crosstalk: Therapeutic targets and perspectives. *IBRO Neuroscience Reports*, *14*, 95–110. https://doi.org/10.1016/J.IBNEUR.2022.12.003/ASSET/27DEAEB8-C72B-40F9-BB9B-A43AC497F4CA/MAIN.ASSETS/GR1.JPG

Morani, F., Doccini, S., Chiorino, G., Fattori, F., Galatolo, D., Sciarrillo, E., Gemignani, F., Züchner, S., Bertini, E. S., & Santorelli, F. M. (2021). Functional Network Profiles in ARSACS Disclosed by Aptamer-Based Proteomic Technology. *Frontiers in Neurology*, *11*. https://doi.org/10.3389/fneur.2020.603774

Morani, F., Doccini, S., Galatolo, D., Pezzini, F., Soliymani, R., Simonati, A., Lalowski, M. M., Gemignani, F., & Santorelli, F. M. (2022). Integrative Organelle-Based Functional Proteomics: In Silico Prediction of Impaired Functional Annotations in SACS KO Cell Model. *Biomolecules*, *12*(8). https://doi.org/10.3390/BIOM12081024

Morani, F., Doccini, S., Sirica, R., Paterno, M., Pezzini, F., Ricca, I., Simonati, A., Delledonne, M., & Santorelli, F. M. (2019). Functional Transcriptome Analysis in ARSACS KO Cell Model Reveals a Role of Sacsin in Autophagy. *Scientific Reports*, *9*(1), 11878. https://doi.org/10.1038/s41598-019-48047-x

Muñoz-Lasso, D. C., Romá-Mateo, C., Pallardó, F. V., & Gonzalez-Cabo, P. (2020). Much More Than a Scaffold: Cytoskeletal Proteins in Neurological Disorders. *Cells 2020, Vol. 9, Page 358*, *9*(2), 358. https://doi.org/10.3390/CELLS9020358

Murtinheira, F., Boasinha, A. S., Belo, J., Macedo, L., Farsetti, E., Robalo, T. T., Torres, V. M., Pinto, F. R., Fernandes, A., Nascimento, P., Rodrigues, M. S., & Herrera, F. (2024). Subcellular, biochemical and biophysical alterations in two glial cell models of ARSACS. *BioRxiv*, 2024.04.15.589510. https://doi.org/10.1101/2024.04.15.589510

Murtinheira, F., Migueis, M., Letra-Vilela, R., Diallo, M., Quezada, A., Valente, C. A., Oliva, A., Rodriguez, C., Martin, V., & Herrera, F. (2022). Sacsin Deletion Induces Aggregation of Glial Intermediate Filaments. *Cells*, *11*(2). https://doi.org/10.3390/cells11020299

Naef, V., Marchese, M., Ogi, A., Fichi, G., Galatolo, D., Licitra, R., Doccini, S., Verri, T., Argenton, F., Morani, F., & Santorelli, F. M. (2021). Efficient Neuroprotective Rescue of Sacsin-Related Disease Phenotypes in Zebrafish. *International Journal of Molecular Sciences*, *22*(16). https://doi.org/10.3390/IJMS22168401

Nanclares, C., Noriega-Prieto, J. A., Labrada-Moncada, F. E., Cvetanovic, M., Araque, A., & Kofuji, P. (2023). Altered calcium signaling in Bergmann glia contributes to spinocerebellar ataxia type-1 in a mouse model of SCA1. *Neurobiology of Disease*, *187*. https://doi.org/10.1016/J.NBD.2023.106318

Nedergaard, M., Ransom, B., & Goldman, S. A. (2003). New roles for astrocytes: Redefining the functional architecture of the brain. *Trends in Neurosciences*, *26*(10), 523–530. https://doi.org/https://doi.org/10.1016/j.tins.2003.08.008

Nekrasova, O. E., Mendez, M. G., Chernoivanenko, I. S., Tyurin-Kuzmin, P. A., Kuczmarski, E. R., Gelfand, V. I., Goldman, R. D., & Minin, A. A. (2011). Vimentin intermediate filaments modulate the motility of mitochondria. *Molecular Biology of the Cell*, *22*(13), 2282–2289. https://doi.org/10.1091/MBC.E10-09-0766

Nishimura, Y., Kasahara, K., & Inagaki, M. (2019). Intermediate filaments and IF-associated proteins: from cell architecture to cell proliferation. *Proceedings of the Japan Academy. Series B, Physical and Biological Sciences*, *95*(8), 479–493. https://doi.org/10.2183/pjab.95.034

Ocana-Santero, G., Díaz-Nido, J., & Herranz-Martín, S. (2021). Future Prospects of Gene Therapy for Friedreich's Ataxia. *International Journal of Molecular Sciences*. https://doi.org/10.3390/ijms22041815

Omary, M. B. (2009). "IF-pathies": a broad spectrum of intermediate filament–associated diseases. *The Journal of Clinical Investigation*, *119*(7), 1756. https://doi.org/10.1172/JCI39894

Omary, M. B., Coulombe, P. A., & McLean, W. H. I. (2004). Intermediate Filament Proteins and Their Associated Diseases. *New England Journal of Medicine*, *351*(20), 2087–2100. https://doi.org/10.1056/NEJMRA040319/ASSET/E6677EEB-4EE4-492E-9BC7-EAAD55D6204D/ASSETS/IMAGES/LARGE/NEJMRA040319_F4.JPG

Parfitt, D. A., Michael, G. J., Vermeulen, E. G. M., Prodromou, N. V, Webb, T. R., Gallo, J.-M., Cheetham, M. E., Nicoll, W. S., Blatch, G. L., & Chapple, J. P. (2009). The ataxia protein sacsin is a functional co-chaperone that protects against polyglutamine-expanded ataxin-1. *Human Molecular Genetics*, *18*(9), 1556–1565. https://doi.org/10.1093/hmg/ddp067

Parkinson, M. H., Bremner, F., & Giunti, P. (2014). Autosomal recessive spastic ataxia of Charlevoix-Saguenay (ARSACS). *Advances in Clinical Neuroscience & Rehabilitation*. https://doi.org/10.47795/DHMP3511

Paul, M. S., & Limaiem, F. (2021). Histology, Purkinje Cells. *StatPearls*. https://www.ncbi.nlm.nih.gov/books/NBK545154/

Paulus-Andres, J. A., & Burnett, M. S. (2021). Three Adult-Onset Autosomal Recessive Ataxias: What Adult Neurologists Need to Know. *Neurology. Clinical Practice*, *11*(3), 256–262. https://doi.org/10.1212/CPJ.0000000000000947

Pekny, M., & Pekna, M. (2014). Astrocyte reactivity and reactive astrogliosis: Costs and benefits. *Physiological Reviews*, *94*(4), 1077–1098. https://doi.org/10.1152/PHYSREV.00041.2013/ASSET/IMAGES/LARGE/Z9J0041427070009.JPEG

Peng, J., Sheng, A., Xiao, Q., Shen, L., Ju, X.-C., Zhang, M., He, S.-T., Wu, C., & Luo, Z.-G. (2019). Single-cell transcriptomes reveal molecular specializations of neuronal cell types in the developing cerebellum. *Journal of Molecular Cell Biology*, *11*(8), 636–648. https://doi.org/10.1093/jmcb/mjy089

Pérez-Sala, D., & Quinlan, R. A. (2024). The redox-responsive roles of intermediate filaments in cellular stress detection, integration and mitigation. *Current Opinion in Cell Biology*, *86*, 102283. https://doi.org/10.1016/J.CEB.2023.102283

Perna, L., Castelli, M., Frasnetti, E., Romano, L. E. L., Colombo, G., Prodromou, C., & Chapple, J. P. (2023). AlphaFold predicted structure of the Hsp90-like domains of the neurodegeneration linked protein sacsin reveals key residues for ATPase activity. *Frontiers in Molecular Biosciences*, *9*, 1074714. https://doi.org/10.3389/FMOLB.2022.1074714/BIBTEX

Peyronnard, J. M., Charron, L., & Barbeau, A. (1979). The Neuropathy of Charlevoix-Saguenay Ataxia: An Electrophysiological and Pathological Study. *Canadian Journal of Neurological Sciences*, *6*(2), 199–203. https://doi.org/10.1017/S031716710011964X

Phatnani, H., & Maniatis, T. (2015). Astrocytes in neurodegenerative disease. *Cold Spring Harbor Perspectives in Biology*, *7*(6), a020628. https://doi.org/10.1101/cshperspect.a020628

Pilotto, F., Del Bondio, A., & Puccio, H. (2024). Hereditary Ataxias: From Bench to Clinic, Where Do We Stand? *Cells 2024, Vol. 13, Page 319*, *13*(4), 319. https://doi.org/10.3390/CELLS13040319

Pilotto, F., & Saxena, S. (2018). Epidemiology of inherited cerebellar ataxias and challenges in clinical research: *Https://Doi.Org/10.1177/2514183X18785258*, *2*(2), 2514183X1878525. https://doi.org/10.1177/2514183X18785258

Pimenta, J., Costa, C., Alonso, I., Filipa Brandão, A., Sequeiros, J., Negrão, L., & Fineza, I. (2017). Autosomal recessive spastic ataxia of Charlevoix-Saguenay in a Portuguese child caused by a novel SACS mutation. *Pediatric Dimensions*, *2*(1). https://doi.org/10.15761/PD.1000137

Pinto, M. V., Santos, F. M. F., Barros, C., Ribeiro, A. R., Pischel, U., Gois, P. M. P., & Fernandes, A. (2021). Bashy dye platform enables the fluorescence bioimaging of myelin debris phagocytosis by microglia during demyelination. *Cells*, *10*(11), 3163. https://doi.org/10.3390/CELLS10113163/S1

Pogoda, K., & Janmey, P. A. (2023). Transmit and protect: The mechanical functions of intermediate filaments. *Current Opinion in Cell Biology*, *85*. https://doi.org/10.1016/J.CEB.2023.102281

Pradeau-Phélut, L., & Etienne-Manneville, S. (2024). Cytoskeletal crosstalk: A focus on intermediate filaments. *Current Opinion in Cell Biology*, *87*, 102325. https://doi.org/10.1016/J.CEB.2024.102325

Prodi, E., Grisoli, M., Panzeri, M., Minati, L., Fattori, F., Erbetta, A., Uziel, G., D'Arrigo, S., Tessa, A., Ciano, C., Santorelli, F. M., Savoiardo, M., & Mariotti, C. (2013). Supratentorial and pontine MRI abnormalities characterize recessive spastic ataxia of Charlevoix-Saguenay. A comprehensive study of an Italian series. *European Journal of Neurology*, *20*(1), 138–146. https://doi.org/10.1111/j.1468-1331.2012.03815.x

Purves, D. et al. (2004). *NEUROSCIENCE: Third Edition* (S. M. Purves, D., Augustine, G. J., Fitzpatrick, D., Hall, W. C., LaMantia, A.-S., McNamara, J. O., & Williams, Ed.; 3rd ed.). Sinauer Associates, Inc.

Qian, N., Wei, T., Yang, W., Wang, J., Zhang, S., Jin, S., Dong, W., Hao, W., Yang, Y., & Huang, R. C. C. (2022). Case Report: Late-Onset Autosomal Recessive Cerebellar Ataxia Associated With SYNE1 Mutation in a Chinese Family. *Frontiers in Genetics*, *13*. https://doi.org/10.3389/fgene.2022.795188

Rahman, M. M., Islam, M. R., Yamin, M., Islam, M. M., Sarker, M. T., Meem, A. F. K., Akter, A., Emran, T. Bin, Cavalu, S., & Sharma, R. (2022). Emerging Role of Neuron-Glia in Neurological Disorders: At a Glance. *Oxidative Medicine and Cellular Longevity*, *2022*(1), 3201644. https://doi.org/10.1155/2022/3201644

Rao, R. V., & Bredesen, D. E. (2004). Misfolded proteins, endoplasmic reticulum stress and neurodegeneration. *Current Opinion in Cell Biology*, *16*(6), 653. https://doi.org/10.1016/J.CEB.2004.09.012

Reemst, K., Noctor, S. C., Lucassen, P. J., & Hol, E. M. (2016). The indispensable roles of microglia and astrocytes during brain development. *Frontiers in Human Neuroscience*, *10*(NOV2016), 215574. https://doi.org/10.3389/FNHUM.2016.00566/BIBTEX

Reipert, S., Steinböck, F., Fischer, I., Bittner, R. E., Zeöld, A., & Wiche, G. (1999). Association of mitochondria with plectin and desmin intermediate filaments in striated muscle. *Experimental Cell Research*, *252*(2), 479–491. https://doi.org/10.1006/EXCR.1999.4626

Rezende Filho, F. M., Bremner, F., Pedroso, J. L., de Andrade, J. B. C., Marianelli, B. F., Lourenço, C. M., Marques-Júnior, W., França, M. C., Kok, F., Sallum, J. M. F., Parkinson, M. H., Barsottini, O. G., & Giunti, P. (2021). Retinal Architecture in Autosomal Recessive Spastic Ataxia of Charlevoix-Saguenay (ARSACS): Insights into Disease Pathogenesis and Biomarkers. *Movement Disorders*, *36*(9), 2027–2035. https://doi.org/10.1002/MDS.28612

Ritchie, M. E., Phipson, B., Wu, D., Hu, Y., Law, C. W., Shi, W., & Smyth, G. K. (2015). limma powers differential expression analyses for RNA-sequencing and microarray studies. *Nucleic Acids Research*, *43*(7), e47. https://doi.org/10.1093/NAR/GKV007

Rivera-Escalera, F., Pinney, J. J., Owlett, L., Ahmed, H., Thakar, J., Olschowka, J. A., Elliott, M. R., & O'Banion, M. K. (2019). IL-1β-driven amyloid plaque clearance is associated with an expansion of transcriptionally reprogrammed microglia. *Journal of Neuroinflammation*, *16*(1), 1–17. https://doi.org/10.1186/S12974-019-1645-7/FIGURES/5

Roberts, L. J., McVeigh, M., Seiderer, L., Harding, I. H., Corben, L. A., Delatycki, M., & Szmulewicz, D. J. (2022). Overview of the clinical approach to individuals with cerebellar ataxia and neuropathy. *Neurology: Genetics*, *8*(5). https://doi.org/10.1212/NXG.0000000000200021/ASSET/7023341C-58F6-40C0-AFA83BFA3D37D5EC/ASSETS/IMAGES/LARGE/NXG.0000000000200021T2.JPG

Robinson, K. J., Tym, M. C., Hogan, A., Watchon, M., Yuan, K. C., Plenderleith, S. K., Don, E. K., & Laird, A. S. (2021). *Flow Cytometry Allows Rapid Detection of Protein Aggregates in Cell Culture and Zebrafish Models of Spinocerebellar Ataxia-3*. https://doi.org/10.1101/2021.03.09.434364

Rolfe, A. J., Bosco, D. B., Broussard, E. N., & Ren, Y. (2017). In Vitro Phagocytosis of Myelin Debris by Bone Marrow-Derived Macrophages. *Journal of Visualized Experiments : JoVE*, *2017*(130). https://doi.org/10.3791/56322

Romano, A., Tessa, A., Barca, A., Fattori, F., de Leva, M. F., Terracciano, A., Storelli, C., Santorelli, F. M., & Verri, T. (2013). Comparative analysis and functional mapping of SACS mutations reveal novel insights into sacsin repeated architecture. *Human Mutation*, *34*(3), 525–537. https://doi.org/10.1002/humu.22269

Romano, L. E. L., Aw, W. Y., Hixson, K. M., Novoselova, T. V., Havener, T. M., Howell, S., Taylor-Blake, B., Hall, C. L., Xing, L., Beri, J., Nethisinghe, S., Perna, L., Hatimy, A., Altadonna, G. C., Graves, L. M., Herring, L. E., Hickey, A. J., Thalassinos, K., Chapple, J. P., & Wolter, J. M. (2022). Multi-omic profiling reveals the ataxia protein sacsin is required for integrin trafficking and synaptic organization. *Cell Reports*, *41*(5). https://doi.org/10.1016/J.CELREP.2022.111580

Ronnebaum, S. M., Patterson, C., & Schisler, J. C. (2014). Emerging evidence of coding mutations in the ubiquitin–proteasome system associated with cerebellar ataxias. *Human Genome Variation 2014 1:1*, *1*(1), 1–7. https://doi.org/10.1038/hgv.2014.18

Roostaei, T., Nazeri, A., Sahraian, M. A., & Minagar, A. (2014). The human cerebellum: a review of physiologic neuroanatomy. *Neurologic Clinics*, *32*(4), 859–869. https://doi.org/10.1016/j.ncl.2014.07.013

Ross, D., & Siegel, D. (2021). The diverse functionality of NQO1 and its roles in redox control. *Redox Biology*, *41*. https://doi.org/10.1016/J.REDOX.2021.101950

Ruffini, N., Klingenberg, S., Heese, R., Schweiger, S., & Gerber, S. (2022). The Big Picture of Neurodegeneration: A Meta Study to Extract the Essential Evidence on Neurodegenerative Diseases in a Network-Based Approach. *Frontiers in Aging Neuroscience*, *14*, 866886. https://doi.org/10.3389/FNAGI.2022.866886/BIBTEX

Salem, I. H., Noreau, A., Bouchard, J.-P., Rouleau, G. A., & Dupré, N. (2020). *Autosomal Recessive Cerebellar Ataxias*. 1–18. https://doi.org/10.1007/978-3-319-97911-3_100-2

Sanghvi-Shah, R., & Weber, G. F. (2017). Intermediate filaments at the junction of mechanotransduction, migration, and development. *Frontiers in Cell and Developmental Biology*, *5*(SEP), 269680. https://doi.org/10.3389/FCELL.2017.00081/BIBTEX

SantaCruz, K. S., Yazlovitskaya, E., Collins, J., Johnson, J., & DeCarli, C. (2004). Regional NAD(P)H:quinone oxidoreductase activity in Alzheimer's disease. *Neurobiology of Aging*, *25*(1), 63–69. https://doi.org/10.1016/S0197-4580(03)00117-9

Schilling, K., Oberdick, J., Rossi, F., & Baader, S. L. (2008). Besides Purkinje cells and granule neurons: an appraisal of the cell biology of the interneurons of the cerebellar cortex. *Histochemistry and Cell Biology 2008 130:4*, *130*(4), 601–615. https://doi.org/10.1007/S00418-008-0483-Y

Schmahmann, J. D. (2004). Disorders of the Cerebellum: Ataxia, Dysmetria of Thought, and the Cerebellar Cognitive Affective Syndrome. *The Journal of Neuropsychiatry and Clinical Neurosciences*, *16*(3), 367–378. https://doi.org/10.1176/jnp.16.3.367

Schwarz, N., & Leube, R. E. (2016). Intermediate Filaments as Organizers of Cellular Space: How They Affect Mitochondrial Structure and Function. *Cells*, *5*(3), 30. https://doi.org/10.3390/CELLS5030030

Sen, S., Lagas, S., Roy, A., & Kumar, H. (2022). Cytoskeleton saga: Its regulation in normal physiology and modulation in neurodegenerative disorders. *European Journal of Pharmacology*, *925*, 175001. https://doi.org/10.1016/J.EJPHAR.2022.175001

Shen, J., Chen, X., Hendershot, L., & Prywes, R. (2002). ER stress regulation of ATF6 localization by dissociation of BiP/GRP78 binding and unmasking of golgi localization signals. *Developmental Cell*, *3*(1), 99–111. https://doi.org/10.1016/S1534-5807(02)00203-4

Shergalis, A. G., Hu, S., Bankhead, A., & Neamati, N. (2020). Role of the ERO1-PDI interaction in oxidative protein folding and disease. *Pharmacology & Therapeutics*, *210*. https://doi.org/10.1016/J.PHARMTHERA.2020.107525

Shi, C. H., Rubel, C., Soss, S. E., Sanchez-Hodge, R., Zhang, S., Madrigal, S. C., Ravi, S., McDonough, H., Page, R. C., Chazin, W. J., Patterson, C., Mao, C. Y., Willis, M. S., Luo, H. Y., Li, Y. S., Stevens, D. A., Tang, M. B., Du, P., Wang, Y. H., … Schisler, J. C. (2018). Disrupted structure and aberrant function of CHIP mediates the loss of motor and cognitive function in preclinical models of SCAR16. *PLoS Genetics*, *14*(9). https://doi.org/10.1371/JOURNAL.PGEN.1007664

Shimazaki, H., & Takiyam, Y. (2012). Autosomal Recessive Spastic Ataxia of Charlevoix-Saguenay (ARSACS): Clinical, Radiological and Epidemiological Aspects. *Spinocerebellar Ataxia*, *May*. https://doi.org/10.5772/28914

Shimizu, F. (2024). [Blood-brain barrier breakdown and autoimmune cerebellar ataxia]. *Rinsho Shinkeigaku=Clinical Neurology*, *64*(3), 148–156. https://doi.org/10.5692/CLINICALNEUROL.CN-001932

Silva, J. S., Pinto, M. M., & Pinto, C. M. (2024). Let the Fibers Guide You: DTI in ARSACS. *Sinapse*, *22*(2), 97–98. https://doi.org/10.46531/sinapse/IN/210083/2022

Singh, A., Kukreti, R., Saso, L., & Kukreti, S. (2019). Oxidative Stress: A Key Modulator in Neurodegenerative Diseases. *Molecules 2019, Vol. 24, Page 1583*, *24*(8), 1583. https://doi.org/10.3390/MOLECULES24081583

Sivaramakrishnan, S., DeGiulio, J. V., Lorand, L., Goldman, R. D., & Ridge, K. M. (2008). Micromechanical properties of keratin intermediate filament networks. *Proceedings of the National Academy of Sciences of the United States of America*, *105*(3), 889–894. https://doi.org/10.1073/PNAS.0710728105

Smeets, C. J. L. M., & Verbeek, D. S. (2014). Cerebellar ataxia and functional genomics: Identifying the routes to cerebellar neurodegeneration. *Biochimica et Biophysica Acta*, *1842*(10), 2030–2038. https://doi.org/10.1016/J.BBADIS.2014.04.004

Sotelo, C. (2015). Molecular Layer Interneurons of the Cerebellum: Developmental and Morphological Aspects. *The Cerebellum*, 1–23. https://doi.org/10.1007/s12311-015-0648-xï

Sparaco, M., Gaeta, L. M., Santorelli, F. M., Passarelli, C., Tozzi, G., Bertini, E., Simonati, A., Scaravilli, F., Taroni, F., Duyckaerts, C., Feleppa, M., & Piemonte, F. (2009). Friedreich's ataxia: Oxidative stress and cytoskeletal abnormalities. *Journal of the Neurological Sciences*, *287*(1–2), 111–118. https://doi.org/10.1016/J.JNS.2009.08.052

Stevens, J. C., Murphy, S. M., Davagnanam, I., Phadke, R., Anderson, G., Nethisinghe, S., Bremner, F., Giunti, P., & Reilly, M. M. (2013). The ARSACS phenotype can include supranuclear gaze palsy and skin lipofuscin deposits. *Journal of Neurology, Neurosurgery & Psychiatry*, *84*(1), 114 LP – 116. https://doi.org/10.1136/jnnp-2012-303634

Stowell, R. D., Wong, E. L., Batchelor, H. N., Mendes, M. S., Lamantia, C. E., Whitelaw, B. S., & Majewska, A. K. (2018). Cerebellar microglia are dynamically unique and survey Purkinje neurons in vivo. *Developmental Neurobiology*, *78*(6), 627–644. https://doi.org/10.1002/DNEU.22572

Stringer, J. L., Gaikwad, A., Gonzales, B. N., Long, D. J., Marks, L. M., & Jaiswal, A. K. (2004). Presence and induction of the enzyme NAD(P)H: Quinone oxidoreductase 1 in the central nervous system. *Journal of Comparative Neurology*, *471*(3), 289–297. https://doi.org/10.1002/CNE.20048

Sultan, T., Scorrano, G., Panciroli, M., Christoforou, M., Raza Alvi, J., Di Ludovico, A., Qureshi, S., Efthymiou, S., Salpietro, V., & Houlden, H. (2024). Clinical and molecular heterogeneity of VPS13D-related neurodevelopmental and movement disorders. *Gene*, *899*, 148119. https://doi.org/10.1016/J.GENE.2023.148119

Sweeney, M. D., Sagare, A. P., & Zlokovic, B. V. (2018). Blood–brain barrier breakdown in Alzheimer disease and other neurodegenerative disorders. *Nature Reviews Neurology 2018 14:3*, *14*(3), 133–150. https://doi.org/10.1038/nrneurol.2017.188

Sweeney, P., Park, H., Baumann, M., Dunlop, J., Frydman, J., Kopito, R., McCampbell, A., Leblanc, G., Venkateswaran, A., Nurmi, A., & Hodgson, R. (2017). Protein misfolding in neurodegenerative diseases: implications and strategies. *Translational Neurodegeneration 2017 6:1*, *6*(1), 1–13. https://doi.org/10.1186/S40035-017-0077-5

Synofzik, M., Puccio, H., Mochel, F., & Schöls, L. (2019). Autosomal Recessive Cerebellar Ataxias: Paving the Way toward Targeted Molecular Therapies. *Neuron*, *101*(4), 560–583. https://doi.org/10.1016/J.NEURON.2019.01.049/ASSET/8F4DFD12-3FB9-4E1D-80AA-31301505EC55/MAIN.ASSETS/GR5.JPG

Synofzik, M., Soehn, A. S., Gburek-Augustat, J., Schicks, J., Karle, K. N., Schüle, R., Haack, T. B., Schöning, M., Biskup, S., Rudnik-Schöneborn, S., Senderek, J., Hoffmann, K.-T., MacLeod, P., Schwarz, J., Bender, B., Krüger, S., Kreuz, F., Bauer, P., & Schöls, L. (2013). Autosomal recessive spastic ataxia of Charlevoix Saguenay (ARSACS): expanding the genetic, clinical and imaging spectrum. *Orphanet Journal of Rare Diseases*, *8*(1), 41. https://doi.org/10.1186/1750-1172-8-41

Takiyama, Y. (2006). Autosomal recessive spastic ataxia of Charlevoix-Saguenay. *Neuropathology : Official Journal of the Japanese Society of Neuropathology*, *26*(4), 368–375. https://doi.org/10.1111/J.1440-1789.2006.00664.X

Takiyama, Y. (2007). Sacsinopathies: Sacsin-related ataxia. *The Cerebellum*, *6*(4), 353–359. https://doi.org/10.1080/14734220701230466

Tan, C. X., Burrus Lane, C. J., & Eroglu, C. (2021). Role of astrocytes in synapse formation and maturation. *Current Topics in Developmental Biology*, *142*, 371–407. https://doi.org/10.1016/BS.CTDB.2020.12.010

Tang, H. L., Lung, H. L., Wu, K. C., Le, A. H. P., Tang, H. M., & Fung, M. C. (2008). Vimentin supports mitochondrial morphology and organization. *Biochemical Journal*, *410*(1), 141–146. https://doi.org/10.1042/BJ20071072

Tang, Y., & Le, W. (2016). Differential Roles of M1 and M2 Microglia in Neurodegenerative Diseases. *Molecular Neurobiology*, *53*(2), 1181–1194. https://doi.org/10.1007/S12035-014-9070-5

Tazir, M., Nouioua, S., Magy, L., Huehne, K., Assami, S., Urtizberea, A., Grid, D., Hamadouche, T., Rautenstrauss, B., & Vallat, J. M. (2009). Phenotypic variability in giant axonal neuropathy. *Neuromuscular Disorders : NMD*, *19*(4), 270–274. https://doi.org/10.1016/J.NMD.2009.01.011

Theunissen, F., West, P. K., Brennan, S., Petrović, B., Hooshmand, K., Akkari, P. A., Keon, M., & Guennewig, B. (2021). New perspectives on cytoskeletal dysregulation and mitochondrial

mislocalization in amyotrophic lateral sclerosis. *Translational Neurodegeneration*, *10*(1), 1–16. https://doi.org/10.1186/S40035-021-00272-Z/FIGURES/2

Tumilaar, S. G., Hardianto, A., Dohi, H., & Kurnia, D. (2024). A Comprehensive Review of Free Radicals, Oxidative Stress, and Antioxidants: Overview, Clinical Applications, Global Perspectives, Future Directions, and Mechanisms of Antioxidant Activity of Flavonoid Compounds. *Journal of Chemistry*, *2024*(1), 5594386. https://doi.org/10.1155/2024/5594386

Türkgenç, B., Şanlıdağ, B., Eker, A., Giray, A., Kütük, Ö., Yakıcıer, C., Tolun, A., & Temel, S. G. (2018). <i>STUB1</I>polyadenylation Signal Variant AACAAA Does Not Affect Polyadenylation but Decreases<i>STUB1</I>translation Causing SCAR16. *Human Mutation*, *39*(10), 1344–1348. https://doi.org/10.1002/humu.23601

Tzoulis, C., Johansson, S., Haukanes, B. I., Boman, H., Knappskog, P. M., & Bindoff, L. A. (2013). Novel SACS Mutations Identified by Whole Exome Sequencing in a Norwegian Family with Autosomal Recessive Spastic Ataxia of Charlevoix-Saguenay. *PLOS ONE*, *8*(6), e66145. https://doi.org/10.1371/JOURNAL.PONE.0066145

Van Essen, D. C., Donahue, C. J., & Glasser, M. F. (2018). Development and Evolution of Cerebral and Cerebellar Cortex. *Brain, Behavior and Evolution*, *91*(3), 158–169. https://doi.org/10.1159/000489943

Vattem, K. M., & Wek, R. C. (2004). Reinitiation involving upstream ORFs regulates ATF4 mRNA translation in mammalian cells. *Proceedings of the National Academy of Sciences of the United States of America*, *101*(31), 11269–11274. https://doi.org/10.1073/PNAS.0400541101/ASSET/86AC6DFB-7D14-475E-B5D2-460B21596D7C/ASSETS/GRAPHIC/ZPQ0310455790005.JPEG

Verheijen, L. M. (2023). *The ubiquitin-proteasome system in neurodegenerative diseases: Lessons from mutant ubiquitin*. https://doi.org/10.26481/DIS.20231024LV

Verkhratsky, A., Butt, A., Li, B., Illes, P., Zorec, R., Semyanov, A., Tang, Y., & Sofroniew, M. V. (2023). Astrocytes in human central nervous system diseases: a frontier for new therapies. *Signal Transduction and Targeted Therapy 2023 8:1*, *8*(1), 1–37. https://doi.org/10.1038/s41392-023-01628-9

Vermeer, S., Meijer, R. P. P., Pijl, B. J., Timmermans, J., Cruysberg, J. R. M., Bos, M. M., Schelhaas, H. J., Van De Warrenburg, B. P. C., Knoers, N. V. A. M., Scheffer, H., & Kremer, B. (2008). ARSACS in the Dutch population: a frequent cause of early-onset cerebellar ataxia. *Neurogenetics*, *9*(3), 207. https://doi.org/10.1007/S10048-008-0131-7

Vermeer, S., van de Warrenburg, B. P., & Kamsteeg, E.-J. (1993). ARSACS. In *GeneReviews®*.

Vermeer, S., van de Warrenburg, B. P., Kamsteeg, E.-J., Brais, B., & Synofzik, M. (1993). *ARSACS.* (M. P. Adam, D. B. Everman, G. M. Mirzaa, R. A. Pagon, S. E. Wallace, L. J. H. Bean, K. W. Gripp, & A. Amemiya, Eds.).

Vivi, E., & Di Benedetto, B. (2024). Brain stars take the lead during critical periods of early postnatal brain development: relevance of astrocytes in health and mental disorders. *Molecular Psychiatry 2024 29:9*, *29*(9), 2821–2833. https://doi.org/10.1038/s41380-024-02534-4

Vogel, A. P., Rommel, N., Oettinger, A., Stoll, L. H., Kraus, E. M., Gagnon, C., Horger, M., Krumm, P., Timmann, D., Storey, E., Schöls, L., & Synofzik, M. (2018). Coordination and timing deficits in speech and swallowing in autosomal recessive spastic ataxia of Charlevoix–Saguenay (ARSACS). *Journal of Neurology*. https://doi.org/10.1007/s00415-018-8950-4

Von Bartheld, C. S., Bahney, J., & Herculano-Houzel, S. (2016). The Search for True Numbers of Neurons and Glial Cells in the Human Brain: A Review of 150 Years of Cell Counting HHS Public Access. *J Comp Neurol*, *524*(18), 3865–3895. https://doi.org/10.1002/cne.24040

Wagner, O. I., Lifshitz, J., Janmey, P. A., Linden, M., McIntosh, T. K., & Leterrier, J. F. (2003). Mechanisms of Mitochondria-Neurofilament Interactions. *The Journal of Neuroscience*, *23*(27), 9046. https://doi.org/10.1523/JNEUROSCI.23-27-09046.2003

Wang, M., & Kaufman, R. J. (2016). Protein misfolding in the endoplasmic reticulum as a conduit to human disease. *Nature*, *529*(7586), 326–335. https://doi.org/10.1038/NATURE17041

Wang, W. Y., Tan, M. S., Yu, J. T., & Tan, L. (2015). Role of pro-inflammatory cytokines released from microglia in Alzheimer's disease. *Annals of Translational Medicine*, *3*(10), 136–136. https://doi.org/10.3978/J.ISSN.2305-5839.2015.03.49

Wang, X., Li, X., Zuo, X., Liang, Z., Ding, T., Li, K., Ma, Y., Li, P., Zhu, Z., Ju, C., Zhang, Z., Song, Z., Quan, H., Zhang, J., Hu, X., & Wang, Z. (2021). Photobiomodulation inhibits the activation of neurotoxic microglia and astrocytes by inhibiting Lcn2/JAK2-STAT3 crosstalk after spinal cord injury in male rats. *Journal of Neuroinflammation*, *18*(1), 1–20. https://doi.org/10.1186/S12974-021-02312-X/FIGURES/8

Wang, X., & Michaelis, E. K. (2010). Selective neuronal vulnerability to oxidative stress in the brain. *Frontiers in Aging Neuroscience*, *2*(MAR), 1224. https://doi.org/10.3389/FNAGI.2010.00012/BIBTEX

Wilson, D. M., Cookson, M. R., Van Den Bosch, L., Zetterberg, H., Holtzman, D. M., & Dewachter, I. (2023). Hallmarks of neurodegenerative diseases. *Cell*, *186*(4), 693–714. https://doi.org/10.1016/J.CELL.2022.12.032

Winter, L., Abrahamsberg, C., & Wiche, G. (2008). Plectin isoform 1b mediates mitochondrion–intermediate filament network linkage and controls organelle shape. *Journal of Cell Biology*, *181*(6), 903–911. https://doi.org/10.1083/JCB.200710151

Winter, L., & Wiche, G. (2013). The many faces of plectin and plectinopathies: pathology and mechanisms. *Acta Neuropathologica*, *125*(1), 77–93. https://doi.org/10.1007/s00401-012-1026-0

Wu, Y. C., Sonninen, T. M., Peltonen, S., Koistinaho, J., & Lehtonen, Š. (2021). Blood–Brain Barrier and Neurodegenerative Diseases—Modeling with iPSC-Derived Brain Cells. *International Journal of Molecular Sciences*, *22*(14), 7710. https://doi.org/10.3390/IJMS22147710

Wyss-Coray, T., & Mucke, L. (2002). Inflammation in neurodegenerative disease - A double-edged sword. *Neuron*, *35*(3), 419–432. https://doi.org/10.1016/S0896-6273(02)00794-8/ASSET/2B14BA72-759A-4A31-AFAD-593CD6C90629/MAIN.ASSETS/GR2.JPG

Yamaguchi, T., Goto, H., Yokoyama, T., Silljé, H., Hanisch, A., Uldschmid, A., Takai, Y., Oguri, T., Nigg, E. A., & Inagaki, M. (2005). Phosphorylation by Cdk1 induces Plk1-mediated vimentin phosphorylation during mitosis. *The Journal of Cell Biology*, *171*(3), 431–436. https://doi.org/10.1083/JCB.200504091

Yim, W. W. Y., & Mizushima, N. (2020). Lysosome biology in autophagy. *Cell Discovery 2020 6:1*, *6*(1), 1–12. https://doi.org/10.1038/s41421-020-0141-7

Yoo, L., & Chung, K. C. (2018). The ubiquitin E3 ligase CHIP promotes proteasomal degradation of the serine/threonine protein kinase PINK1 during staurosporine-induced cell death. *Journal of Biological Chemistry*, *293*(4), 1286–1297. https://doi.org/10.1074/jbc.M117.803890

Yoshida, H., Matsui, T., Yamamoto, A., Okada, T., & Mori, K. (2001). XBP1 mRNA is induced by ATF6 and spliced by IRE1 in response to ER stress to produce a highly active transcription factor. *Cell*, *107*(7), 881–891. https://doi.org/10.1016/S0092-8674(01)00611-0

Yuan, A., Rao, M. V., Veeranna, & Nixon, R. A. (2017). Neurofilaments and Neurofilament Proteins in Health and Disease. *Cold Spring Harbor Perspectives in Biology*, *9*(4), a018309. https://doi.org/10.1101/CSHPERSPECT.A018309

Zhang, S. J., Ye, F., Xie, R. F., Hu, F., Wang, B. F., Wan, F., Guo, D. S., & Lei, T. (2011). Comparative study on the stem cell phenotypes of C6 cells under different culture conditions. *Chinese Medical Journal*, *124*(19), 3118–3126. https://doi.org/10.3760/CMA.J.ISSN.0366-6999.2011.19.030

Zhang, Y., Sloan, S. A., Clarke, L. E., Caneda, C., Plaza, C. A., Blumenthal, P. D., Vogel, H., Steinberg, G. K., Edwards, M. S. B., Li, G., Duncan, J. A., Cheshier, S. H., Shuer, L. M., Chang, E. F., Grant, G. A., Gephart, M. G. H., & Barres, B. A. (2016). Purification and Characterization of Progenitor and Mature Human Astrocytes Reveals Transcriptional and Functional Differences with Mouse. *Neuron*, *89*(1), 37–53. https://doi.org/10.1016/J.NEURON.2015.11.013

Zhao, J., Fu, Y., Yamazaki, Y., Ren, Y., Davis, M. D., Liu, C. C., Lu, W., Wang, X., Chen, K., Cherukuri, Y., Jia, L., Martens, Y. A., Job, L., Shue, F., Nguyen, T. T., Younkin, S. G., Graff-Radford, N. R., Wszolek, Z. K., Brafman, D. A., … Bu, G. (2020). APOE4 exacerbates synapse loss and neurodegeneration in Alzheimer's disease patient iPSC-derived cerebral organoids. *Nature Communications 2020 11:1*, *11*(1), 1–14. https://doi.org/10.1038/s41467-020-19264-0

Zhao, Y. ;, Huang, Y. ;, Cao, Y. ;, Quintas, C., Zhao, Y., Huang, Y., Cao, Y., & Yang, J. (2024). Astrocyte-Mediated Neuroinflammation in Neurological Conditions. *Biomolecules 2024, Vol. 14, Page 1204*, *14*(10), 1204. https://doi.org/10.3390/BIOM14101204

Zheng, X., Shen, G., Yang, X., & Liu, W. (2007). Most C6 Cells Are Cancer Stem Cells: Evidence from Clonal and Population Analyses. *Cancer Research*, *67*(8), 3691 LP – 3697. https://doi.org/10.1158/0008-5472.CAN-06-3912

Zheng, Z. V., Chen, J., Lyu, H., Erica Lam, S. Y., Lu, G., Chan, W. Y., & Wong, G. K. C. (2022). Novel role of STAT3 in microglia-dependent neuroinflammation after experimental subarachnoid haemorrhage. *Stroke and Vascular Neurology*, *7*(1), 62–70. https://doi.org/10.1136/SVN-2021-001028

Zhu, H., Jian, Z., Zhong, Y., Ye, Y., Zhang, Y., Hu, X., Pu, B., Gu, L., & Xiong, X. (2021). Janus Kinase Inhibition Ameliorates Ischemic Stroke Injury and Neuroinflammation Through Reducing NLRP3 Inflammasome Activation via JAK2/STAT3 Pathway Inhibition. *Frontiers in Immunology*, *12*, 714943. https://doi.org/10.3389/FIMMU.2021.714943/BIBTEX

Zöller, T., Schneider, A., Kleimeyer, C., Masuda, T., Potru, P. S., Pfeifer, D., Blank, T., Prinz, M., & Spittau, B. (2018). Silencing of TGFβ signalling in microglia results in impaired homeostasis. *Nature Communications 2018 9:1*, *9*(1), 1–13. https://doi.org/10.1038/s41467-018-06224-y

ITQB NOVA, Avenida da República, 2780-157 Oeiras, Portugal | Tel +351 214 469 100 | itqb.unl.pt